# The *in silico* Investigation of the Perplexity of Synergistic Duality: Inter-Molecular Mechanisms of Communication in Bcr–Abl

**Mr. Ahmed Abd Elkader Abd Elkader Mohamed Elrashedy**

**2019**

A thesis submitted to the School of Health Sciences, University of KwaZulu-Natal, Westville, in fulfilment for the degree of Doctor of Philosophy

**The *in silico* investigation of the Perplexity of Synergistic Duality: Inter-Molecular Mechanisms of Communication in Bcr–Abl**

**Mr. Ahmed Abd Elkader Abd Elkader Mohamed Elrashedy**

**217064947**

**2019**

A thesis submitted to the School of Pharmacy and Pharmacology, Faculty of Health Sciences, University of KwaZulu-Natal, Westville, for the degree of Doctor of Philosophy.

The thesis is set-up with chapters written as a set of discrete research publications, with an overall introduction and final summary. Typically, these chapters will have been published in internationally recognized, peer-reviewed journals.

This is to certify that the contents of this thesis are the original research work of Mr. Ahmed Elrashedy.

As the candidate's supervisor, I have approved this thesis for submission.

Supervisor:

Signed: Mahmoud E. Soliman Name: Prof Mahmoud Soliman

Date: 31 August 2019

## PREFACE

This thesis is divided into seven chapters, including this one:

**Chapter 1:**

This is an introductory chapter that addresses the background, rationale, and relevance of the study as well as the proposed aim and objectives. The general outline and structure of the thesis conclude this chapter.

**Chapter 2:**

This chapter provides a comprehensive literature review on the inhibition of Bcr-Abl mechanism as a driver for chronic myeloid leukemia. The background, function and structural characteristics are included in this chapter.

**Chapter 3:**

This chapter expounds on computer-aided drug design by discussing various molecular dynamic approaches and applications that were employed to investigate the various conformational changes, structural conformations and the impact of the induced single active site mutation and dual active site and activation loop mutations on co-bound and singly-bound to Bcr-Abl

**Chapter 4: (Published work- this chapter is presented in the required format of the journal and is the final version of the accepted manuscript)**

This chapter presents results from the study titled " The Perplexity of Synergistic Duality: Inter-Molecular Mechanisms of Communication in Bcr-Abl". The research article has been already published in Anti-Cancer Agents in Medicinal Chemistry (IF = 2.18) in 2019.

**Chapter 5: (Published work- this chapter is presented in the required format of the journal and is the final version of the published manuscript)**

This chapter reveals the second objective of the thesis and is entitled “Dual Drug Targeting of Mutant Bcr-Abl Induces Inactive Conformation: New Strategy for the Treatment of Chronic Myeloid Leukemia and Overcoming Monotherapy Resistance”. This article has been accepted in Chemistry& Biodiversity (IF = 1.449) in 2018.

**Chapter 6: (Published work- this chapter is presented in the required format of the journal and is the final version of the submitted manuscript)**

This chapter entitled “A Synergistic Combination Against Chronic Myeloid Leukemia: An Intra-molecular Mechanism of Communication in Bcr–Abl Resistance”. This article has been accepted in The Protein journal (IF = 1.029) in 2019.

**Chapter 7:**

This is the final chapter that proposes concluding remarks and future work.

## ABSTRACT

Due to their important role in normal cellular physiology, protein kinase activity is tightly regulated and their aberrant activation can lead to cancer. Chronic myeloid leukaemia (CML) is a blood cancer described by unregulated growth of myeloid cells caused by a fusion protein, Bcr-Abl, a constitutively active form of the Abelson tyrosine kinase (Abl). Drug targeting of either the ATP binding pocket or allosteric pocket has led to durable therapeutic response, however the development of drug resistance still poses a major clinical challenge. Recent studies exploring synergistic inhibition as an effective approach, by dual targeting of Bcr-Abl using both catalytic and allosteric binding inhibitors.

This thesis implements the use of advanced computational tools to unravel molecular insights to aid in the suppression of the emergence of resistance to Bcr-Abl when Nilotinib and ABL001 are co-administered to target both the catalytic and allosteric binding site of Bcr-Abl protein, respectively. Our studies revealed co-binding induced a stable Bcr-Abl protein structure, increased the degree of compactness of binding site residues around Nilotinib and subsequently improved the binding affinity of Nilotinib.

Findings in this thesis further provide an atomistic perspective underlying the developed resistance of Nilotinib by point mutation at the catalytic active site only and both catalytic and activation loop sites. We also recognized and rationalized the structural interplay of this single and double mutation upon co-binding of Nilotinib with the novel inhibitor, ABL001. Our findings report the distortion of the overall conformational landscape of Bcr-Abl fusion oncoprotein caused by the mutation, resulting in a reduction of binding affinity of Nilotinib upon single binding. Interesting, co-administration with ABL001 impacted by the mutation results in a more compact and stable protein conformation. Findings reveal a structural mechanism by which the novel inhibitor ABL001 stabilizes Bcr-Abl fusion oncoprotein upon co-binding with Nilotinib, thus suppressing Nilotinib resistance.

We also provide vital conformational dynamics and structural mechanisms of the mutant enzyme at the catalytic site-ligand interaction and mutant enzyme at both catalytic and activation loop ligand interactions which could potentially shift the current therapeutic protocol in chronic myeloid leukemia treatment, thus aiding in the design of novel inhibitors with improved therapeutic features against the mutant proteins.

## DECLARATION I -PLAGIARISM

I, Ahmed Elrashedy, declare that

1. The research reported in this thesis, except where otherwise indicated, is my original research.

2. This thesis has not been submitted for any degree or examination at any other university.

3. This thesis does not contain other persons' data, pictures, graphs or other information unless specifically acknowledged as being sourced from other persons.

4. This thesis does not contain other persons' writing unless specifically acknowledged as being sourced from other researchers. Where other written sources have been quoted, then:

    a. Their words have been re-written but the general information attributed to them has been referenced.

    b. Where their exact words have been used, then their writing has been placed in italics and inside quotation marks and referenced.

5. This thesis does not contain text, graphics or tables copied and pasted from the internet, unless specifically acknowledged, and the source being detailed in the thesis and in the References sections.

A detailed contribution to publications that form part and/or include research presented in this thesis is stated (include publications submitted, accepted, in the press and published).

Signed: A. A. E. Elrashedy

## DECLARATION II- LIST OF PUBLICATIONS

1. Ahmed A. Elrashedy, Pritika Ramharack, Mahmoud E.S. Soliman (2019) The Perplexity of Synergistic Duality: Inter-Molecular Mechanisms of Communication in Bcr-Abl. Anti-Cancer Agents in Medicinal Chemistry, Anticancer Agents Med Chem. Jun 20. DOI: 10.2174/1871520619666190620120144.. (Published).

   **Contribution:**

   Ahmed A ElRashedy:: contributed to the project by performing all the experimental work and manuscript preparation and writing.

   Pritika Ramharack: Contributed to the manuscript writing and providing technical support

   Mahmoud E.S. Soliman: Supervisor

   *Appendix A: Pdf version of the publication*

2. Ahmed A. El Rashedy, Fisayo A. Olotu and Mahmoud E. S. Soliman (2018) Dual Drug Targeting of Mutant Bcr-Abl Induces Inactive Conformation: New Strategy for the Treatment of Chronic Myeloid Leukemia and Overcoming Monotherapy Resistance, *Chem. Biodiversity 2018, 15, e1700533. (Published)*

   **Contribution:**

   Ahmed A ElRashedy: contributed to the project by performing all the experimental work and manuscript preparation and writing.

   Fisayo A. Olotu: Contributed to the manuscript writing and providing technical support

   Mahmoud E.S. Soliman: Supervisor

   *Appendix B: Pdf version of the publication*

3. Ahmed A. El Rashedy, Patrick Appiah-Kubi and Mahmoud E. S. Soliman (2019) A Synergistic Combination Against Chronic Myeloid Leukemia: An Intra-molecular Mechanism of Communication in BCR–ABL1 Resistance, *The Protein Journal 38: 1-9*. (*Published*)

**Contribution:**

Ahmed A ElRashedy: contributed to the project by performing all the experimental work and manuscript preparation and writing.

Patrick Appiah-Kubi: Contributed to the manuscript writing and providing technical support

Mahmoud E.S. Soliman: Supervisor

*Appendix C: Pdf version of the publication*

## RESEARCH OUTPUT

### *A- LIST OF PUBLICATIONS*

1. Ahmed A. Elrashedy, Pritika Ramharack, Mahmoud E.S. Soliman (2019) The Perplexity of Synergistic Duality: Inter-Molecular Mechanisms of Communication in Bcr-Abl. Anticancer Agents Med Chem. 2019 Jun 20. DOI: 10.2174/1871520619666190620120144.
2. Ahmed A. El Rashedy, Fisayo A. Olotu and Mahmoud E. S. Soliman (2018) Dual Drug Targeting of Mutant Bcr-Abl Induces Inactive Conformation: New Strategy for the Treatment of Chronic Myeloid Leukemia and Overcoming Monotherapy Resistance, Chem. Biodiversity 2018, 15, e1700533.
3. Ahmed A. El Rashedy, Patrick Appiah-Kubi and Mahmoud E. S. Soliman (2019) A Synergistic Combination Against Chronic Myeloid Leukemia: An Intra-molecular Mechanism of Communication in BCR–ABL1 Resistance, *The Protein Journal 38: 1-9.*

### *B- Other research outputs*

1. Metwally K, Pratsinis H, Kletsas D, Quattrini L, Coviello V, Motta C, El-Rashedy AA, Soliman ME, Novel quinazolinone-based 2,4-thiazolidinedione-3-acetic acid derivatives as potent aldose reductase inhibitors. Future Med Chem. 2017 Nov 3. doi: 10.4155/fmc-2017-0149
2. Metwally K, Pratsinis H, Kletsas D, Quattrini L, Coviello V, Motta C, El-Rashedy AA, Soliman ME, Novel quinazolinone-based 2,4-thiazolidinedione-3-acetic acid derivatives as potent aldose reductase inhibitors. Future Med Chem. 2017 Nov 3. doi: 10.4155/fmc-2017-0149
3. El-Sayed S, Metwally K, El-Shanawani AA, Abdel-Aziz LM, El-Rashedy AA, Soliman MES, Quattrini L, Coviello V, la Motta C. Quinazolinone-based rhodanine-3-acetic acids as potent aldose reductase inhibitors: Synthesis, functional evaluation and molecular modeling study. Bioorg Med Chem Lett. 2017 Oct 15;27(20):4760-4764
4. Monu Joy , Ahmed A. Elrashedy , Bijo Mathew , Ashona Singh Pillay , Annie Mathews , Sanal Dev , Mahmoud E.S. Soliman , C. Sudarsanakumar , Discovery of new class of

methoxy carrying isoxazole derivatives as COX-II inhibitors: Investigation of a detailed molecular dynamics study, Journal of Molecular Structure 1157 (2018) 19e28

5. Imane Bjij, Fisayo A. Olotu, Clement Agoni, Emmanuel Adeniji, Shama Khan, Ahmed El Rashedy, and Mahmoud E.S. Soliman (2018) Covalent Inhibition in Drug Discovery: Filling the Void in Literature, Current Topics in Medicinal Chemistry,18(13):1135-1145.
6. Fisayo A. Olotu, Emmanuel A. Adeniji, Shama Khan, Imane Bjij, Clement Agoni , Ahmed Elrashedy and Mahmoud E.S. Soliman (2018) An update on the discovery and development of selective heat shock protein inhibitors as anti-cancer therapy, Expert Opinion On Drug Discovery, 13(10):903-918.
7. Murtala A. Ejalonibu, Ahmed A. Elrashedy, Monsurat M. Lawal, Mahmoud E. Soliman, Sphelele C. Sosibo, Hezekiel M. Kumalo, Ndumiso N. Mhlongo Dual targeting approach for Mycobacterium tuberculosis drug discovery: insights from DFT calculations and molecular dynamics simulations. Structural Chemistry (accepted)
8. Ahmed A Elrashedy, Khalid Ahmed, Mahmoud E. S. Soliman, The influence of pH/pKa on controlled loading and release of Ibuprofen-silica nanoparticles - A molecular insight (submitted).
9. Khalid Ahmed, Ahmed A Elrashedy, Mahmoud E. S. Soliman, Dual drug targeting of Mtb PKNA/PKNB: Anew strategy for the selective treatment of tuberculosis disease (submitted)
10. Aimen Aljoundi , Ahmed El Rashedy, Imane Bjij , and Mahmoud E. S. Soliman, “Covalent versus Non-covalent Enzyme Inhibition: Which Route should we take? A Compactional Molecular Modelling perspective” (submitted)

***B- CONFERENCES***

1. Poster Presentation “Dual Drug Targeting of Mutant Bcr-Abl Induces Inactive Conformation: New Strategy for the Treatment of Chronic Myeloid Leukemia and Overcoming Monotherapy Resistance” CHPC National Conference, 3-7, 2017, Velmore Hotel Estate, Pretoria, South Africa.
2. Poster Presentation “A Synergistic Combination Against Chronic Myeloid Leukemia: An Intra-molecular Mechanism of Communication in Bcr–Abl Resistance” CHPC National Conference, 2-6, 2018, Century City Conference Centre, Cape Town, South Africa.

3. Poster Presentation “The influence of pH/pKa on controlled loading and release of Ibuprofen-silica nanoparticles - A molecular insight” Nanotechenology platform symposium program, Senate Chamber-Westville Campus, University of KwaZulu-Natal, South Africa.

## ACKNOWLEDGEMENTS

***First and foremost, I would like to thank God. You have given me the power to believe in myself and carry on in my life. I could never have done this with the faith I have in you, the Almighty*.**

This thesis marks the end of my journey in obtaining my Ph.D. I have not travelled alone and I have been kept on track thanks to the support of numerous people. I am delighted to dedicate these few words to all those who contributed in many ways to my Ph.D. These 3 years have been a period of intense learning, not only scientifically, but mostly on a personal level.

- I would like to express my appreciation and thanks to my advisor **Prof. M.E.S Soliman**. He supported me greatly and was constantly available to guide me during my Ph.D. I thank you for your willingness to share your knowledge and time with me.
- My colleagues, in the UKZN **Molecular Modeling and Drug Design Group** for sharing their knowledge of research methodologies and computational chemistry. Also, their constant support, love, and motivation during my PhD
- I am so grateful for my supportive family, and especially my wife, mother, and father. Thank you for allowing me to achieve my goals, live my dreams and for supporting me.
- My two angels, **Abd Allah** and **Maryum** – God bless and protect them.
- The **Centre for High Performance Computing (CHPC)** for the computational resources.
- To the **College of Health Sciences** for financial support.

## LIST OF ABREVIATIONS

| | |
|---|---|
| CML | chronic myeloid leukaemia |
| TKIs | Tyrosine kinase inhibitors |
| FDA | Food and Drug Administration |
| CTKs | Cytoplasmic tyrosine kinases |
| ATP | Adenosine Triphosphate |
| RTKs | Transmembrane receptor tyrosine kinases |
| SH3 | Src-homology 3 |
| SH2 | Src-homology 2 |
| CADD | Computer-Aided Drug Design |
| 3D | Three-Dimensional |
| PH | Pleckstrin homology |
| TH | Tec-homology |
| MM/GBSA | Molecular Mechanics/Generalized Born Surface Area |
| MM/PBSA | Molecular Mechanics/Poisson-Boltzmann Surface Area |
| WHO | World Health Organization |
| F-BAR | Bin-Amphiphysin-Rvs |
| SAM | Sterile-α-motif |
| CRIB | Cdc42/Rac-interactive-binding-motif |
| FERM | protein-ezrin-radixin-moesin |
| B | Beta |
| A | Alpha |

| | |
|---|---|
| FAT | focal adhesion- targeting |
| Ph | Philadelphia chromosome |
| NLS | Nuclear localization signal |
| DBN | DNA binding domain |
| FBD | F-actin binding domain |
| CDK4/6 | Cyclin-dependent kinases (CDK) 4/6 |
| QM | Quantum Mechanics |
| MM | Molecular Mechanics |
| MD | Molecular Dynamics |
| DNA | Deoxyribonucleic acid |
| MC | Monte Carlo |
| RMSD | Root Mean Square Deviation |
| RoG | Radius of Gyration |
| ΔG | Free Binding energy |
| SASA | Solvent accessible surface area |
| RMSF | Root Mean Square Fluctuation |
| PCA | Principal Component Analysis |
| PDB | Protein data bank |
| ORF | Open Reading Frame |
| UTR | Un-Translated Region |
| PRED | Per Residue Decomposition |
| RSCB | Research Collaboratory for Structural Bioinformatics |
| RESP | Restrained Electrostatic Potential |

| | |
|---|---|
| GAFF | General amber Force Field |
| Ps | Picoseconds |
| Ns | Nanoseconds |
| K | Kelvin |
| Å | Amperes |
| PME | Particle-mesh Ewald method |
| EGFR | Epidermal growth factor receptor |
| ErbB2 | Receptor tyrosine-protein kinase erbB-2 |
| ErbB4 | Receptor protein-tyrosine kinase erbB-4 |
| ALK | Anaplastic lymphoma kinase |
| JAK1/2 | Janus kinase1/2 |
| MEK1/2 | Mitogen Activated Protein Kinase Kinase |
| MET | MNNG HOS transforming gene |
| BRAF | A serine/threonine protein kinase activating the MAP kinase/ERK-signaling pathway. |
| AML | Acute myeloid leukemia |
| Bcr | breakpoint cluster region gene |

## LIST OF AMINO ACIDS

| Three Letter Code | Amino Acid |
|---|---|
| Ala | Alanine |
| Arg | Arginine |
| Asn | Asparagine |
| Asp | Aspartic Acid |
| Cys | Cysteine |
| Gln | Glutamine |
| Glu | Glutamic Acid |
| Gly | Glycine |
| His | Histidine |
| Ile | Isoleucine |
| Leu | Leucine |
| Lys | Lysine |
| Met | Methionine |
| Phe | Phenylalanine |
| Pro | Proline |
| Ser | Serine |
| Thr | Threonine |
| Trp | Tryptophan |
| Tyr | Tyrosine |
| Val | Valine |

## TABLE OF CONTENTS

## LIST OF FIGURES

## LIST OF TABLES

# CHAPTER 1

## 1 Introduction

### *1.1 Background and Rational*

The information presented in this thesis is geared towards comprehending and giving molecular insights into Bcr-Abl fusion protein while unraveling the potential of co-inhibition as a solution of Nilotinib resistance in chronic myeloid leukemia (CML) treatment. One of the main setbacks associated with the treatment of CML is the occurrence of mutations within the Bcr-Abl kinase domain(Hochhaus *et al.*, 2002; Gambacorti-Passerini *et al.*, 2003) , which leads to the ineffectiveness of several potent tyrosine kinase inhibitors (Shah *et al.*, 2002; Milojkovic and Apperley, 2009) . Firstly, *in silico* exploration of the conformational properties of the protein followed by investigation of the mechanism of either tyrosine kinase or allosteric inhibitor resistance provides valuable information in the search for a solution to either tyrosine kinase inhibitor or allosteric inhibitor resistance. This insight will provide a rational basis for combination therapy using both inhibitors for Bcr-Abl pathway in CML treatment.

The discovery of Bcr – Abl as a necessity in CML pathogenesis and the essential function of ABL tyrosine-kinase interaction in facilitated Bcr – Abl transformation has highlighted the Abl receptor an appealing therapy target for CML procedures (Ren, 2005). This has resulted in a substantial transformation in the therapeutic landscape of CML with the development of tyrosine kinase inhibitors (TKIs) that may potentially inhibit the interaction of Bcr-Abl and ATP. This approach has resulted in a 10-year survival rate improvement from 20% to 80%- 90% (Huang, Cortes and Kantarjian, 2012; Jabbour and Kantarjian, 2018). Recently, Wylie *et al* (2017) reported conclusive experimental proof that both catalytic and allosteric site co-administration of Nilotinib and ABL001 suppresses the emergence of resistance (Wylie et al., 2017a). Therefore, it is essential to obtain insight into the structural basis for future dual inhibition with the accessibility of drugs target specific to both allosteric and active sites. This will improve our understanding of the efficacy of CML co-administrative therapy. The combined blockade of Bcr-Abl by Nilotinib and ABL-001 makes a synergistic impact on Bcr-Abl inducing a more stable and compact protein conformation. The binding energy assessment reveals that the joint effect

of the two drugs was substantially higher in comparison to the bonding impacts of each drug individually.

Molecular modeling methods have emerged as close counterparts that complement experimental studies in current drug discovery process and have substantially aided in the understanding of very complicated biological processes (Chaudhari *et al.*, 2017). Different computational tools such as Molecular dynamic simulation and advanced post dynamic analysis played an important role in the precise molecularlevel understanding of the interaction between drug molecules to targets. In this thesis , MD simulations and enhanced post analysis techniques e.g Root Mean Square Deviation (RMSD), Root Mean Square Fluctuation (RMSF), Radius of Gyration (RoG), Molecular Mechanics energies combined with the Poisson–Boltzmann or Generalized Born and Surface area continuum solvation (MM/PBSA and MM/GBSA) based binding free energy analysis were used to recognize the detailed molecular impact of single catalytic active site mutation only and catalytic and activation loop mutation on the binding landscape of Nilotinib amidst single and co-binding with ABL001 and to also unveil the molecular structural and conformations of single and co-binding of both Nilotinib and ABL001 on Bcr-Abl oncoprotein .

### *1.2 Aim and Objectives*

The primary purpose of this thesis is to identify and characterize the principal target proteins of Bcr-Abl and subsequently utilize Computer-Aided Drug Design techniques (CADD) to investigate potential small molecule inhibitors against these proteins.

To accomplish this, the following objectives were outlined:

1. To explore the structural dynamics and in turn, the Bcr-Abl inhibition mechanism when bound to both ATP-competitive inhibitor (Nilotinib) and Allosteric inhibitor (ABL001). This will provide insight on the binding mechanism at the ATPase active site, thereby helping to develop efficient inhibitors against this Bcr-Abl target.These objective is achieved by:

1.1. Performing MD simulation on unbound Bcr-Abl, complex of Bcr-Abl with Nilotinib, complex of Bcr-Abl with ABL001, and complex of Bcr-Abl with both Nilotinib and ABL001 (Apo, Asciminib, Nilotinib and complex )

1.2. Calculating the binding free energy of Nilotinib and ABL001 when each is bounded individually and when co-administrated to Bcr-Abl.

1.3. Characterizing the binding landscape of Bcr-Abl and its structural alteration when bound to Nilotinib and ABL001 concurrently.

1.4. Performing per-residue based decomposition for the active site residues of Nilotinib and ABL001.

2. To investigate the molecular impact of an amino acid mutation in a single active site on Bcr-Abl of Nilotinib and the novel allosteric inhibitor ABL001. These objective is achieved by:

2.1. Generating a Bcr-Abl mutant by replacing Thr 334 with leucine at Nilotinib's active site with Chimera.

2.2. Performing MD simulation on the following system: complex of Nilotinib bound to Bcr-Abl, complex of Bcr-Abl bound to both Nilotinib and ABL001 (nilotinib, dual ).

2.3. Investigating the stability of the different simulated systems over the simulation period.

2.4. Performing multiple post dynamic analysis to understand the effect of gatekeeper T334I mutation on the binding of Nilotinib at the catalytic site.

3. To understand the molecular impact of amino acid mutations at both catalytic active site and activation loop site on Bcr-Abl of Nilotinib and the novel allosteric inhibitor ABL001. In order to accomplish this:

3.1. Perform MD simulation on unbound Bcr-Abl, complex of Bcr-Abl with Nilotinib, complex of Bcr-Abl with ABL001, and complex of Bcr-Abl with both Nilotinib and ABL001 (BA-Apo, BA-Nilotinib, BA-ABL001, and BA-Co-inhibition).

3.2. Calculate the Nilotinib and ABL001 potential free energy when each is bounded individually and when co-administrated to Bcr-Abl.

3.3. Characterize the binding landscape of Bcr-Abl and its structural alteration when bound to Nilotinib and ABL001 concurrently.
3.4. Perform per-residue based decomposition for the active site residues of Nilotinib and ABL001.

### *1.3 Novelty and Significance of Study:*

A recent study by Wylie et al (2017) reported conclusive experimental proof that both catalytic and allosteric site co-administration of ABL001 at the allosteric, myristoyl pocket of the protein and Nilotinib at the catalytic pocket suppresses the emergence of resistance (Wylie *et al.*, 2017b). These findings showed that ABL001 was bound in a comparable conformation to myristate and led to tumor regression in mice when bound in conjunction with Nilotinib. It was important to note that no proof of tumor regrowth was observed even after the combination dosage stopped. A phase 1 clinical trial was launched to further evaluate the dosage of ABL001 in CML patients (ClinicalTrials.gov identifier: NCT02081378) (Wylie *et al.*, 2017b). A crystal structure of the protein in combination with both Nilotinib and AB L001 was recorded to further validate the research (PDB code: 5MO4) (Wylie *et al.*, 2017b). Preliminary findings in patients receiving an increased dose of a compound disclosed well-tolerated dose-dependent pharmacokinetics. Other studies by Cowan-Jacob (2016) and Schoepfer et al (2018) further illustrated ABL001's potency as an allosteric inhibitor against the Bcr-Abl protein in CML(Cowan-Jacob, 2016; Schoepfer *et al.*, 2018). On the basis of the above experimental research, we present the first account of the structural inhibition mechanism caused by the co-binding of allosteric (ABL001) and catalytic (Nilotinib) inhibitors. We will also provide insights into the Nilotinib resistance mechanism by unveiling the impact of catalytic active site mutation only and both catalytic active site and activation loop mutations on the binding affinity of Nilotinib and ABL001 amidst single binding or co-binding. The research conducted in this study gives rise to new possibilities for the treatment of resistance in CML and helps to design novel and selective inhibitors as dual anti-cancer drugs.

## *1.4 References:*


Chaudhari, R. *et al.* (2017) 'Computational polypharmacology: a new paradigm for drug discovery', *Expert Opinion on Drug Discovery*. Taylor & Francis, 12(3), pp. 279–291. DOI: 10.1080/17460441.2017.1280024.

Cowan-Jacob, S. W. (2016) 'The role of structure and biophysics in the discovery of allosteric kinase inhibitors: ABL001, a potent and specific inhibitor of BCR-ABL', *Acta. Crystallogr*, 72(a1), pp. s4–s5. Available at: http://journals.iucr.org/a/issues/2016/a1/00/a54007/a54007.pdf (Accessed: 22 August 2019).

Gambacorti-Passerini, C. B. *et al.* (2003) 'Molecular mechanisms of resistance to imatinib in Philadelphia-chromosome-positive leukaemias', *The Lancet Oncology*. Elsevier, 4(2), pp. 75–85. doi: 10.1016/S1470-2045(03)00979-3.

Hochhaus, A. *et al.* (2002) 'Molecular and chromosomal mechanisms of resistance to imatinib (STI571) therapy', *Leukemia*. Nature Publishing Group, 16(11), pp. 2190–2196. doi: 10.1038/sj.leu.2402741.

Huang, X., Cortes, J. and Kantarjian, H. (2012) 'Estimations of the increasing prevalence and plateau prevalence of chronic myeloid leukemia in the era of tyrosine kinase inhibitor therapy.', *Cancer*. United States, 118(12), pp. 3123–3127. doi: 10.1002/cncr.26679.

Jabbour, E. and Kantarjian, H. (2018) 'Chronic myeloid leukemia: 2018 update on diagnosis, therapy and monitoring', *American journal of hematology*. Wiley Online Library, 93(3), pp. 442–459.

Milojkovic, D. and Apperley, J. (2009) 'Mechanisms of Resistance to Imatinib and Second-Generation Tyrosine Inhibitors in Chronic Myeloid Leukemia.', *Clinical cancer research : an official journal of the American Association for Cancer Research*. American Association for Cancer Research, 15(24), pp. 7519–7527. doi: 10.1158/1078-0432.CCR-09-1068.

Ren, R. (2005) 'Mechanisms of BCR–ABL in the pathogenesis of chronic myelogenous

leukaemia', *Nature Reviews Cancer*. Nature Publishing Group, 5(3), p. 172.

Schoepfer, J. *et al.* (2018) 'Discovery of Asciminib (ABL001), an Allosteric Inhibitor of the Tyrosine Kinase Activity of Bcr-Abl1'. doi: 10.1021/acs.jmedchem.8b01040.

Shah, N. P. *et al.* (2002) 'Multiple BCR-ABL kinase domain mutations confer polyclonal resistance to the tyrosine kinase inhibitor imatinib (STI571) in chronic phase and blast crisis chronic myeloid leukemia.', *Cancer cell*, 2(2), pp. 117–25. Available at: http://www.ncbi.nlm.nih.gov/pubmed/12204532 (Accessed: 22 March 2018).

Wylie, A. A. *et al.* (2017a) 'The allosteric inhibitor ABL001 enables dual targeting of BCR–ABL1', *Nature*. Nature Research, 543(7647), pp. 733–737. doi: 10.1038/nature21702.

Wylie, A. A. *et al.* (2017b) 'The allosteric inhibitor ABL001 enables dual targeting of Bcr-Abl', *Nature*, 543(7647), pp. 733–737. doi: 10.1038/nature21702.

# CHAPTER 2

## 2. Overview of Cancer:

Despite advances in diagnosis and treatment of cancer, cancer remains the second leading cause of death in the western world. It has been shown that cancer can be transmitted within or between cells (Dhillon et al., 2007). Cancer is a complicated genetic disease that is caused mostly by environmental factors such as food poisoning, water contaminants, chemicals, and air pollution (Anand *et al.*, 2008).

Until recently, standard treatments using endocrine therapy, radiation therapy, chemotherapy, and surgery have been the available options for cancer patients. This has improved survival in many types of solid tumour, but unfortunately, treatment-associated toxicity and emergence of resistance have been the primary cause of mortality and morbidity (Abou-Jawde et al., 2003). Therefore, a new and more effective therapy is urgently needed to enhance patient outcomes.

Rapid scientific progress in recent years has enhanced our knowledge of cancer biology which has led to the discovery of several novel targets, which results in treatments with better efficiency, high selectivity and low toxicity (Singh and Salnikova, 2015). Among these novel targets are protein kinases. Protein kinases are a phosphate transferase family that is essential for phosphorylation reactions and is considered to be one of the most significant groups of post-translational protein changes (Masterson et al., 2012). From a pharmacological viewpoint, small molecule inhibitors that are highly selective for protein kinases results in the inhibition of kinase functions at any step of cellular development (Dar and Shokat, 2011).

### 2.1 Protein kinases in cancer

Protein kinases (PKs) play an important role in controlling several biological processes in establishing the correct cell functionality, and constitute nearly 2% of human gene (Manning *et al.*, 2002). Protein phosphorylation is a key biochemical hallmark of metazoans mediated by transferring a $\gamma$-phosphate of ATP and covalently attaching it to serine, threonine ,tyrosine or histidine residues belonging to peptide or proteins (Hunter, 2012) (**Figure 2.1**). About a third of all proteins in human cells are phosphorylated by

protein kinase (Cohen, 2002b) .A significant change on the structure of the substrate protein occurs upon phosphorylation by protein kinases (Johnson and Lewis, 2001; Kuriyan and Eisenberg, 2007). This phosphorylation consequentially results in cell proliferation, migration and survival (Tarrant and Cole, 2009). Hence, Protein kinases are considered as key regulators of cell biology that are monitoring a number of signaling pathways which are vital for cell growth and survival. However, the overexpression of these kinases have been implicated in the initiation, promotion, progression as well as the reoccurrence of cancer and other diseases such as diabetes, vascular disease, inflammatory, and neurological diseases(Kang, 2014).

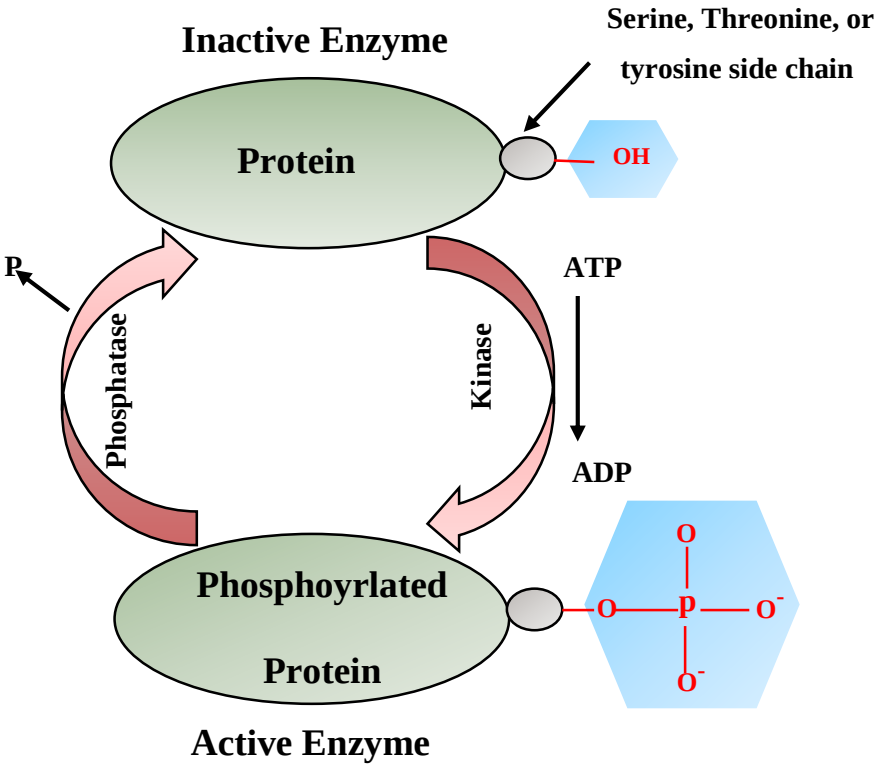


**Figure 2.1:** Protein phosphorylation pathways (Image prepared by author).

This makes the inhibition or the modulation of protein kinases activity an attractive target in the treatment of several diseases especially cancer. Nearly 45 protein kinase inhibitors have been approved by US FDA, and thousands of clinical studies targeting kinases are ongoing(Kornev and Taylor, 2015; Wu, Nielsen and Clausen, 2015) **(Figure 2.2)**.

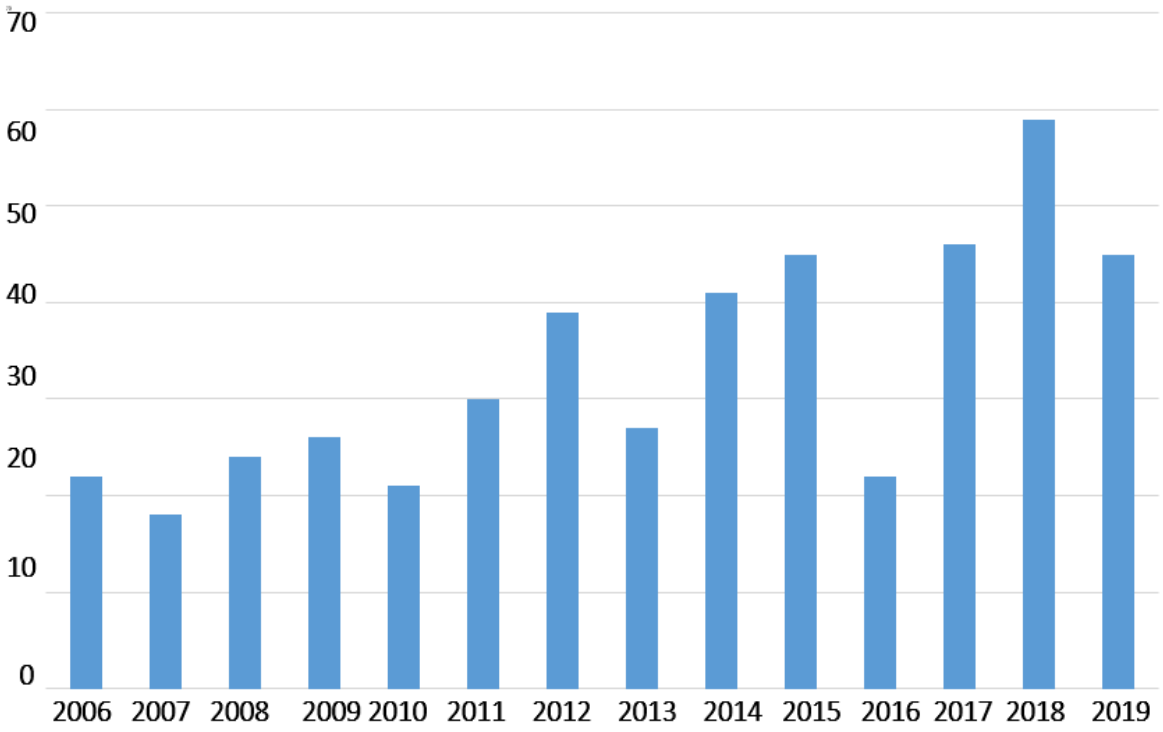


**Figure 2.2:** FDA approved protein kinase inhibitors (Image prepared by author).

### 2.2 Classification of protein kinases

The human genome encodes 518 kinases from which about 90 are tyrosine kinases (Manning et al., 2002). The protein kinase family is divided into two types: cytoplasmic tyrosine kinases (CTKs), and transmembrane receptor tyrosine kinases (RTKs) which are further grouped into subfamilies based on protein sequence homology. The cytoplasmic tyrosine kinase (CTK) consist of 34 known members , all containing non-catalytic domains and a catalytic kinase domain (Robinson, Wu and Lin, 2000) **(Figure 2.3)**.

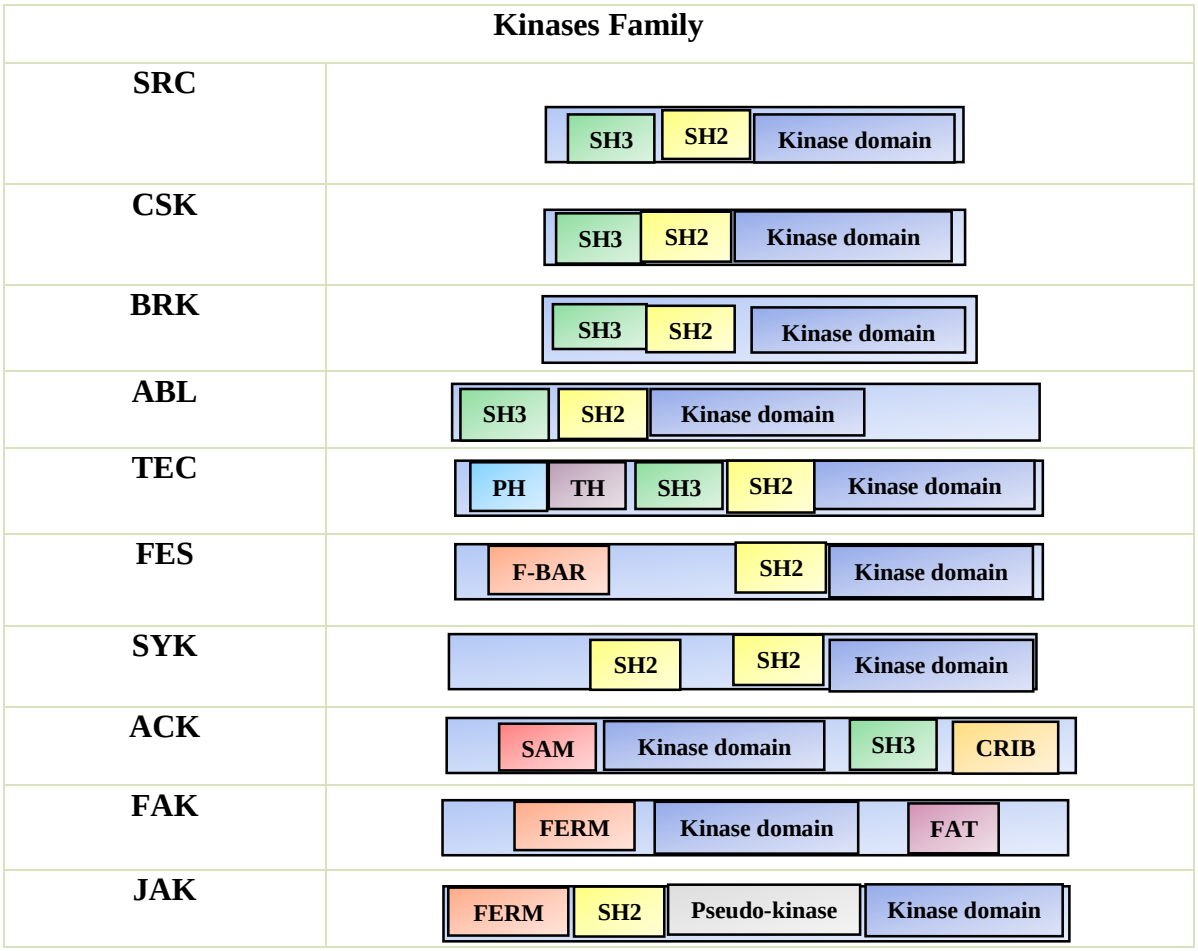


**Figure 2.3:** Structural organization of cytoplasmic tyrosine kinases (Image prepared by author).

Non-catalytic domain names are the following. **SH2/SH3**: Src-homology; **PH**: Pleckstrin homology; **TH**: Tec-homology; **F-BAR**: Bin-Amphiphysin-Rvs; **SAM**: Sterile-$\alpha$-motif; **CRIB**: Cdc42/Rac-interactive-binding-motif; **FERM**: protein-ezrin-radixin-moesin; **FAT**: focal adhesion- targeting.

### *2.2.1 Non-catalytic domain*

Non catalytic domain is of interest because of its high diversity as well as its significant role in cellular localization (Kung and Jura, 2016). For instance, non-catalytic domains such as SH2 which binds phospho-tyrosines allows spatial regulation and specific binding of CTKS to tyrosine-phosphrylated target proteins (Neet and Hunter, 1996). SH3 domains also play an important role in cellular substrate recognition, protein regulation and

improved SH2-dependent phosphorylation (Pellicena and Miller, 2001). Other non-catalytic domains such as SAM, and CRIB are implicated in protein-protein interaction complexes. For example, the CRIB domain in ACK kinase plays an important role in its interaction with the activated form of Cdc42 GTPase to promote cell survival and multiplication (Kato-Stankiewicz et al., 2001). While, PH and FERM domains play a critical role on the localization of the membrane through binding to phospholipids which is significant for protein kinase activation pathways (Leonard and Hurley, 2011). Vihinen et al. has shown, the location of plasma membrane in Bruton tyrosine kinase (Btk) protein is an important step in B-cell activation, and the mutation of its PH domain can lead to X-linked agammaglobulinemia (XLA) (Vihinen et al., 1994).

### *2.2.2 Kinase domain*

Kinase domain is a highly conserved protein kinase domain that spans about 300 amino acids and catalyzes the transfer of phosphates to the hydroxyl group of protein substrates (Kornev *et al.*, 2006). The structure of the kinase domain can subdivide into two domains N and C. The N domain consists of one prominent α helix and five stranded β-sheets. In contrast, the C domain is a larger and mostly helical segment (Cox, Radzio-Andzelm and Taylor, 1994). ATP interacted with the deep cleft located between these two domains just below the conserved glycine-rich loop. An optimal phosphate transfer requires a specific sequence of spatial arrangements of several residues located in the αC helix , the catalytic loop ,and the glycine rich loop (Huse and Kuriyan, 2002) (Figure 2.4).

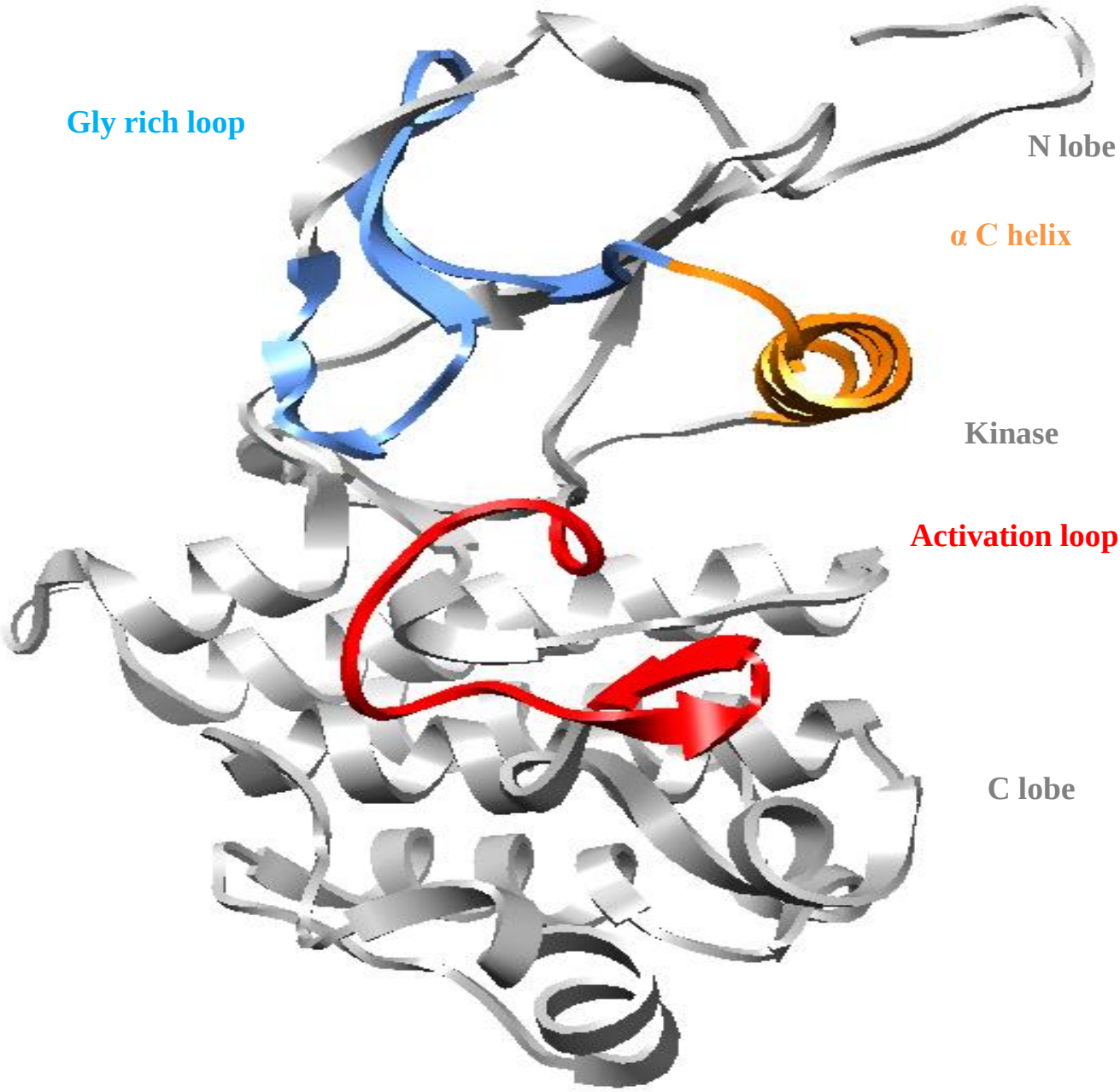


**Figure 2.4**: Cartoon representation of structural organization of the Abl kinase domain (PDB: 1IEP). N- and C- lobes are shown in gray. αC helix is shown in orange. The activation loop and the glycine rich loop are shown in red and blue respectively (Image prepared by author).

### *2.2.3 Role of cytoplasmic tyrosine kinases in cancer*

Cytoplasmic tyrosine kinase has a significant role in cellular signaling and deregulation by point mutation , translocation, deletions or duplications are usually combined by an over-activation that leads to cancer (Hubbard and Till, 2000; Blume-Jensen and Hunter, 2001). In 1978, Levinson et al discovered that there is a correlation between Src-family kinases (SFKs) and tumor progression of malignancy such as breast, colorectal, prostate or lung cancer (Zhang and Yu, 2012) .

## 2.3 c-Abelson (Abl) kinase: a prototypic cytoplasmic tyrosine kinase

### *2.3.1 The Abl kinase family*

c-Abl is a member of the cytoplasmic tyrosine kinase which is localized at several sites in the cell including nucleus, cytoplasm, mitochondria and endoplasmic reticulum (Wetzler *et al.*, 1993) . c-Abl is the prototype of a subfamily which includes two members : c-Abl (Abl1) and its paralogue Arg (Abl2,Abl related gene)(Sirvent, Benistant and Roche, 2008). Members of this family are highly conserved throughout the metazoans and ubiquitously expressed. Abl play a significant role in signaling pathways that is critical for cellular function such as adhesions, differentiation, division and stress response(Sirvent, Benistant and Roche, 2008).

## 2.4 Chronic myeloid leukemia and Bcr-Abl fusion protein

### *2.4.1 Chronic myeloid leukemia*

Deregulation of Abl activity by mutation are usually combined with diverse pathologies such as solid tumors, neurodegenerative diseases, and inflammatory disorders. (Khatri, Wang and Pendergast, 2016) The most common Abl- related diseases is the chronic myelogenous leukemia (CML) , a form of leukemia represented by the unregulated growth of myeloid cells in the bone marrow resulting in sufficient amounts of normal red blood cells, white blood cells, and platelets(Houshmand *et al.*, 2019) (Figure 2.5).

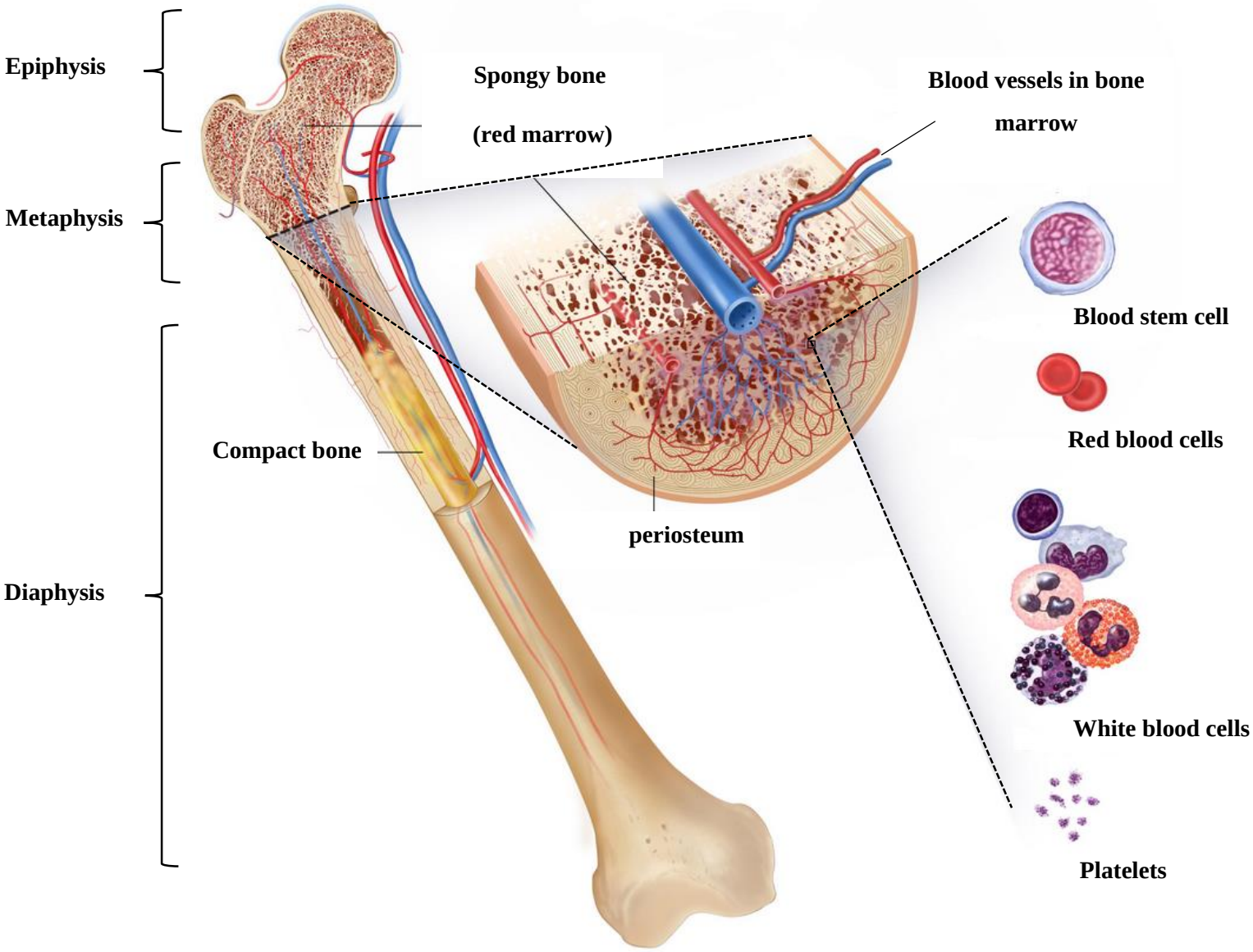


**Figure 2.5:** Effect of CML on bone marrow and blood components. (Image adapted from (Krause *et al.*, 2015).

CML is present in about 15-25% of all adult leukemia patients(Granatowicz *et al.*, 2015). The annual incidence rate of CML is 1 to 2 cases per 100 000 and can occur at any age, being most prominent in 60-65 year old (Baccarani *et al.*, 2012) (Figure 2.6).

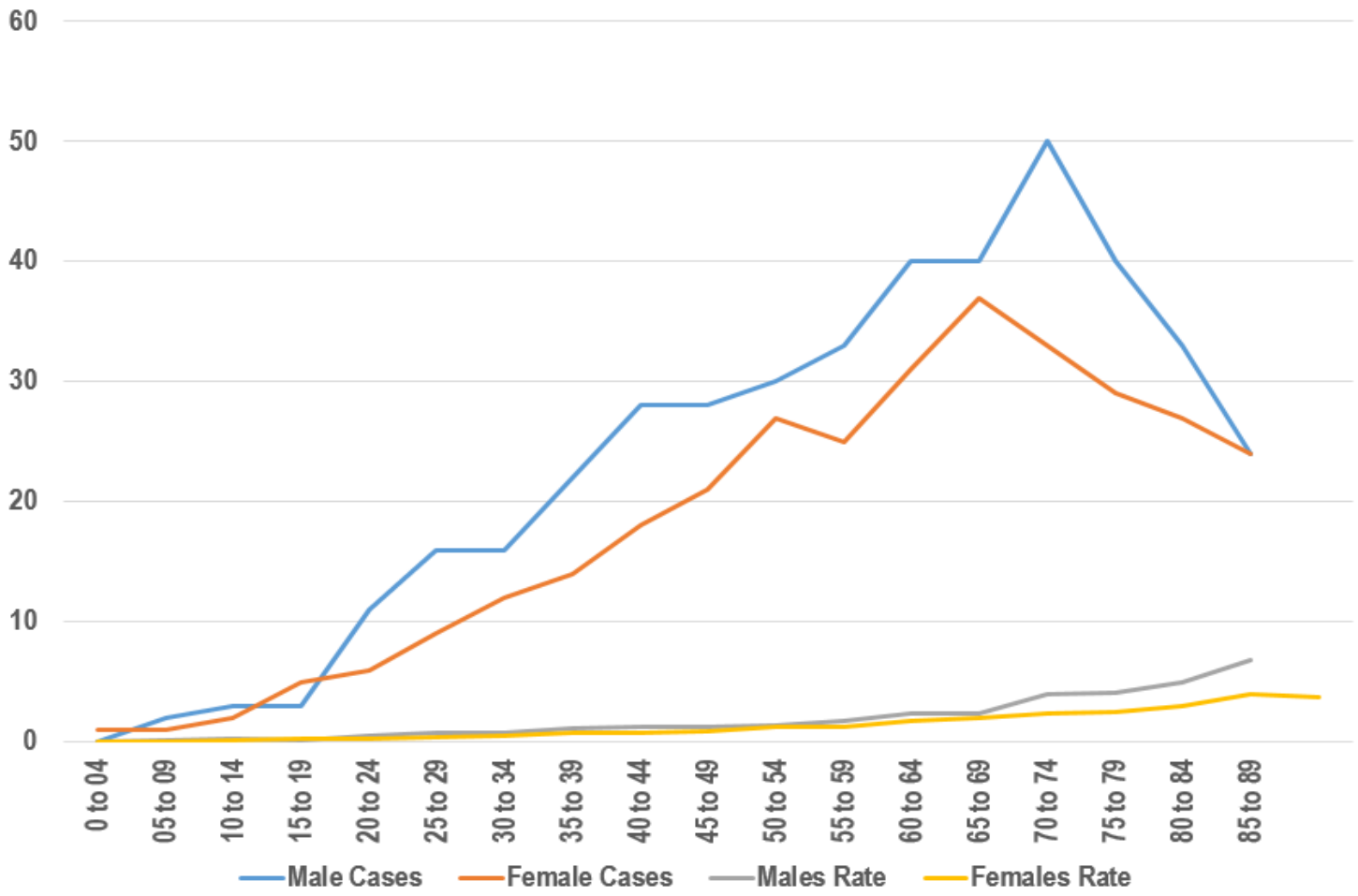


**Figure 2.6**: Incidence of Chronic Myeloid Leukemia, Average Number of New Cases per Year and Age-Specific Incidence Rates per 100,000 Population (Prepared by Author).

### *2.4.2 Bcr-Abl fusion gene*:

The expression of the fusion protein (Bcr-Abl) was formed by the conjugation between the Abl1 gene on chromosome 9 with the breakpoint cluster region gene (Bcr) on chromosome 22 generating ( Philadelphia chromosome (Ph)) (ROWLEY, 1973). The resulting fusion protein is an integral activated form of the Abl kinase (Bcr-Abl form) that enables unrestrained production of cancerous cells in blood (Wong and Witte, 2004) (Figure 2.7).

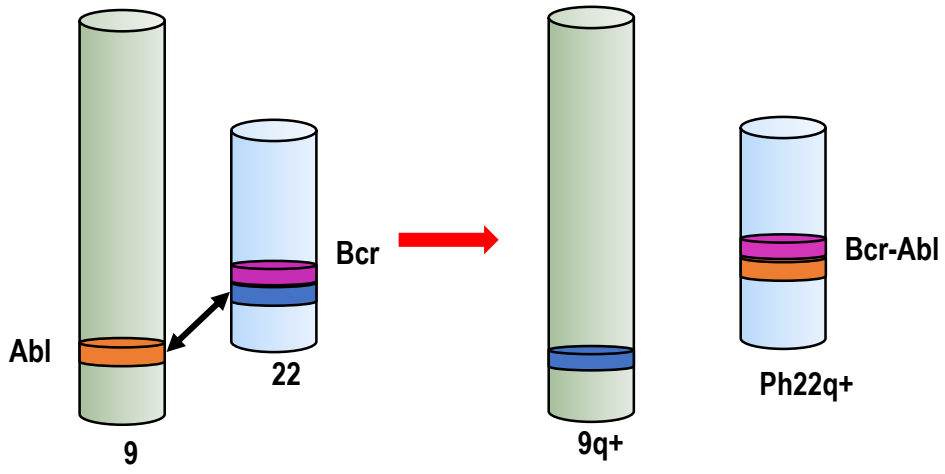


**Figure 2.7**: Chromosomal translocation that generates the Philadelphia chromosome and its Bcr-Abl fusion gene (Prepared by Author).

### *2.4.3 Bcr-Abl: driver of chronic myeloid leukemia*:

Bcr-Abl p210 is considered as one of the most common type for Bcr-Abl fusion. It contains all the c-Abl tyrosine kinase sequence except the N-terminal regions which is replaced by Bcr. Absence of N terminal (cap regions ) interferes with the myristoylation of the protein and inhabited the release of c-Abl tyrosine kinase from auto inhibition (McWhirter and Wang, 1991) .Abl1 gene can be subdivided into two different splicing transcripts: Abl1a, and Abl1b . The 1b splicing variant is myristoylated at the N-terminus (glycine 2) whereas the 1a variant is 19 amino acids shorter and are not myristoylated (Renshaw, Capozza and Wang, 1988) (Figure 2.8).

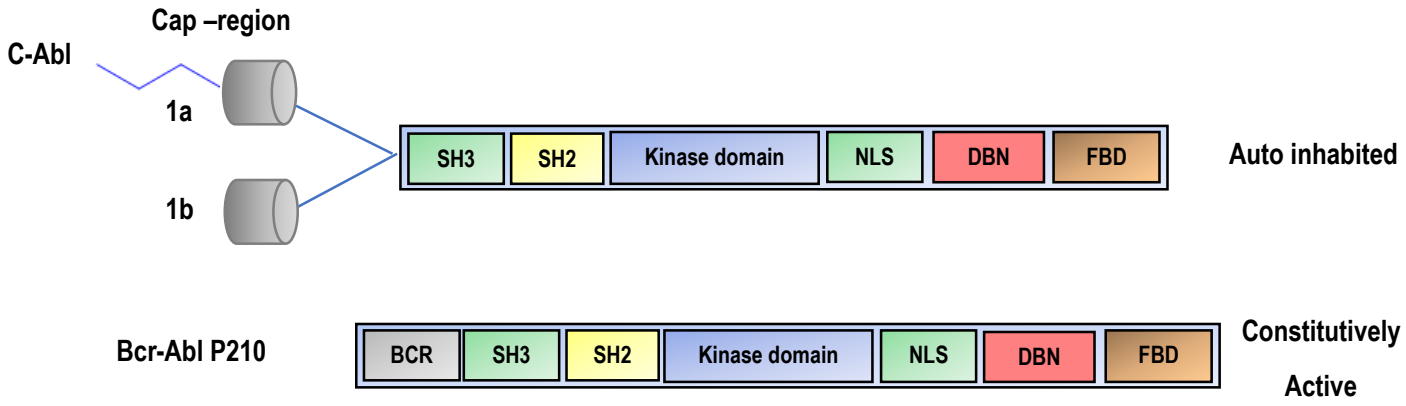


**Figure 2.8**: Structural organization of c-Abl and Bcr-Abl. On the top, Domain structures of Abl kinase and on the bottom, the oncogenic Bcr-Abl kinase. **NLS**: Nuclear localization signal, **DBN**: DNA binding domain, **FBD**: F-actin binding domain (Prepared by Author).

c-Abl tyrosine kinase is implicated in a diverse range of cellular activities ranging from the regulation of cell growth, survival, oxidative stress and DNA damage response to actin dynamics and cell migration (Van Etten, 1999). The two variants of c-Abl have a modular organization like that Src family members. It is characterized by a core tyrosine kinase domain which is preceded by SH2 and SH3 domains. c-Abl is exclusively having last exon region along carboxy-terminal extension that is containing a nuclear localization signals (NLS) that permit the protein to shuttle between cytoplasm and nucleus (Taagepera *et al.*, 1998) ,and involves in the interaction with F-actin (Hantschel *et al.*, 2005) . It is also having a proline -rich motifs that function as binding sites for SH3 domains of adaptor proteins.(Hantschel *et al.*, 2005) .

### *2.4.4 Auto-inhibition mechanism:*

The tyrosine kinase activity of c-abl is very tightly controlled and c-Abl is mostly inactive in cells (Vihinen *et al.*, 1996; Van Etten, 1999). Structural and biochemical studies have shown a multiple auto inhibitory mechanisms. The auto inhibition relies on a complex set of intramolecular interactions that preserve the kinase in a closed and inactive conformation. The myristoyl group in the cap region has an important role in the

autoinhibition of c-Abl 1b (Hantschel *et al.*, 2003). The SH2 domain is formed by a central antiparallel sheet flanked by a α-helices on each side. The mystrate can interact deeply into the hydrophobic pocket in the kinase C-lobe therefore forcing the SH2 and SH3 domain to dock against the kinase lobes and keeping the kinase inactive (Pluk, Dorey and Superti-Furga, 2002; Nagar *et al.*, 2003) (Figure 2.9) .

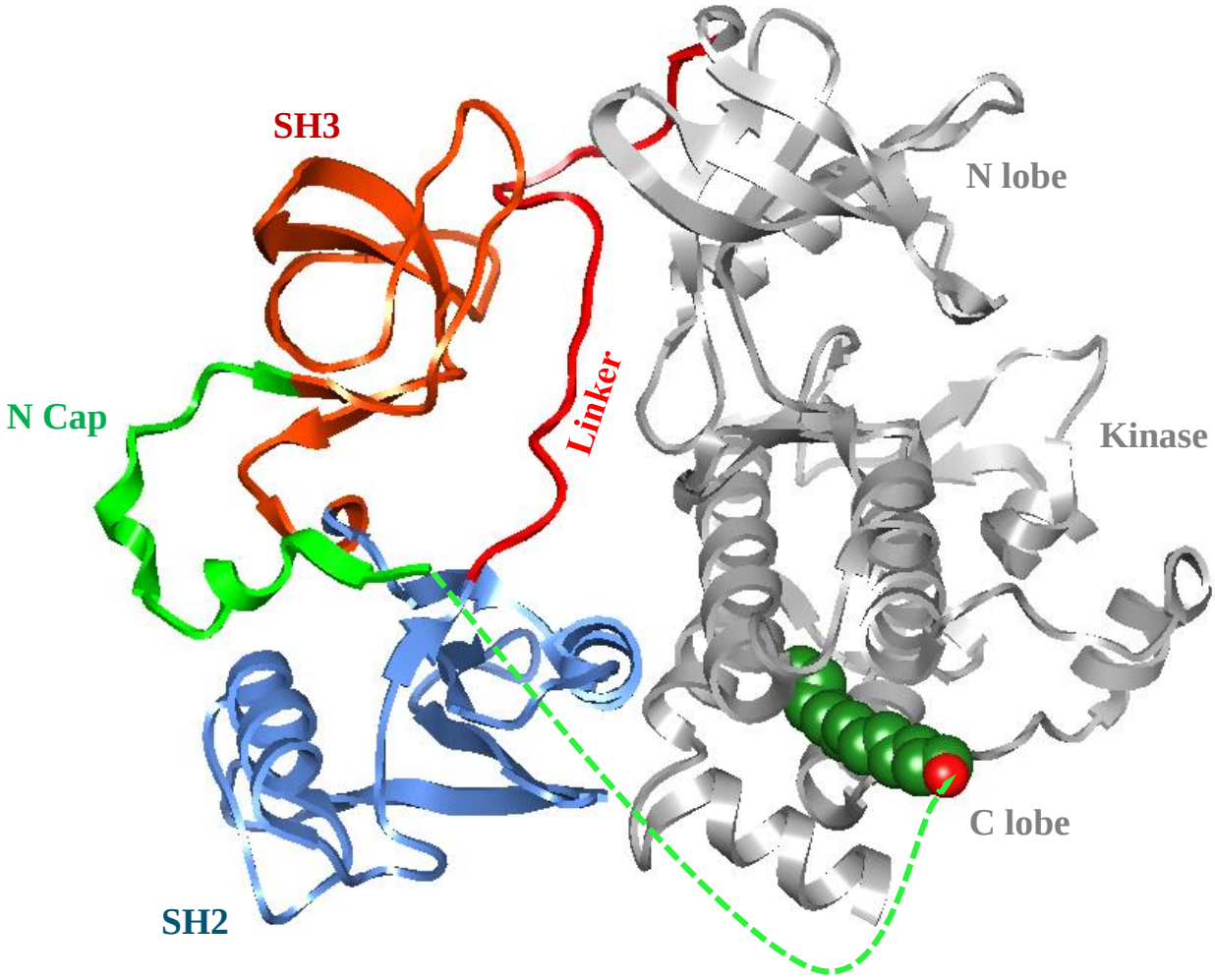


**Figure 2.9** : The 3-D crystal structure of the Bcr-Abl protein (PDB code: 2FO0(Nagar *et al.*, 2006)). The N-cap, SH3, SH2 and kinase domains are shown in green, orange, blue and gray, respectively. The SH2-kinase linker is depicted in red, and the green dashed line represented the importance of N cap to the stabilization of the downregulated conformation of the kinase upon myristate binding (Image prepared by author).

## 2.5 Inhibition of Bcr-Abl

Many of the drugs that are present in market bind to the orthostatic pocket at the ATP binding pocket in Abl kinase (Bcr-Abl). Based on their molecular mechanism of activity, the Bcr-Abl orthostatic inhibitor can be divided into two class, type 1, and type 2 . First generation inhibitors interact with the active conformation of the kinase, where the catalytic important residues are in the optimal position raised the catalysis, i.e. the DFG in the *in conformation*, and the Activation -loop is opened. On the other side, the type 2 inhibitors bind to the in active conformation of the Bcr-Abl. i.e the DFG in the *out* conformation, and the Activation -loop is closed or open conformation(Reddy and Aggarwal, 2012) (Figure 2.10).

### *2.5.1 Targeted therapy and development of resistances*

Imatinib (STI-571 ,or CGP-57148) is the first Bcr-Abl inhibitor which was approved in the year 2001 as the drug of choice for the treatment of CML (Zuccotto *et al.*, 2010). Imatinib is a type 2 inhibitors with $IC_{50}$ of 10 nM (Zimmermann *et al.*, 1997) . Nevertheless, the extended mutation across the Abl protein, makes this drug poorly or incompletely active against certain enzymes. The most common mutation are H395P/R, G250E , M351T,F359V, , M244V, F317L, Y253H/F, Q252H, E355G, E255K/V and gatekeeper T315I. The second generation of Bcr-Abl inhibitors such as Nilotinib and Dasatinib have been approved for the treatment of imatinib –resistant patients with the exception of the gate keeper T315I. (Figure 2.11). Nilotinib (Tasigna, AMN107; Novartis) is a type 2 inhibitors with $IC_{50}$ of 38nM.In 2012, FDA has approved Ponatinib as a third generation ATP competitive tyrosine kinase inhibitor that is efficiently targets for both Bcr-Abl wild type and the Bcr-Abl T315I mutation with $IC_{50}$=0.37nM,2.0nM respectively (Figure 2.10) (O'Hare *et al.*, 2009).

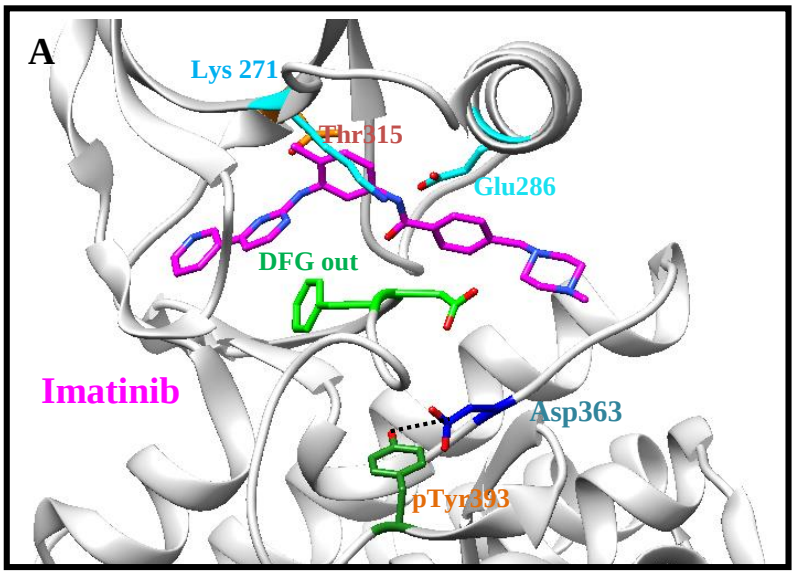


**In active Kinase Conformation**

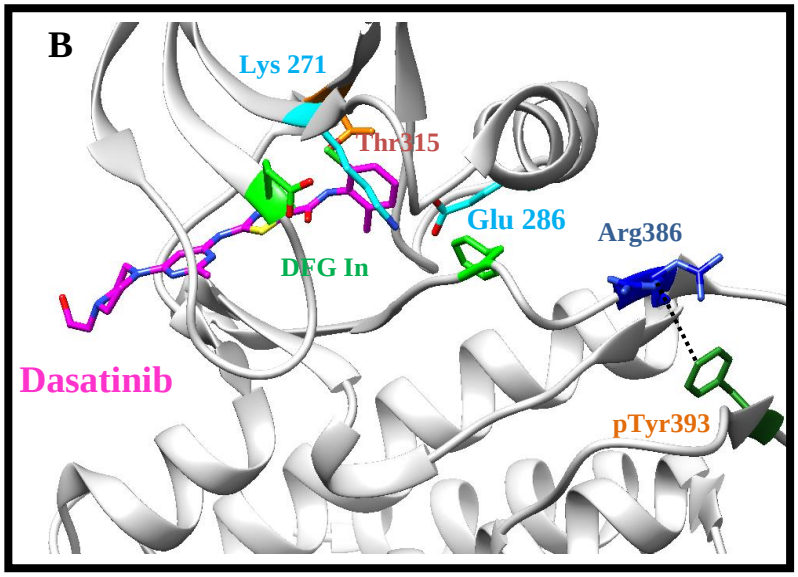


**Active kinase conformation**

**Figure 2.10:** (A) The crystal structure of the Abl kinase domain bound to imatinib (PDB: 1IEP) (Nagar *et al.*, 2002) shows the important features of the inactive configuration of the active site. The ionic interaction between lys 271 and Glu 286 is maintained while the DFG (Asp-Phe-Gly) motif is flipped out. The activation loop is folded towards the active site and Tyr393 forms a hydrogen bond with the preserved Asp363 (catalytic aspartate). (B)

Abl kinase domain crystal structure bind to dasatinib (PDB: 2GQG, (Tokarski *et al.*, 2006) , shows significant characteristics of active kinase conformation. To coordinate the ATP phosphate group, the ionic interaction between Lys271 and Glu286 is essential. The phosphorylated Tyr393 forms an Arg386 hydrogen bond and helps stabilize the active conformation (Image prepared by author) .

Allosteric binding inhibitors have also been found to inhibit the Abl activation, for instance , DCC-2036 is switch pocket inhibitor that allosterically binds to the Arg386/Glu282 residues in the switch regions and hinder Abl from adopting an active conformation(Chan *et al.*, 2011). DCC-2036 has been found to overcome most of imatinib mutation including T315I mutation. DCC-2036 is now under Phase I clinical trials with T315I mutation CML patients, with the study currently awaiting results (Figure 2.11)(Chan *et al.*, 2011).

Other examples include GNF-2 and GNF-5 which were able to inhibit Bcr-Abl growth with the exception of T315I mutation (Webersinke, 2016). Similarly, ABL001 is allosterically bound to Bcr-Abl with $IC_{50}$ = 1-12nM (Schoepfer *et al.*, 2018), recent studies have shown that monotherapy using ABL001 which led to tumor regression in mice xenografted with KCL22 CML cell line. Unfortunately, the tumors eventually recurred (Figure 2.11) (Wylie *et al.*, 2014, 2017; Eadie *et al.*, 2015).

However, dual targeting of GNF-2 with Nilotinib or ABL001 with Nilotinib have shown a highly synergistic effect compared to mono therapeutic treatment, being able to overcome gatekeeper T315I mutation. Therefore dual targeting of both ATP binding r, and allosteric inhibitors represents an innovative way to overcome mono therapeutic resistance (Iacob *et al.*, 2011) (Wylie *et al.*, 2017). This may be attributed to the effect of GNF5 when bound to the myristate pocket stabilizing the in active form of the T315I mutant, and the new state enable confirmation where I 315 no longer limits access of Nilotinib to the hydrophobic binding pocket . In this case, the allosteric targeting of Abl can cause dynamic perturbations to the ATP binding site residues and this explains the mechanism by which synergistic interaction occurs (Zhang *et al.*, 2010) .

Recently, Mono bodies shows a highly allosterically inhibition to Bcr-Abl by interfering with the SH2-Kinase domain complex. This induces the apoptosis in CML cell lines and primary human CML cells.(Hantschel, Grebien and Superti-Furga, 2012).

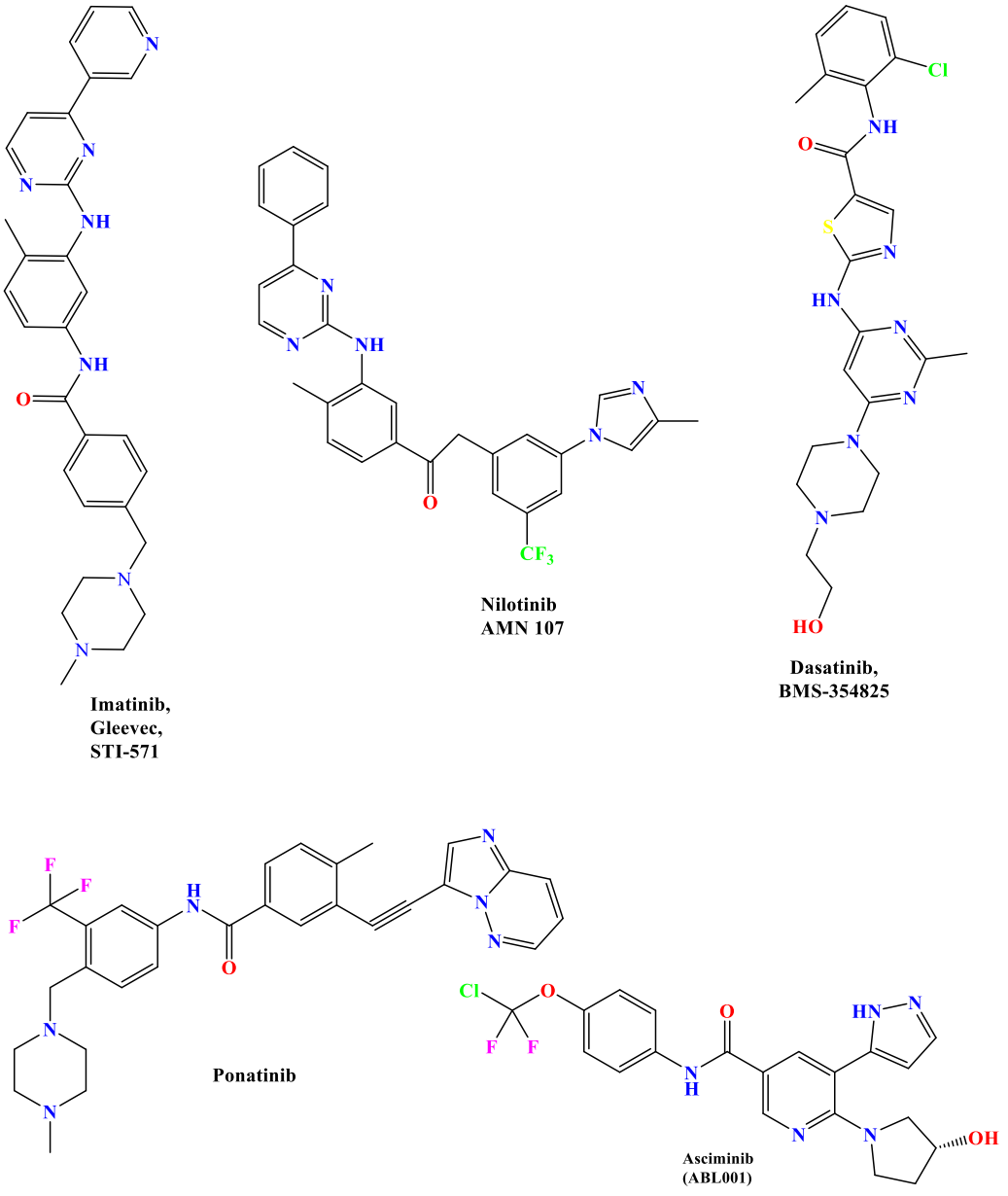


**Figure 2.11**: The 2D structures of some kinase inhibitors.

**2.6 Clinical Developments of Protein kinase inhibitors:**

Protein kinase inhibitors are rapidly growing in drug discovery, as protein kinases are considered as the second most significant group of drug targets after G-protein-coupled receptors. They account for about 20–30% of the drug discovery program of many companies (Vlahovic and Crawford, 2003)(Cohen, 2002a)**.** Recently, FDA has approved 49 compounds which have been identified as protein kinase inhibitors (Table 1) . Despite these encouraging results, response to these protein kinase inhibitors are surrounded by the development of resistance, toxicity ,and efficiency which remains challengeable (Fabbro, Cowan-Jacob and Moebitz, 2015) .Furthermore, Accomplishing the selectively of the kinase inhibitors for particular protein kinases remain a significant challenge(DAVIES et al., 2000; Noble, Endicott and Johnson, 2004). Computational methods can have a key effect on Protein kinase inhibitors design and will stand to be an important feature for the development of these inhibitors (Ferrè, Palmeri and Helmer-Citterich, 2014), so that , many researcher have been motivated to overcome various limitation of kinase inhibition , particularly evading the treatment-related drug resistance .

**Table 2.1**: list of FDA-approved small molecule protein kinase inhibitors.

| Name | Structure | Target | Domain |
|---|---|---|---|
| **Abemaciclib** | 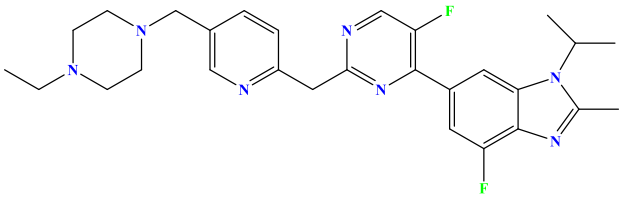 | **CDK4/6** | **Breast cancer** (Lu, 2015) |
| **Acalabrutinib** | 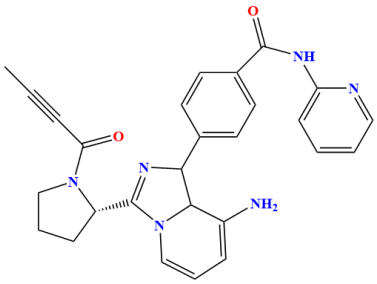 | **Bruton tyrosine kinase** | **Mantle cell lymphoma**(Markham and Dhillon, 2018)() |
| **Afatinib** | 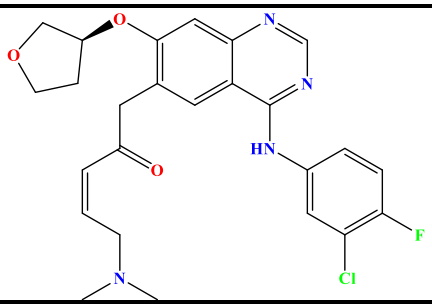 | **EGFR, ErbB2, ErbB4** | **NSCLC** (Minkovsky and Berezov, 2008) |
| **Alectinib** | 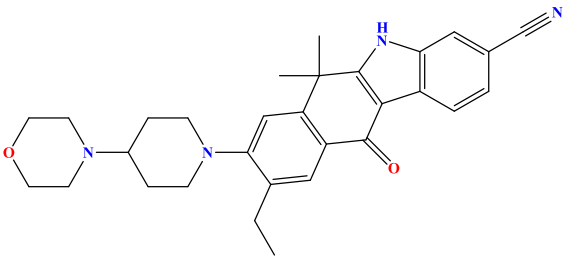 | **ALK , RET** | **Anaplastic lymphoma kinase** (McKeage, 2015) |
| **Baricitinib** | 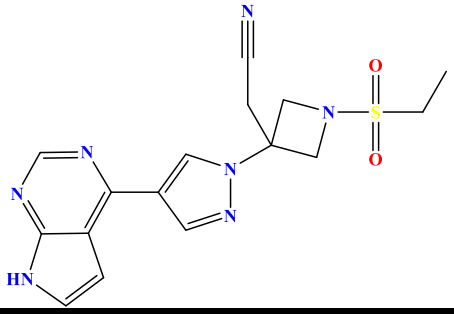 | **JAK1/2** | **Rheumatoid arthritis** (Richez *et al.*, 2017) |

| | | | |
|---|---|---|---|
| **Binimetinib** | 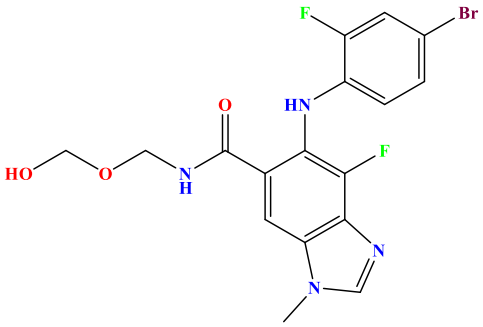 | **MEK1/2** | **Cancer** (Koelblinger, Dornbierer and Dummer, 2017) |
| **Bosutinib** | 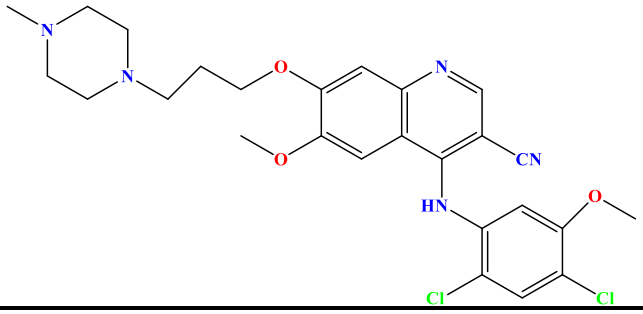 | **Bcr-Abl, Src, Lyn, Hck** | **CML**(Daud *et al.*, 2012) |
| **Brigatinib** | 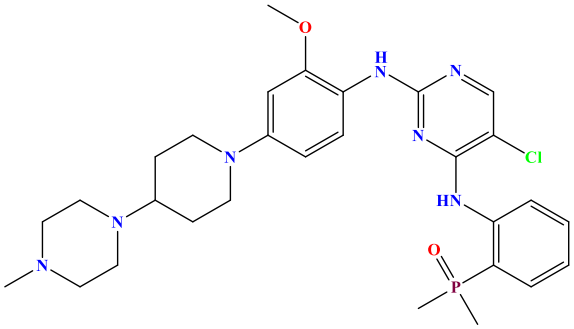 | **ALK, EGFR** | **Cancer** (Huang *et al.*, 2016) |
| **Cobozantinib** | 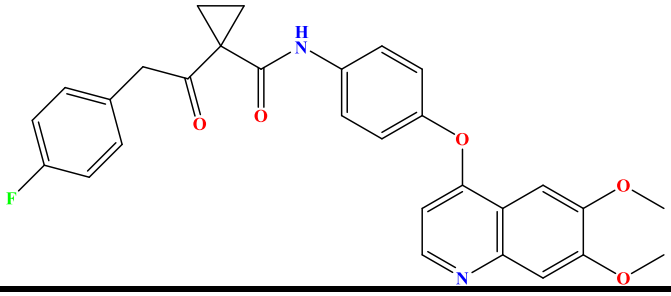 | **Met, VEGFR2, Axl** | **Cancer** (Choueiri *et al.*, 2015) |

| | | | |
|---|---|---|---|
| **Ceritinib** | 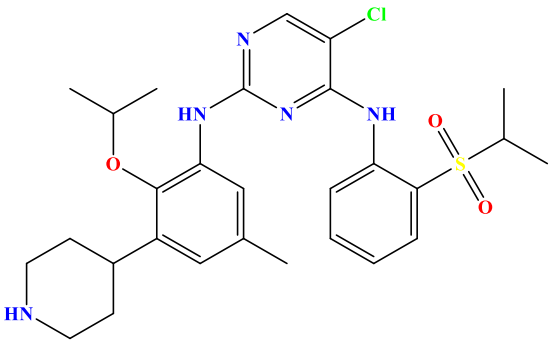 | **ALK** | **NSCLC** (Soria *et al.*, 2017) |
| **Dacomitinib** | 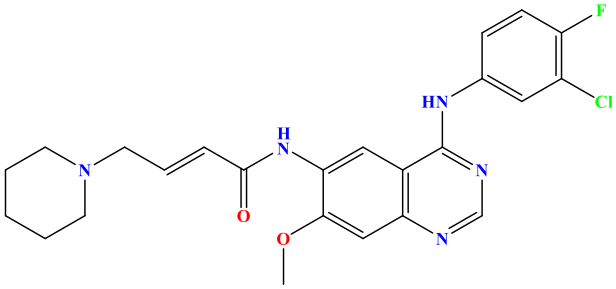 | **EGFR** | **NSCLC**(Shirley, 2018) |
| **Dasatinib** | 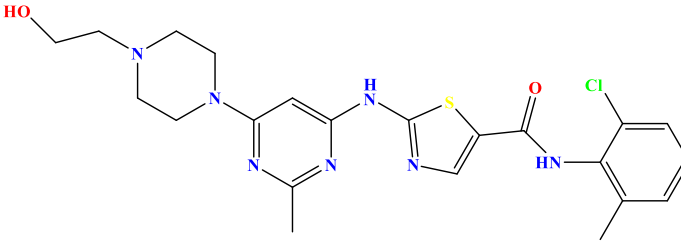 | **Bcr-Abl** | **CML**(Tokarski *et al.*, 2006) |
| **Encorafenib** | 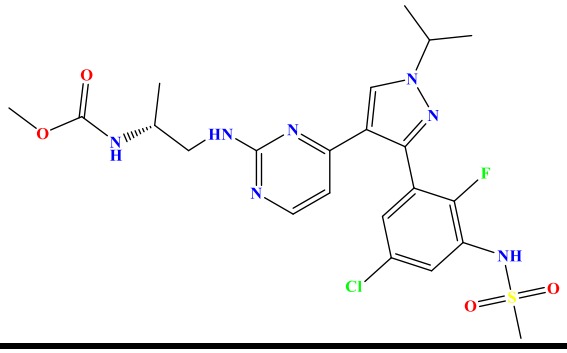 | **B-Raf$^{V600E/K}$** | **Cancer** (Koelblinger, Thuerigen and Dummer, 2018) |

| | | | |
|---|---|---|---|
| **Fostamatinib** | 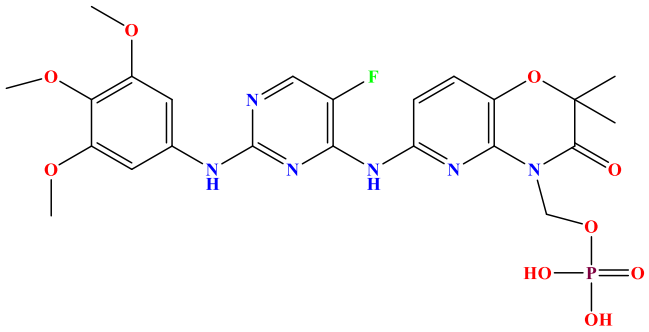 | **Spleen tyrosine kinase (syk)** | **Autoimmune disorders**(Braselmann *et al.*, 2006) |
| **Gilteritinib** | 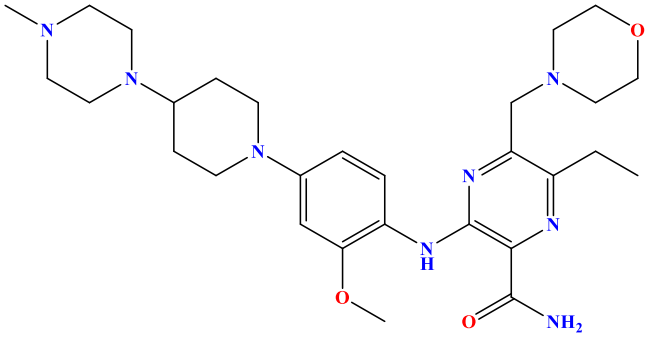 | **FLT3 Mutation** | **AML** (Perl *et al.*, 2017) |
| **Larotrectinib** | 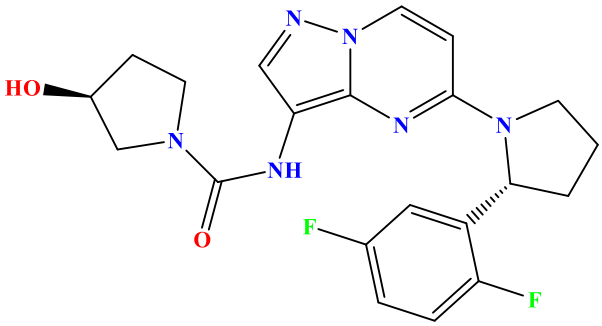 | **NTRK** | **Cancer** (Berger, Martens and Bochum, 2018) |
| **Lorlatinib** | 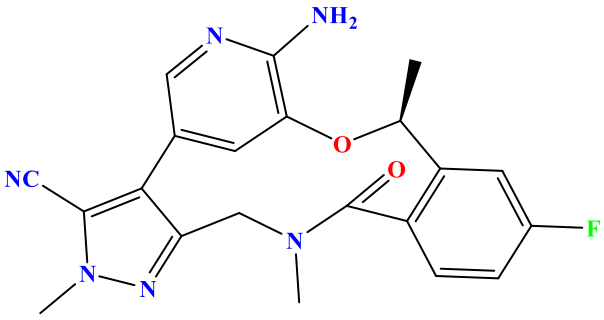 | **ALK** | **NSCLC** (Shaw *et al.*, 2017) |

| | | | |
|---|---|---|---|
| **Netarsudil** | 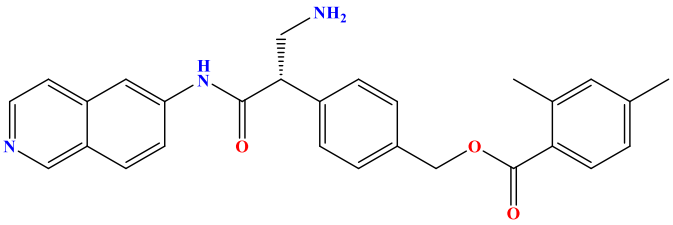 | **Rho kinase** | **Ocular hypertension** (Lin *et al.*, 2018) |
| **Imatinib** | 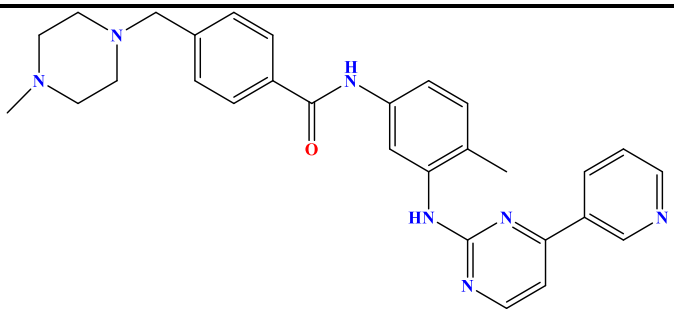 | **Bcr-Abl kinase** | CML (Capdeville *et al.*, 2002) |
| **Lenvatinib** | 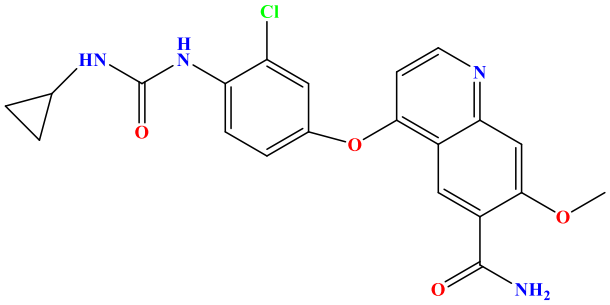 | **VEGFRs, FGFRs, PDGFR, Kit, RET** | **Cancer** (Matsui *et al.*, 2008) |
| **Ponatinib** | 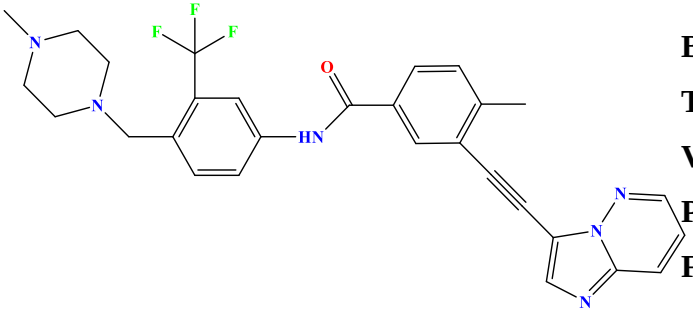 | **Bcr-Abl, T315I, VEGFR, PDGFR, FGFR** | **Cancer** (Huang *et al.*, 2010) |

| | | | |
|---|---|---|---|
| **Nilotinib** | 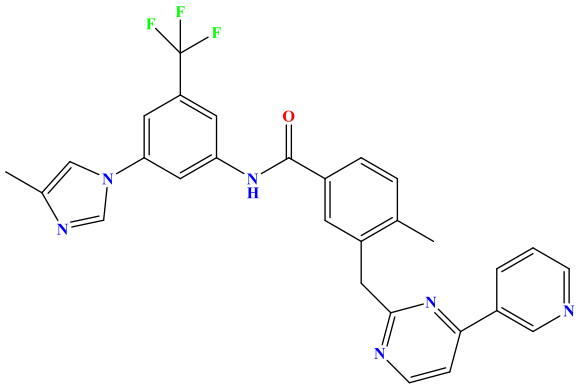 | **Bcr-Abl, PDGFR,** | **CML** (Golemovic *et al.*, 2005) |
| **Neratinib** | 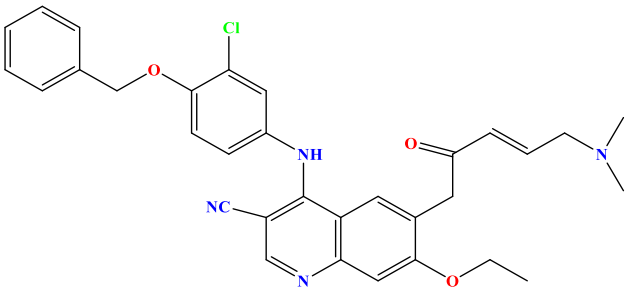 | **ErbB2/HER2** | **Cancer** (Gandhi *et al.*, 2017) |
| **Osimertinib** | 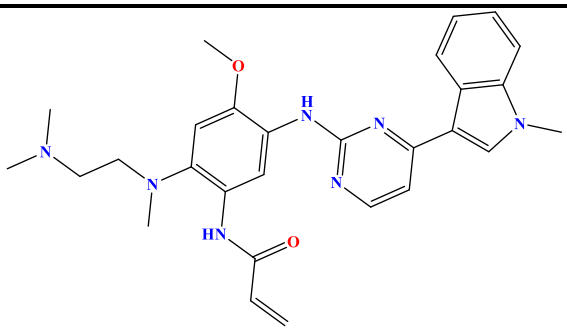 | **EGFR T970M** | **NSCLC** (Ayeni, Politi and Goldberg, 2015) |
| **Palbociclib** | 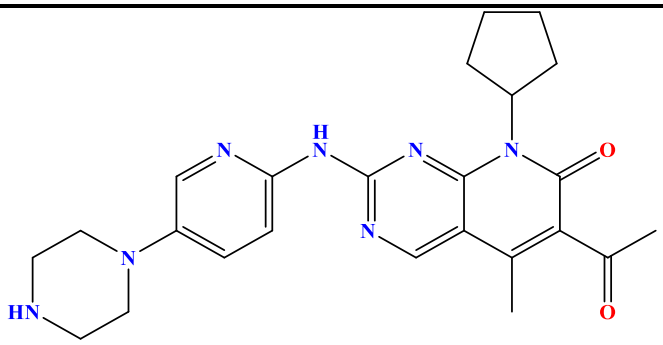 | **CDK4/6** | **Cancer** (Finn *et al.*, 2009) |

| | | | |
|---|---|---|---|
| **Pazopanib** | 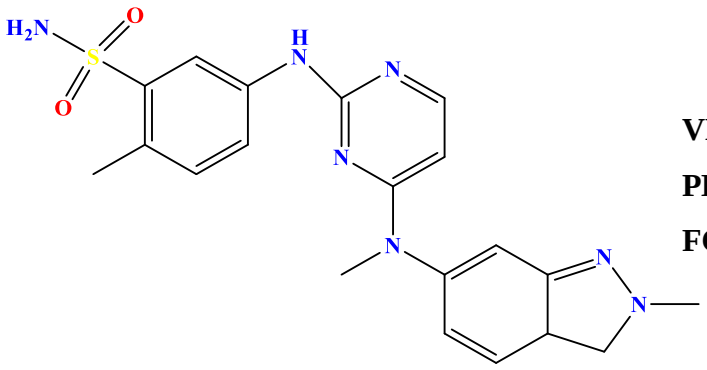 | **VEGFR, PDGFR, FGFR** | **Cancer** (Verheijen *et al.*, 2017) |
| **Ribociclib** | 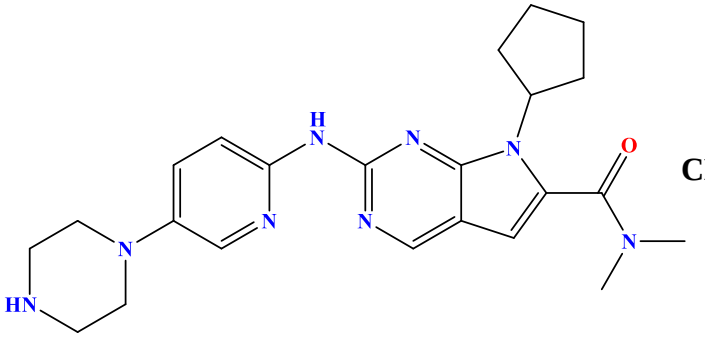 | **CDK4/6** | **Cancer**(Samson, 2014) |

## 2.7 References:


Abou-Jawde, R. *et al.* (2003) 'An overview of targeted treatments in cancer', *Clinical Therapeutics*. Elsevier, 25(8), pp. 2121–2137. doi: 10.1016/S0149-2918(03)80209-6.

Anand, P. *et al.* (2008) 'Cancer is a Preventable Disease that Requires Major Lifestyle Changes', *Pharmaceutical Research*, 25(9), pp. 2097–2116. doi: 10.1007/s11095-008-9661-9.

Ayeni, D., Politi, K. and Goldberg, S. B. (2015) 'Emerging Agents and New Mutations in EGFR-Mutant Lung Cancer', *Clinical Cancer Research*, 21(17), pp. 3818–3820. doi: 10.1158/1078-0432.CCR-15-1211.

Baccarani, M. *et al.* (2012) 'Chronic myeloid leukemia: ESMO Clinical Practice Guidelines for diagnosis, treatment and follow-up', *Annals of Oncology*. Karger, Basel, 23(suppl 7), pp. 72–77. doi: 10.1093/annonc/mds228.

Berger, S., Martens, U. M. and Bochum, S. (2018) 'Larotrectinib (LOXO-101)', in *Recent results in cancer research. Fortschritte der Krebsforschung. Progres dans les recherches sur le cancer*, pp. 141–151. doi: 10.1007/978-3-319-91442-8_10.

Blume-Jensen, P. and Hunter, T. (2001) 'Oncogenic kinase signalling.', *Nature*, 411(6835), pp. 355–365. doi: 10.1038/35077225.

Braselmann, S. *et al.* (2006) 'R406, an Orally Available Spleen Tyrosine Kinase Inhibitor Blocks Fc Receptor Signaling and Reduces Immune Complex-Mediated Inflammation', *Journal of Pharmacology and Experimental Therapeutics*, 319(3), pp. 998–1008. doi: 10.1124/jpet.106.109058.

Capdeville, R. *et al.* (2002) 'Glivec (STI571, imatinib), a rationally developed, targeted anticancer drug.', *Nature reviews. Drug discovery*, 1(7), pp. 493–502. doi: 10.1038/nrd839.

Chan, W. W. *et al.* (2011) 'Conformational control inhibition of the Bcr-Abl tyrosine kinase, including the gatekeeper T315I mutant, by the switch-control inhibitor DCC-2036.', *Cancer cell*, 19(4), pp. 556–68. doi: 10.1016/j.ccr.2011.03.003.

Choueiri, T. K. *et al.* (2015) 'Cabozantinib versus everolimus in advanced renal-cell carcinoma', *New England Journal of Medicine*. Mass Medical Soc, 373(19), pp. 1814–1823.

Cohen, P. (2002a) 'Protein kinases — the major drug targets of the twenty-first century?', *Nature Reviews Drug Discovery*. Nature Publishing Group, 1(4), pp. 309–315. doi: 10.1038/nrd773.

Cohen, P. (2002b) 'The origins of protein phosphorylation.', *Nature cell biology*, 4(5), pp. E127-30. doi: 10.1038/ncb0502-e127.

Cox, S., Radzio-Andzelm, E. and Taylor, S. S. (1994) 'Domain movements in protein kinases', *Current Opinion in Structural Biology*. Elsevier Current Trends, 4(6), pp. 893–901. doi: 10.1016/0959-440X(94)90272-0.

Dar, A. C. and Shokat, K. M. (2011) 'The Evolution of Protein Kinase Inhibitors from Antagonists to Agonists of Cellular Signaling', *Annual Review of Biochemistry*, 80(1), pp. 769–795. doi: 10.1146/annurev-biochem-090308-173656.

Daud, A. I. *et al.* (2012) 'Phase I study of bosutinib, a src/abl tyrosine kinase inhibitor, administered to patients with advanced solid tumors', *Clinical Cancer Research*. AACR, 18(4), pp. 1092–1100.

DAVIES, S. P. *et al.* (2000) 'Specificity and mechanism of action of some commonly used protein kinase inhibitors', *Biochemical Journal*, 351(1), p. 95. doi: 10.1042/0264-6021:3510095.

Dhillon, A. S. *et al.* (2007) 'MAP kinase signalling pathways in cancer.', *Oncogene*, 26(22), pp. 3279–90. doi: 10.1038/sj.onc.1210421.

Eadie, L. N. *et al.* (2015) 'The Allosteric Inhibitor ABL001 Is Susceptible to Resistance in Vitro Mediated By Overexpression of the Drug Efflux Transporters ABCB1 and ABCG2', *Blood*, 126(23), pp. 4841–4841. Available at: http://www.bloodjournal.org/content/126/23/4841?sso-checked=true (Accessed: 23 February 2018).

Van Etten, R. A. (1999) 'Cycling, stressed-out and nervous: cellular functions of c-Abl.',

*Trends in cell biology*, 9(5), pp. 179–86. Available at: http://www.ncbi.nlm.nih.gov/pubmed/10322452 (Accessed: 4 April 2018).

Fabbro, D., Cowan-Jacob, S. W. and Moebitz, H. (2015) 'Ten things you should know about protein kinases: IUPHAR Review 14', *British Journal of Pharmacology*, 172(11), pp. 2675–2700. doi: 10.1111/bph.13096.

Ferrè, F., Palmeri, A. and Helmer-Citterich, M. (2014) 'Computational methods for analysis and inference of kinase/inhibitor relationships.', *Frontiers in genetics*. Frontiers Media SA, 5, p. 196. doi: 10.3389/fgene.2014.00196.

Finn, R. S. *et al.* (2009) 'PD 0332991, a selective cyclin D kinase 4/6 inhibitor, preferentially inhibits proliferation of luminal estrogen receptor-positive human breast cancer cell lines in vitro', *Breast Cancer Research*, 11(5), p. R77. doi: 10.1186/bcr2419.

Gandhi, L. *et al.* (2017) 'MA04.02 Neratinib ± Temsirolimus in HER2-Mutant Lung Cancers: An International, Randomized Phase II Study', *Journal of Thoracic Oncology*. Elsevier, 12(1), pp. S358–S359. doi: 10.1016/J.JTHO.2016.11.398.

Golemovic, M. *et al.* (2005) 'AMN107, a novel aminopyrimidine inhibitor of Bcr-Abl, has in vitro activity against imatinib-resistant chronic myeloid leukemia.', *Clinical cancer research : an official journal of the American Association for Cancer Research*. American Association for Cancer Research, 11(13), pp. 4941–7. doi: 10.1158/1078-0432.CCR-04-2601.

Granatowicz, A. *et al.* (2015) 'An Overview and Update of Chronic Myeloid Leukemia for Primary Care Physicians.', *Korean journal of family medicine*. Korean Academy of Family Medicine, 36(5), pp. 197–202. doi: 10.4082/kjfm.2015.36.5.197.

Hantschel, O. *et al.* (2003) 'A myristoyl/phosphotyrosine switch regulates c-Abl.', *Cell*, 112(6), pp. 845–57. Available at: http://www.ncbi.nlm.nih.gov/pubmed/12654250 (Accessed: 12 February 2018).

Hantschel, O. *et al.* (2005) 'Structural Basis for the Cytoskeletal Association of Bcr-Abl/c-Abl', *Molecular Cell*, 19(4), pp. 461–473. doi: 10.1016/j.molcel.2005.06.030.

Hantschel, O., Grebien, F. and Superti-Furga, G. (2012) 'The growing arsenal of ATP-

competitive and allosteric inhibitors of BCR-ABL.', *Cancer research*, 72(19), pp. 4890–5. doi: 10.1158/0008-5472.CAN-12-1276.

Houshmand, M. *et al.* (2019) 'Chronic myeloid leukemia stem cells', *Leukemia*. Nature Publishing Group, 33(7), pp. 1543–1556. doi: 10.1038/s41375-019-0490-0.

Huang, W.-S. *et al.* (2010) 'Discovery of 3-[2-(imidazo[1,2-b]pyridazin-3-yl)ethynyl]-4-methyl-N-{4-[(4-methylpiperazin-1-yl)methyl]-3-(trifluoromethyl)phenyl}benzamide (AP24534), a potent, orally active pan-inhibitor of breakpoint cluster region-abelson (BCR-ABL) kinase including the T315I gatekeeper mutant.', *Journal of medicinal chemistry*, 53(12), pp. 4701–19. doi: 10.1021/jm100395q.

Huang, W.-S. *et al.* (2016) 'Discovery of brigatinib (AP26113), a phosphine oxide-containing, potent, orally active inhibitor of anaplastic lymphoma kinase', *Journal of medicinal chemistry*. ACS Publications, 59(10), pp. 4948–4964.

Hubbard, S. R., and Till, J. H. (2000) 'Protein Tyrosine Kinase Structure and Function', *Annual Review of Biochemistry*, 69(1), pp. 373–398. doi: 10.1146/annurev.biochem.69.1.373.

Hunter, T. (2012) 'Why nature chose phosphate to modify proteins.', *Philosophical transactions of the Royal Society of London. Series B, Biological sciences*. The Royal Society, 367(1602), pp. 2513–6. doi: 10.1098/rstb.2012.0013.

Huse, M. and Kuriyan, J. (2002) 'The Conformational Plasticity of Protein Kinases', *Cell*. Cell Press, 109(3), pp. 275–282. doi: 10.1016/S0092-8674(02)00741-9.

Iacob, R. E. *et al.* (2011) 'Allosteric interactions between the myristate- and ATP-site of the Abl kinase.', *PloS one*. Edited by F. Rodrigues-Lima, 6(1), p. e15929. doi: 10.1371/journal.pone.0015929.

Johnson, L. N. and Lewis, R. J. (2001) 'Structural Basis for Control by Phosphorylation', *Chemical Reviews*, 101(8), pp. 2209–2242. doi: 10.1021/cr000225s.

Kang, J.-H. (2014) 'Protein Kinase C (PKC) Isozymes and Cancer', *New Journal of Science*. Hindawi, 2014, pp. 1–36. doi: 10.1155/2014/231418.

Kato-Stankiewicz, J. *et al.* (2001) 'Epidermal Growth Factor Stimulation of the ACK1/Dbl Pathway in a Cdc42 and Grb2-Dependent Manner', *Biochemical and Biophysical Research Communications*. Academic Press, 284(2), pp. 470–477. doi: 10.1006/BBRC.2001.5004.

Khatri, A., Wang, J. and Pendergast, A. M. (2016) 'Multifunctional Abl kinases in health and disease.', *Journal of cell science*, 129(1), pp. 9–16. doi: 10.1242/jcs.175521.

*Kisqali - FDA prescribing information, side effects and uses* (no date). Available at: https://www.drugs.com/pro/kisqali.html (Accessed: 1 August 2019).

Koelblinger, P., Dornbierer, J. and Dummer, R. (2017) 'A review of binimetinib for the treatment of mutant cutaneous melanoma', *Future Oncology*, 13(20), pp. 1755–1766. doi: 10.2217/fon-2017-0170.

Koelblinger, P., Thuerigen, O. and Dummer, R. (2018) 'Development of encorafenib for BRAF-mutated advanced melanoma', *Current Opinion in Oncology*, 30(2), p. 1. doi: 10.1097/CCO.0000000000000426.

Kornev, A. P. *et al.* (2006) 'Surface comparison of active and inactive protein kinases identifies a conserved activation mechanism.', *Proceedings of the National Academy of Sciences of the United States of America*. National Academy of Sciences, 103(47), pp. 17783–8. doi: 10.1073/pnas.0607656103.

Kornev, A. P. and Taylor, S. S. (2015) 'Dynamics-Driven Allostery in Protein Kinases.', *Trends in biochemical sciences*, 40(11), pp. 628–647. doi: 10.1016/j.tibs.2015.09.002.

Krause, S.D. and Scadden,T .D (2015) 'A Hostel For The Hostile: The Bone Marrow Niche InHematologicNeoplasms'.*Haematologica*',100:1376-1387;doi:10.3324/haematol.2014. 113852

Kung, J. E. and Jura, N. (2016) 'Structural Basis for the Non-catalytic Functions of Protein Kinases.', *Structure (London, England : 1993)*. Elsevier, 24(1), pp. 7–24. doi: 10.1016/j.str.2015.10.020.

Kuriyan, J. and Eisenberg, D. (2007) 'The origin of protein interactions and allostery in

colocalization.', *Nature*, 450(7172), pp. 983–90. doi: 10.1038/nature06524.

Leonard, T. A. and Hurley, J. H. (2011) 'Regulation of protein kinases by lipids.', *Current opinion in structural biology*. NIH Public Access, 21(6), pp. 785–91. doi: 10.1016/j.sbi.2011.07.006.

Lin, C.-W. *et al.* (2018) 'Discovery and Preclinical Development of Netarsudil, a Novel Ocular Hypotensive Agent for the Treatment of Glaucoma', *Journal of Ocular Pharmacology and Therapeutics*, 34(1–2), pp. 40–51. doi: 10.1089/jop.2017.0023.

Lu, J. (2015) 'Palbociclib: a first-in-class CDK4/CDK6 inhibitor for the treatment of hormone-receptor positive advanced breast cancer.', *Journal of hematology & oncology*. BioMed Central, 8, p. 98. doi: 10.1186/s13045-015-0194-5.

Manning, G. *et al.* (2002) 'The Protein Kinase Complement of the Human Genome', *Science*, 298(5600), pp. 1912–1934. doi: 10.1126/science.1075762.

Markham, A. and Dhillon, S. (2018) 'Acalabrutinib: First Global Approval', *Drugs*, 78(1), pp. 139–145. doi: 10.1007/s40265-017-0852-8.

Masterson, L. R. *et al.* (2012) 'Allostery and Binding Cooperativity of the Catalytic Subunit of Protein Kinase A by NMR Spectroscopy and Molecular Dynamics Simulations', *Advances in Protein Chemistry and Structural Biology*. Academic Press, 87, pp. 363–389. doi: 10.1016/B978-0-12-398312-1.00012-3.

Matsui, J. *et al.* (2008) 'Multi-kinase inhibitor E7080 suppresses lymph node and lung metastases of human mammary breast tumor MDA-MB-231 via inhibition of vascular endothelial growth factor-receptor (VEGF-R) 2 and VEGF-R3 kinase.', *Clinical cancer research : an official journal of the American Association for Cancer Research*, 14(17), pp. 5459–65. doi: 10.1158/1078-0432.CCR-07-5270.

McKeage, K. (2015) 'Alectinib: A Review of Its Use in Advanced ALK-Rearranged Non-Small Cell Lung Cancer', *Drugs*, 75(1), pp. 75–82. doi: 10.1007/s40265-014-0329-y.

McWhirter, J. R. and Wang, J. Y. (1991) 'Activation of tyrosinase kinase and microfilament-binding functions of c-abl by bcr sequences in bcr/abl fusion proteins.', *Molecular and cellular biology*. American Society for Microbiology (ASM), 11(3), pp.

1553–65. Available at: http://www.ncbi.nlm.nih.gov/pubmed/1705008 (Accessed: 5 April 2018).

Minkovsky, N. and Berezov, A. (2008) 'BIBW-2992, a dual receptor tyrosine kinase inhibitor for the treatment of solid tumors.', *Current opinion in investigational drugs (London, England : 2000)*, 9(12), pp. 1336–46. Available at: http://www.ncbi.nlm.nih.gov/pubmed/19037840 (Accessed: 1 August 2019).

Nagar, B. *et al.* (2002) 'Crystal structures of the kinase domain of c-Abl in complex with the small molecule inhibitors PD173955 and imatinib (STI-571).', *Cancer research*, 62(15), pp. 4236–43. Available at: http://www.ncbi.nlm.nih.gov/pubmed/12154025 (Accessed: 22 March 2018).

Nagar, B. *et al.* (2003) 'Structural basis for the autoinhibition of c-Abl tyrosine kinase.', *Cell*, 112(6), pp. 859–71. Available at: http://www.ncbi.nlm.nih.gov/pubmed/12654251 (Accessed: 18 January 2018).

Nagar, B. *et al.* (2006) 'Organization of the SH3-SH2 unit in active and inactive forms of the c-Abl tyrosine kinase.', *Molecular cell*, 21(6), pp. 787–98. doi: 10.1016/j.molcel.2006.01.035.

Neet, K. and Hunter, T. (1996) 'Vertebrate non-receptor protein-tyrosine kinase families.', *Genes to cells : devoted to molecular & cellular mechanisms*, 1(2), pp. 147–69. Available at: http://www.ncbi.nlm.nih.gov/pubmed/9140060 (Accessed: 3 April 2018).

Noble, M. E. M., Endicott, J. A. and Johnson, L. N. (2004) 'Protein kinase inhibitors: insights into drug design from structure.', *Science (New York, N.Y.)*, 303(5665), pp. 1800–5. doi: 10.1126/science.1095920.

O'Hare, T. *et al.* (2009) 'AP24534, a Pan-BCR-ABL Inhibitor for Chronic Myeloid Leukemia, Potently Inhibits the T315I Mutant and Overcomes Mutation-Based Resistance', *Cancer Cell*, 16(5), pp. 401–412. doi: 10.1016/j.ccr.2009.09.028.

Pellicena, P. and Miller, W. T. (2001) 'Processive Phosphorylation of p130Cas by Src Depends on SH3-Polyproline Interactions', *Journal of Biological Chemistry*, 276(30), pp. 28190–28196. doi: 10.1074/jbc.M100055200.

Perl, A. E. *et al.* (2017) 'Selective inhibition of FLT3 by gilteritinib in relapsed or refractory acute myeloid leukaemia: a multicentre, first-in-human, open-label, phase 1–2 study', *The Lancet Oncology*, 18(8), pp. 1061–1075. doi: 10.1016/S1470-2045(17)30416-3.

Pluk, H., Dorey, K. and Superti-Furga, G. (2002) 'Autoinhibition of c-Abl.', *Cell*, 108(2), pp. 247–59. Available at: http://www.ncbi.nlm.nih.gov/pubmed/11832214 (Accessed: 28 June 2017).

Reddy, E. P. and Aggarwal, A. K. (2012) 'The ins and outs of bcr-abl inhibition.', *Genes & cancer*, 3(5–6), pp. 447–54. doi: 10.1177/1947601912462126.

Renshaw, M. W., Capozza, M. A. and Wang, J. Y. (1988) 'Differential expression of type-specific c-abl mRNAs in mouse tissues and cell lines.', *Molecular and cellular biology*, 8(10), pp. 4547–51. Available at: http://www.ncbi.nlm.nih.gov/pubmed/2460747 (Accessed: 4 April 2018).

Richez, C. *et al.* (2017) 'Efficacy of baricitinib in the treatment of rheumatoid arthritis', *Expert Opinion on Pharmacotherapy*, 18(13), pp. 1399–1407. doi: 10.1080/14656566.2017.1359256.

Robinson, D. R., Wu, Y.-M. and Lin, S.-F. (2000) 'The protein tyrosine kinase family of the human genome', *Oncogene*, 19(49), pp. 5548–5557. doi: 10.1038/sj.onc.1203957.

ROWLEY, J. D. (1973) 'A New Consistent Chromosomal Abnormality in Chronic Myelogenous Leukaemia identified by Quinacrine Fluorescence and Giemsa Staining', *Nature*. Nature Publishing Group, 243(5405), pp. 290–293. doi: 10.1038/243290a0.

Singh, M. and Salnikova , M. (2015) *Novel Approaches and Strategies for Biologics, Vaccines and Cancer Therapies*. Elsevier. doi: 10.1016/C2013-0-00324-6.

Samson, K. (2014) 'LEE011 CDK Inhibitor Showing Early Promise in Drug-Resistant Cancers', *Oncology Times*, 36(3), pp. 39–40. doi: 10.1097/01.COT.0000444043.33304.c1.

Schoepfer, J. *et al.* (2018) 'Discovery of Asciminib (ABL001), an Allosteric Inhibitor of the Tyrosine Kinase Activity of Bcr-Abl', *Journal of Medicinal Chemistry*. American Chemical Society, 61(18), pp. 8120–8135. doi: 10.1021/acs.jmedchem.8b01040.

Shaw, A. T. *et al.* (2017) 'Lorlatinib in non-small-cell lung cancer with ALK or ROS1 rearrangement: an international, multicentre, open-label, single-arm first-in-man phase 1 trial', *The Lancet Oncology*, 18(12), pp. 1590–1599. doi: 10.1016/S1470-2045(17)30680-0.

Shirley, M. (2018) 'Dacomitinib: First Global Approval', *Drugs*, 78(18), pp. 1947–1953. doi: 10.1007/s40265-018-1028-x.

Sirvent, A., Benistant, C. and Roche, S. (2008) 'Cytoplasmic signalling by the c-Abl tyrosine kinase in normal and cancer cells', *Biol. Cell*, 100, pp. 617–631. doi: 10.1042/BC20080020.

Soria, J.-C. *et al.* (2017) 'First-line ceritinib versus platinum-based chemotherapy in advanced ALK-rearranged non-small-cell lung cancer (ASCEND-4): a randomised, open-label, phase 3 study', *The Lancet*. Elsevier, 389(10072), pp. 917–929.

Taagepera, S. *et al.* (1998) 'Nuclear-cytoplasmic shuttling of C-ABL tyrosine kinase.', *Proceedings of the National Academy of Sciences of the United States of America*. National Academy of Sciences, 95(13), pp. 7457–62. Available at: http://www.ncbi.nlm.nih.gov/pubmed/9636171 (Accessed: 4 April 2018).

Tarrant, M. K. and Cole, P. A. (2009) 'The chemical biology of protein phosphorylation.', *Annual review of biochemistry*. NIH Public Access, 78, pp. 797–825. doi: 10.1146/annurev.biochem.78.070907.103047.

Tokarski, J. S. *et al.* (2006) 'The structure of Dasatinib (BMS-354825) bound to activated ABL kinase domain elucidates its inhibitory activity against imatinib-resistant ABL mutants.', *Cancer research*, 66(11), pp. 5790–7. doi: 10.1158/0008-5472.CAN-05-4187.

Verheijen, R. B. *et al.* (2017) 'Clinical Pharmacokinetics and Pharmacodynamics of Pazopanib: Towards Optimized Dosing', *Clinical Pharmacokinetics*, 56(9), pp. 987–997. doi: 10.1007/s40262-017-0510-z.

Vihinen, M. *et al.* (1994) 'Structural basis for pleckstrin homology domain mutations in X-linked agammaglobulinemia', *Biochemistry* , 91, pp. 12803–12807. Available at: https://www.pnas.org/content/pnas/91/26/12803.full.pdf (Accessed: 1 August 2019).

Vihinen, M. *et al.* (1996) 'BTKbase, mutation database for X-linked agammaglobulinemia (XLA).', *Nucleic acids research*. Oxford University Press, 24(1), pp. 160–5. Available at: http://www.ncbi.nlm.nih.gov/pubmed/8594569 (Accessed: 3 April 2018).

Vlahovic, G. and Crawford, J. (2003) 'Activation of Tyrosine Kinases in Cancer', *The Oncologist*. AlphaMed Press, 8(6), pp. 531–538. doi: 10.1634/THEONCOLOGIST.8-6-531.

Webersinke, G. (2016) 'Molecular pathogenesis of chronic myeloid leukemia', *memo - Magazine of European Medical Oncology*. Springer Vienna, 9(4), pp. 163–167. doi: 10.1007/s12254-016-0294-0.

Wetzler, M. *et al.* (1993) 'Subcellular localization of Bcr, Abl, and Bcr-Abl proteins in normal and leukemic cells and correlation of expression with myeloid differentiation.', *Journal of Clinical Investigation*, 92(4), pp. 1925–1939. doi: 10.1172/JCI116786.

Wong, S. and Witte, O. N. (2004) 'The BCR-ABL story: bench to bedside and back.', *Annual review of immunology*, 22(1), pp. 247–306. doi: 10.1146/annurev.immunol.22.012703.104753.

Wu, P., Nielsen, T. E. and Clausen, M. H. (2015) 'FDA-approved small-molecule kinase inhibitors.', *Trends in pharmacological sciences*, 36(7), pp. 422–39. doi: 10.1016/j.tips.2015.04.005.

Wylie, A. *et al.* (2014) 'ABL001, a Potent Allosteric Inhibitor of BCR-ABL, Prevents Emergence of Resistant Disease When Administered in Combination with Nilotinib in an in Vivo Murine Model of Chronic Myeloid Leukemia', *Blood*, 124, pp. 398–398. Available at: http://www.bloodjournal.org/content/124/21/398.

Wylie, A. A. *et al.* (2017) 'The allosteric inhibitor ABL001 enables dual targeting of BCR?ABL1', *Nature*, 543(7647), pp. 733–737. doi: 10.1038/nature21702.

Zhang, J. *et al.* (2010) 'Targeting Bcr-Abl by combining allosteric with ATP-binding-site inhibitors.', *Nature*, 463(7280), pp. 501–6. doi: 10.1038/nature08675.

Zhang, S. and Yu, D. (2012) 'Targeting Src family kinases in anti-cancer therapies: turning promise into triumph.', *Trends in pharmacological sciences*. NIH Public Access, 33(3),

pp. 122–8. doi: 10.1016/j.tips.2011.11.002.

Zimmermann, J. *et al.* (1997) 'Potent and selective inhibitors of the Abl-kinase: phenylamino-pyrimidine (PAP) derivatives', *Bioorganic & Medicinal Chemistry Letters*, 7(2), pp. 187–192. doi: 10.1016/S0960-894X(96)00601-4.

Zuccotto, F. *et al.* (2010) 'Through the "Gatekeeper Door": Exploiting the Active Kinase Conformation', *J. Med. Chem*, 53, pp. 2681–2694. doi: 10.1021/jm901443h.

# CHAPTER 3

## 3 Computational Approaches for Biomolecular Structure and Drug Design

### *3.1 Introduction*

In the medical world today, there has been a paradigm shift in the design of drugs, novel methods of drug design are constantly being exploited in an endeavor to improve efficiency and encounter challenges faced during the drug design process (Zheng *et al.*, 2013; Ramírez, 2016). Molecular modeling (also known as computational chemistry ) is the science and art of studying molecular function structure through model building and computing using computational methods to simulate the behavior of molecules (Ramachandran, Deepa, and Namboori, 2008). Molecular modeling is a rapidly growing discipline of science in the research community. In the medical domain, molecular modeling is the mainstream of drug design and discovery. It entails the use of algorithms to carry out calculation, data processing, and automated reasoning tasks to elucidate chemical properties problems(Young, 2001). Simulations use an equation that elucidate the behaviour of matter on an atomic level to analyse structural properties of molecules such as gases, liquid, solids to predict and explain chemical phenomena. (Young, 2001; Jensen, 2002; Leszczynski, 2012). It gives a platform for scientists to expect chemical reactions using computer software so that saving time, and experimental costs (Montoya, Mondragón and Truong, 2002; Bajorath, 2012; Rohland and Reich, 2012).

Molecular modeling covers a wide range of topics including quantum chemistry, molecular mechanics and molecular dynamics (Lewars, 2011). There are two fundamental molecular modeling principle that are used to establish the energetics and conformational changes to the drug-target system (Figure 3.1):

1) Quantum Mechanics
2) Molecular Mechanics

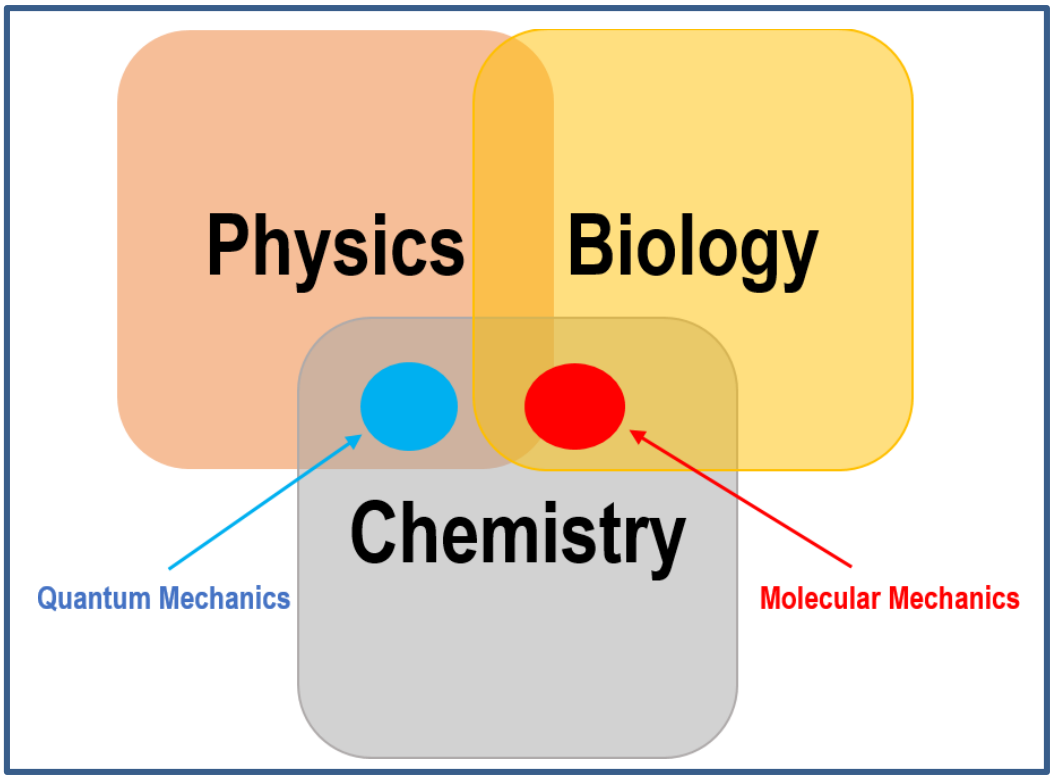


**Figure 3.1:** The scientific domains in which Applications of Quantum and Molecular Mechanics fit into (Prepared by Author).

In this chapter, quantum mechanics, molecular mechanics and molecular dynamics simulations will be explained on, to get more insight into the rationale behind the chosen energy descriptors for this study. The principle behind each of the computational tools employed in the study will also be further explained

### *3.2 The Principle of Quantum Mechanics*

Quantum mechanics (also known as Quantum physics or Quantum field theory) is one of the most successful branches of classical physics in the history of science. It identifies the characteristic behavior of matter and energy at molecular, atomic, nuclear and smaller microscopic levels (Griffiths, 2005; Zettili, 2009). The principle of quantum Mechanics hypothesis was suggested by Max Planck in the early 20$^{th}$ century in 1900 (Bose, 1924). It states that any energy-radiating atomic system can be theoretically split into a number of different energy components so that each of the energy elements is equivalent to the

frequency with which each of them radiates separately (Müller, 2008). In biological process, QM plays a significant role in understanding this process at the molecular level such as bond forming /breaking atomic transfer and electron excitation.

Planck theorized that energy was transferred in portions called quanta, hence the name quantum hypothesis. It is illustrated by the equation below:

$$\mathbf{E=hv} \qquad \text{(Eq 3.2.1)}$$

where E is energy, h is Planck's constant, equal to $6.626068 \times 10^{-34}$ Joule-second (J-s) and the Greek letter v is the photon's frequency (Hull, Tessner and Diamond Jr., 1978; Mittelstaedt, 2008; Quincey, 2013).

The quantum phenomena can be best clarified by the Copenhagen interpretation. Danish physicist Niels Bohr and German physicist Werner Heisenberg approached a set of statements which attempt to clarify how QM explains our understanding of nature (Stapp, 1972). It stated that physical systems normally do not have certain properties prior to being measured, and quantum mechanics can only expect the probabilities that measurements will produce certain results (Hanson, 1959; Kober, 2009; Hollowood, 2013).

Despite there were many challenges to the Copenhagen interpretation, but it still remains the frequently taught explanations of quantum mechanics(Zinkernagel, 2011).The quantum hypothesis laid a foundation for many physicists like Albert Einstein, Niels Bohr, Werner Heisenberg, Erwin Schrödinger, and many others to further develop the field of quantum physics (Zettili, 2009; D'Espagnat, 2011).

### *3.2.1 The Schrödinger Wave Function*

In January 1926, the atom's quantum mechanical model was suggested by Austrian biologist Erwin Schrödinger. Expanding on the Bohr atom template, which suggests that atoms are placed around a core in concentrated linear positions, Schrödinger used mathematical formulas to define the likelihood of placing an electron on a precise route. The model is depicted as a nucleus encircled by an elevated and small density electron

cloud (Dronamraju, 1999; Leach, 2001; Atkins and Friedman, 2011) (Figure 3.2). According to quantum mechanics, all particles are termed as a wave function with no defined position or momentum until they are detected. The probability of each possible observation may be determined by the wave function(Leach, 2001; Atkins and Friedman, 2011).

Schrödinger found that by adding the properties of an atom, being the mass and charge, to the equation, he was able to predict a series of shapes showing the wave pattern of electrons in an atom (Bahrami *et al.*, 2014)

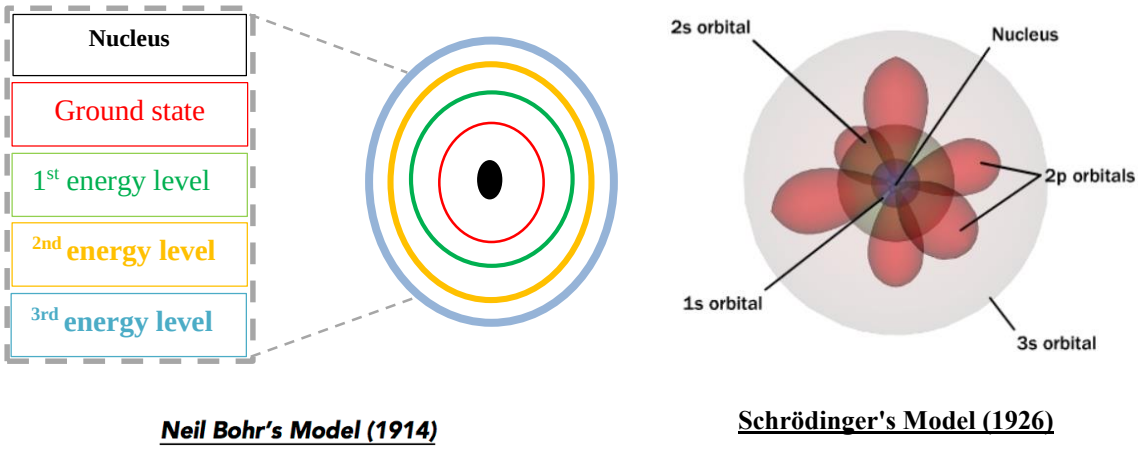


**Figure 3.2:** The Bohr Model demonstrated the atom to have a positively charged nucleus that was orbited by negatively charged electrons. This model was corrected by the equation, which evidenced electrons to have wave functions dependent on mass and charge of the atom. The two models are the fundamentals of what we now know as Quantum mechanics (Prepared by Author).

In its simplest form, the Schrödinger wave equation(Laskin, 2002) may be represented as:

$$\mathbf{H\psi = E\psi} \qquad \text{(Eq 3.2.2)}$$

Where, **H** is called Hamiltonian operator (contains derivatives with respect to atom location)**, Ψ** is the wave function and ***E,*** is the energy of the system also referred to as the

operator energy eigenvalue(Jensen, 2007; Lewars, 2011).This description is a probabilistic description of electron location but can't predicate their precise location so that in order to get a disclose physical model of Schrödinger's equation, the wave function must be continuous, single-valued and antisymmetric relative to electrons interchange(Young, 2001). The molecular Hamiltonian operator is derived from the sum of the atom's total potential energy (V) and the kinetic energy (T) represented as

$$\mathbf{H} = \mathbf{T} + \mathbf{V} \qquad \text{(Eq 3.2.3)}$$

When considering particles as point masses, and neglecting relativistic effects, the Hamiltonian will, therefore, constitute all the kinetic and potential energy operators for all the electrons and nuclei in a molecule.

An advanced Hamiltonian can then be presented as:

$$\hat{H} = \left[ -\frac{\mathbf{h^2}}{\mathbf{8\pi^2}} \sum_{\mathbf{i}} \frac{\mathbf{1}}{\mathbf{m_j}} \left( \frac{\mathbf{\partial^2}}{\mathbf{\partial x^2}} + \frac{\mathbf{\partial^2}}{\mathbf{\partial y^2}} + \frac{\mathbf{\partial^2}}{\mathbf{\partial z^2}} \right) \right] + \sum_{\mathbf{i}} \sum_{\mathbf{<j}} \left( \frac{\mathbf{e_i e_j}}{\mathbf{r_{ij}}} \right) \qquad \text{(Eq 3.2.4)}$$

*3.2.2 The Born- Oppenheimer Approximation Theory*

In 1927, Max Born and J. Robert Oppenheimer proposed the Born-Oppenheimer approximation theory (Born and Oppenheimer, 1927). This theory assumes that the motion of atomic nuclei and electrons in a molecule can be separated. In mathematical terminology, it allows the wave function of a molecule to broken into its electronic and nuclear components. Electrons are considered to be of lighter weight than the nuclei. This leads to the electrons having a greater velocity and moving instantaneously to nuclei movement. The distribution of electrons within a molecule is therefore defined by the location of the nuclei (Bludman and Daitch, 1954; Woolley and Sutcliffe, 1977; Wudka, 1990; Matsika, 2010).

The disparity in velocities of the nuclei and electrons allow the application of the Born-Oppenheimer approximation, thus minimizing the complexity of the wave function of the Hamiltonian equation.

The simplified wave function is as follows:

$$\boldsymbol{\psi}(\mathbf{r_{elec}}) = \boldsymbol{\psi}(\mathbf{r_{elec}})\,(\boldsymbol{\psi}(\mathbf{r_{nucl}}) \qquad \text{(Eq 3.2.5)}$$

Eq 3.2.2 is converted:

$$\boldsymbol{H_{EN}}\boldsymbol{\psi}(\mathbf{r_{elec}}) = \boldsymbol{E_{EN}}\boldsymbol{\psi}(\mathbf{r_{elec}}) \qquad \text{(Eq 3.2.6)}$$

Where $H_{EN}$ denotes a difference between terms based activity to fixed nuclear positions ($V_{NN}$) or their activity to the non-fixed electron positions. Eq. 3.2.5 shows $E_{EN,}$ which is derived from the sources being the fluctuating electron co-ordinates and fixed nuclear co-ordinates.

$$(\mathbf{H_{el}} + \mathbf{V_{NN}})\,\boldsymbol{\psi}(\mathbf{r_{el}}) = \mathbf{E_{EN}}\boldsymbol{\psi}(\mathbf{r_{el}}) \qquad \text{(Eq 3.2.7)}$$

Electronic motion is best described by the electronic Schrödinger equation. This approximation is more accurate when it is applied to ground electronic states. (Deslauriers, 2011; Beringer and Others, 2014).

### *3.2.3 Potential Energy Surface*

The potential energy surface is an effective mathematical representation between molecular vibrational motions of a molecule, along with its geometry and its nuclear probability distribution by finding solutions to the time-dependent Schrödinger equation. This concept is birthed from the Born-Oppenheimer approximation elucidated above, where electrons differ according to the positional states of the nuclei in a manner such that the potential energy surface is taken as the potential of atoms to collide with each other in a molecule (Woolley, 1991; Atkins and Friedman, 2011). A potential energy surface displays high potential energy regions, indicating high-energy nuclear arrangements or molecular conformations and low energy regions indicating low nuclear energy conformations. The potential energy surface is utilized in computational chemistry to

analyze the lowest energy state and the positional geometry of a molecule at this state (Elsawy, Hodgson and Caves, 2005; Atkins and Paula, 2009) (Figure 3.3).

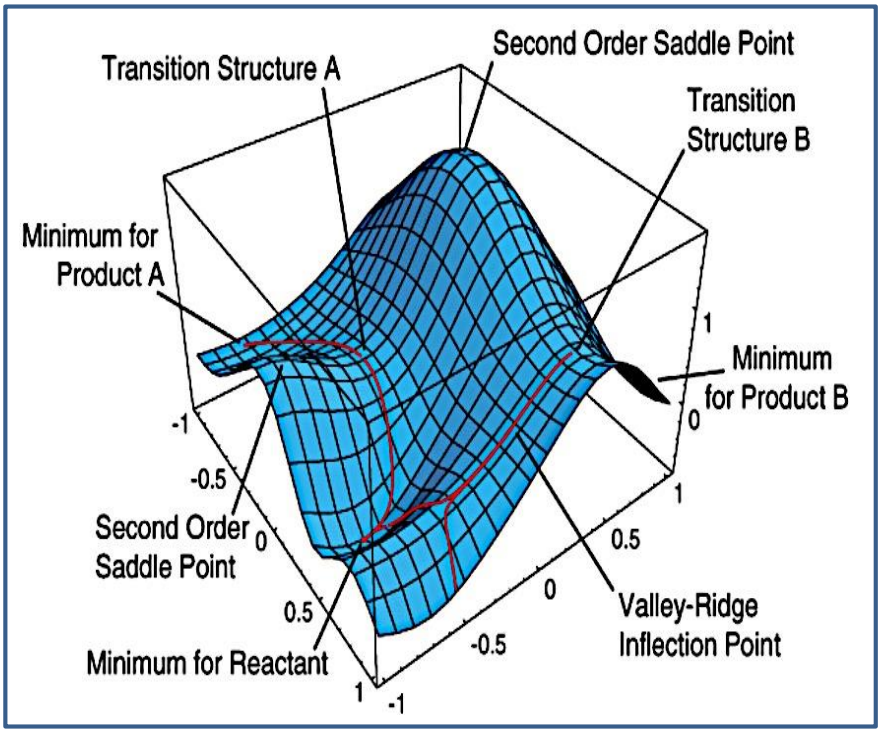


**Figure 3.3:** graphical representation of a two-dimensional potential energy surface (PES) (Adapted from The California State University 2017).

### *3.3 The Principle of Molecular Mechanics*

Molecular mechanics (MM) or force-field methods is a technique that is used to predict the energy of a molecule as a function of its conformation. This involves predictions of equilibrium geometries, transition states, and relative energies between conformers or between different molecules (Shattuck, 2003; Vanommeslaeghe *et al.*, 2014).

Molecular mechanics is a computational method that computes the potential energy surface for a specific order of atoms by the use of potential functions that are obtained by using classical physics (Tsai, 2002; Bowen and Allinger, 2007).

It depends on the following assumptions:

1) Electrons are treated around a nucleus that is a perfect sphere.
2) The molecular bonds are regarded as springs.
3) Potential features are dependent on experimental parameters such as force constants and equilibrium values.
4) the potential energy function is the total functions for bond stretching, angle bending, torsional energies, and non-bonding interactions.

Molecular mechanics requires less computing cost than QM methods. It is however restricted by certain parameters of equations such as the different force-field for different types of atoms. Moreover, it is inapplicable for electronic properties (Hu, Elstner and Hermans, 2003; Wallrapp and Guallar, 2011).

Molecular mechanics can be useful for large molecules such as proteins so that its mainly used in the molecular dynamics field (Marques and Brown, 2002; Cournia, Smith and Ullmann, 2005).

### *3.3.1 Potential Energy Function*

In the force field, all atoms are known as building block whereas electrons are not considered as single entities. This implies that rather than finding solutions to the Schrödinger equation, explicit bonding information must be specified (González, 2011). In the force field, molecules are described by a "ball and spring" analogy, with atoms of different sizes and different bond length. It was founded that different molecules might have structural similarity due to the atoms they are made up of. The notion atom types were then coined and are dependent on the atomic number and chemical bonding fixating it in place (Jensen, 2007)(Guest and Sherwood, 2002).

The potential energy function (PEF) force field of a molecular system may be assembled in terms of a set of force field energy equations that are solely based on Newtonian classical physics. These equations calculate the energy of the system as well as the atom types that construct the molecule (Huang *et al.*, 2010).

The following equations best describe the sum of all individual molecular components that make up the total potential energy:

1. Bond stretching (between directly bonded atoms)

$$\mathbf{E_r} = \sum \mathbf{K_r}(\mathbf{r} - \mathbf{r_0})^2 \qquad \text{(Eq 3.3.1)}$$

2. Angle bending (atoms bounded to same central atoms)

$$\mathbf{E_\theta} = \sum \mathbf{K_\theta}(\boldsymbol{\theta} - \boldsymbol{\theta_0})^2 \qquad \text{(Eq 3.3.2)}$$

3. Bond torsion

$$\mathbf{E_\phi} = \sum \mathbf{K_\phi}[\mathbf{1} + \mathbf{cos}(\mathbf{n}\boldsymbol{\phi} - \boldsymbol{\phi_0})] \qquad \text{(Eq 3.3.3)}$$

4. Non-bonded interactions (van der Waals and electrostatic)

$$\mathbf{E_{nb}} = \left[\sum \sum \left(\frac{\mathbf{A_{ij}}}{\mathbf{r_{ij}}^{12}} - \frac{\mathbf{B_{ij}}}{\mathbf{r_{ij}}^{6}}\right)\right] + \left[\sum \sum \left(\frac{\mathbf{q_i q_j}}{\mathbf{D r_{ij}}}\right)\right] \qquad \text{(Eq 3.3.4)}$$

Where: $K_r$, $K_\theta$, $K_\phi$ are force constants for a bond, angle, and dihedral angle and $r_o$, $\theta_o$, $\phi_o$ are the equilibrium distance, angle, and phase angle. Parameter $r_{ij}$ is distance, while $A_{ij}$ and $B_{ij}$ are van der Waal parameters. D is the molecular dielectric constant; $q_i$ and $q_j$ are charge points.

The final potential energy function equation is, therefore:

$$\boldsymbol{E_{total}} = \boldsymbol{E_r} + \boldsymbol{E_\theta} + \boldsymbol{E_\emptyset} + \boldsymbol{E_{nb}} \qquad (Eq\ 3.3.4)$$

Where, $\boldsymbol{E_{total}}$ donate total energy, $\boldsymbol{E_r}$ denote bond-stretching energy, $\boldsymbol{E_\emptyset}$ donate angle-bending energy, $\boldsymbol{E_\emptyset}$ donate bond rotation energy, and $\mathbf{E_{nb}}$ donate non-bonded interactions(Figure 3.4).

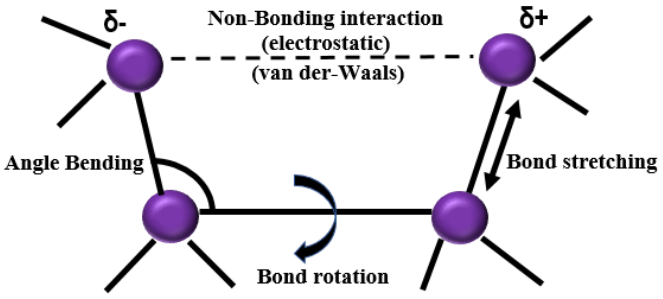


Figure 3.4: Diagrammatic representation of bonded and non-bonded interactions acting in molecular motion (Prepared by Author).

### *3.4 Quantum Mechanics/Molecular Mechanics (QM/MM)*

To decline negative implications associated with using Quantum Mechanics (QM) and Molecular Mechanics (MM) approaches so that computational chemists have established combinational QM/MM algorithms, which merge QM descriptors with the low-cost computing rate of MM (Levitt, 1976; Shurki and Warshel, 2003; Adcock and McCammon, 2006a) (Figure 3.5). QM/MM methods employ algorithm that combined the description accuracy of QM and the low computational cost of MM (Sauer and Sierka, 2000; Senn and Thiel, 2009; Lu *et al.*, 2016). The technique of QM/MM involves two step-wise domains. The reactive domain defined by QM, whereas, the non-reactive domain treated with MM (Bornemann, Nettesheim and Schütte, 1998). Although QM calculations are very precise at describing the electronic structure of molecular systems, it is highly computationally expensive and time-consuming (Honarparvar *et al.*, 2014).so that hybrid QM/MM propose to accurately describe quantum mechanics with the low cost applied to molecular mechanics.

Amongst the notable advantages of hybrid QM/MM method over QM and MM, that QM or MM may not be appropriate for every structure-based drug design study; therefore, further investigation of the technique may be required(Lu *et al.*, 2016), so that hybrid QM/MM is a vital computational tool in drug design.

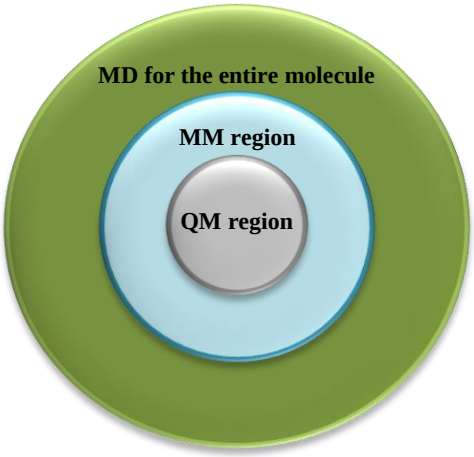


Figure 3.5: A schematic representation of a hybrid QM/MM/MD model (Prepared by Author).

### *3.5 Force Field*

In 1970s the first Molecular Mechanics (MM) force field was formulated (González, 2011). A force field is a mathematical function with a delineated set of parameters. These parameters describe the molecular energy systems to specific particle coordinates (Kang, Liu and Guo, 2014). Commonly used biomolecular force fields include AMBER (Wang *et al.*, 2005), CHARMM (Brooks *et al.*, 2009), NAMD (Phillips *et al.*, 2005), GROMOS (Christen *et al.*, 2005) and OPLS-AA(Guvench and MacKerell, 2008). All force field parameters are obtained from either experimental data sources, ab initio or semi-empirical QM (González, 2011). Force field functions are assumed to be wholly dependent on atomic orientations. They have been used as representatives for describing potential energy surface for different types of molecular systems with varying degrees of freedom (Ponder and Case, 2003). This force field function is used to understand the specific forces acting within the molecular system. In this thesis, the AMBER14 force field was implemented to characterize the Bcr-Abl protein, whilst GAFF was used to interpret the ABL001 and Nilotinib ligands (Halgren and Damm, 2001). The AMBER14 force field provides a favorable balance in energy between the helical and extended regions of the peptide and protein backbones with improved dihedral torsions (Wang *et al.*, 2004).

### *3.6 The principle of Molecular Dynamics*

Over the year's crystallographic studies, Nuclear Magnetic Resonance Spectroscopy (NMR), and biological assays have been engaged to credibly determine the crucial role of protein flexibility in ligand binding and to provide insights into the biomolecular structures (Nair and Miners,2014). In late 1950, Molecular dynamic first emerged were Alder, Wainwright, and Rahman established simulation methods for the dynamics of liquids. The computational chemistry domain has developed since then and from the early 1970s, molecular dynamics has become the most widely used method to study structure and dynamics of macromolecules such as DNA or protein (Tsai, 2002).There are two common types of simulation techniques classical MD, and Monto Carlo method(Adcock and McCammon, 2006b). Monto Carlo method depends on the prospects by creating a large number of conformation and transition from one state to the other in a specific statistical manner (Earl and Deem, 2008). On the other hand, classical MD simulation, trajectories of atoms and molecules are created by mathematically solving Newton's equation of motion for a system of interacting particles, in which forces between the particles and potential energy are defined by molecular mechanics force fields(Cornell *et al.*, 1995). Recently, there are many hybrid techniques have also been released. One of the main advantages of MD over MC is its capacity to allow for dynamical properties of a system such as rheological properties and time-dependent responses(Nair and Miners, 2014). Molecular dynamics is especially valuable in biochemistry and molecular biology as it affords the occasion to identify and categorizes on an atomic scale that may impact the biological properties of a system (Jarosaw Meller, 2001).

In MD, complex systems are modeled at atomic level and Newton's equations of motion are mathematically solved to indicate the time of evolution of a specific system, allowing a derivation of its kinetic energy and thermodynamic properties through the application of computational tools (Jarosaw Meller, 2001; Case *et al.*, 2005; Atkins and Paula, 2009) (Figure 3.6).

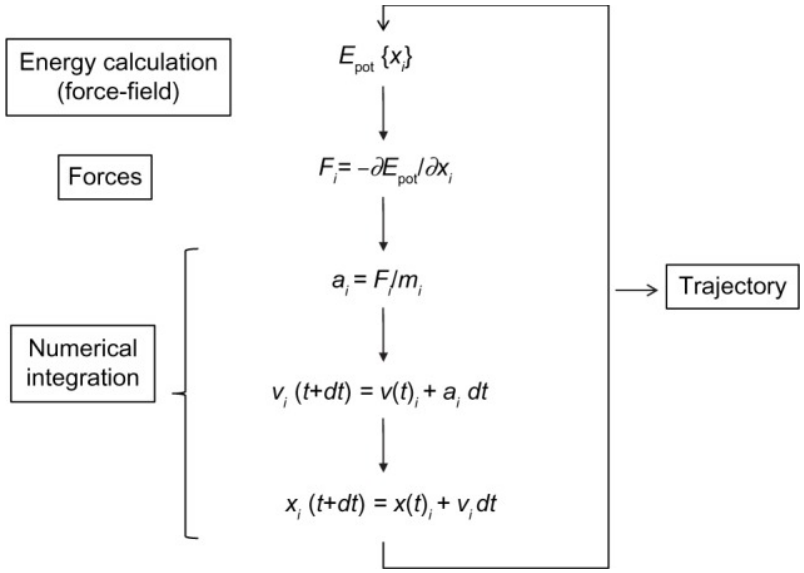


**Figure 3.6:** Basic algorithm of Molecular Dynamics. Where Epot = potential energy; t = simulation time; dt = iteration time; x = tom co-ordinates; F = force component; a = acceleration; m = atom mass and v = velocity (Image adapted from (Hospital *et al.*, 2015).

The overall purpose of this computational technique is to utilize Newton's equations to solve and understand the energies and structural dynamics of a molecular network system. The following initial particle conditions are required:

1. Positions and velocities of each particle

2. A good force field to characterize the forces between atoms, e.g. AMBER or CHARMM

3. Boundary conditions that need to be engaged

Atomic trajectories are generated through the integration of Newton's equations of motion for atoms on an energy surface.

The classical equation of motion may then be solved:

$$\mathbf{F_i} = \mathbf{m_i}\frac{\mathbf{d^2 r_i(t)}}{\mathbf{dt^2}} \qquad \text{(Eq 3.4.1)}$$

Where $r_i$ (t) is the particle position vector, t is time-evolution, m is the mass of the particle and $F_i$ depicts the interacting force on the particle.

Molecular dynamics can be categorized into 4 continuous technical steps that are repeated numerously to generate a trajectory (Figure 3.7).

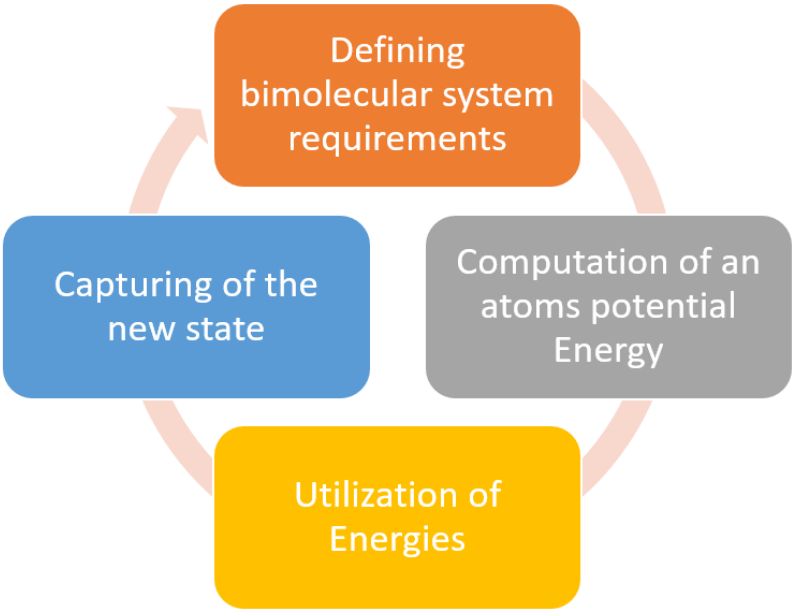


**Figure 3.7.** The cycle of molecular dynamics steps (Prepared by Author).

The steps are outlined below:

1) The fundamental requirements of the biomolecular system are defined:
    - The coordinates of each atom
    - The bond characteristics between each atom
    - The acceleration of atoms

2) Each atom's potential energy is computed.
3) The energies from the step are then utilized to solve the equation of motion.
4) The new state of the system needs to be saved, and the atoms' co-ordinates changed, and step forward in the simulation taken. The cycle then restarts from step 1.

Once the trajectory is fully generated, quantitative analysis of the system's time- evolution can proceed.

### *3.6.1 Molecular Dynamics Post-Analysis*

Molecular dynamics trajectories are created from the production run of the simulation. The trajectories can be defined as sequential snapshots that are characterized by both positional co-ordinates and velocity vectors and detail the time evolution of the system in phase space (Jarosaw Meller, 2001; Likhachev, Balabaev and Galzitskaya, 2016).

When choosing analytical software, three requirements are essential:

1. Qualitative visualization software that will not only display the trajectory's video clips but also generates high-quality snapshots/images.
2. The software should have prompt processors that will accommodate large volumes of data.
3. A variety of analysis options should be available on one program.

The selected post-dynamic techniques and calculations should be dependent on the nature of the MD study; however, critical quantitative evaluation is necessary to support any visual systemization.

For the purpose of this study, the post dynamic analysis of the trajectories is critical to determining the:

1. energetic and conformational stability of the biomolecular system.
2. The characteristics of the system's small molecule binding landscape and the thermodynamic energy fluctuations along the system's clustered trajectory.
3. dynamic conformational features or variability of the biomolecular system.

#### *3.6.1.1 System Stability*

Convergence:

Convergence is an empirical description of protein dynamics. It specifically describes protein dynamics based on bond types and bond angle vibrations during the unfolding of a protein. This fusion toward equilibrium and portrayal of a conclusive plateau is impertinent

for an MD trajectory to be accurate and reproducible. At this plateau, the protein-ligand system displays energetically stable conformations (Galindo-Murillo, Roe and Cheatham, 2015).

Root Mean Square Deviation (RMSD):

Spatial difference between two static structures of the same trajectory measures the deviation of a complex (Brüschweiler, 2003). The RMSD of a trajectory is defined as:

$$\mathbf{RMSD} = \left(\frac{\sum_{\mathbf{N}}(\mathbf{R_i} - \mathbf{R_1^0})^2}{\mathbf{N}}\right)^{\frac{1}{2}} \qquad \text{(Eq 3.4.2)}$$

Root Mean Square Fluctuation (RMSF):

The root mean fluctuation (RMSF) of a protein measures residue's Cα atom fluctuations is based on the average protein structure along the system's trajectory. The RMSF captures the fluctuation for each atom around its average position (Martínez, 2015; Margreitter and Oostenbrink, 2017). It is calculated using the equation below:

$$\mathbf{sRMSF} = \frac{(\mathbf{RMSF_i} - \overline{\mathbf{RMSF}})}{\boldsymbol{\sigma}\,(\mathbf{RMSF})} \qquad \text{(Eq 3.4.3)}$$

Where: $RMSF_i$ is the RMSF of the $i^{th}$ residue, from which the average RMSF is subtracted. This is then divided by the RMSF's standard deviation to yield the resultant standardized RMSF.

Radius of Gyration (RoG):

The radius of gyration in a protein can be calculated as the root mean square distance of the atoms from their common centroid/centre of gravity(Lobanov, Bogatyreva and Galzitskaya, 2008). This allows for the estimation of compactness of a protein complex along a trajectory(Huang and Paul, 2007; Pan and Patterson, 2013). RoG can determine how folded or unfolded a biomolecule over a given simulation period(Lobanov,

Bogatyreva and Galzitskaya, 2008), in addition, the overall stability of biomolecular structure over a given period can be determined from RoG calculation

Mathematically, RoG is calculated as follows;

$$\boldsymbol{r^2}\mathbf{gyr} = \left(\frac{\sum_{i-1}^{n} \boldsymbol{wi}\,(\boldsymbol{r_i} - \boldsymbol{r}^{-})\dot{\mathbf{2}}}{\sum_{i-1}^{n} \boldsymbol{wi}}\right) \qquad \text{(Eq 3.4.9)}$$

Where $r_i$ represents the position of the atom $i^{th}$ atom whiles r is the center weight of atom i.

The average RoG is calculated by taking the average over the number of frames in a

trajectory (Lobanov, Bogatyreva and Galzitskaia, no date).

Solvent Accessible Surface Area (SASA)

The solvent-accessible surface area (SASA), is a derivative of the area over which absolute contact between the proteins' Van der Waals surface and the solvent arises. This feature gives information relative to the compactness of the structure as well as the magnitude of hydrophobicity in the interior of the folded protein which is important for biomolecular stability (Richmond, 1984).

*3.6.1.2 Thermodynamic Energy Calculations*

Calculations of binding energy are crucial in computational chemistry studies as they are the endpoint method that accounts for the ligand-receptor interactions. Approximations of binding free energy lead to the development of various algorithms including energy perturbations, thermodynamic integration, molecular docking calculations, etc (Vakal, 2017).

The Molecular Mechanics/Generalized Born Surface Area method (MM/GBSA) methods have been regarded as the most accurate and efficient method in estimating binding free energies for biological macromolecules (Homeyer and Gohlke, 2012). The free binding energy computed by these methods for a protein system which comprises of the complex, ligand and receptor can be represented as:

$$\Delta G_{bind} = G_{complex} - G_{receptor} - G_{ligand} \quad \text{(Eq 3.4.4)}$$

$$\Delta G_{bind} = E_{gas} + G_{sol} - TS \quad \text{(Eq 3.4.5)}$$

$$E_{gas} = E_{int} + E_{vdw} + E_{ele} \quad \text{(Eq 3.4.6)}$$

$$G_{sol} = G_{GB/PB} + G_{SA} \quad \text{(Eq 3.4.7)}$$

$$G_{SA} = \gamma SASA \quad \text{(Eq 3.4.8)}$$

Here, Egas symbolizes gas-phase energy consisting the internal energy $E_{int}$; Coulomb energy $E_{ele}$ and the van der Waals energy $E_{vdw}$. The $E_{gas}$ was calculated from the FF14SB. $G_{sol}$ is the solvation free energy that was computed from the polar states, non-polar states, and $G_{GB/PB}$ energy contribution. GSA is the non-polar solvation energy. $G_{SA}$ was calculated from the solvent accessible surface area (SASA) by utilizing a water probe radius of 1.4 Å, while the polar solvation $G_{GB/PB}$ involvement was calculated by solving the equation of GB/PB (Rastelli *et al.*, 2010; Genheden and Ryde, 2015).T and S signifies the total entropy of the temperature and solute respectively. The MM/GBS and MM/PBSA algorithms propose quantifiable analysis of the binding affinity of the inhibitor to the protein and thus enables to explain molecular docked structures.

## 3.7 Other Molecular Modeling Tools Used in this Study

### *3.7.1 Molecular Docking*

Molecular docking has become a fundamental tool in the drug discovery industry. It employs multiple methods to predict the binding affinity and configuration of a complex. Most general use of docking is in ligand-receptor complexes, although other uses are documented. There are two major steps in docking:

1. Sample conformations of a ligand in the active site of the protein.

   Different algorithms may be used when sampling the numerous conformations of the docked complex. This can be the “lock and key” model which describes the

ligand and receptor as rigid structures, or the ligand may reflect flexibility by random or simulation-based methods. The latter algorithm is the frequently used method as it permits a more realistic fit of the ligand to the protein (Morris and Lim-Wilby, 2008).

2. Ranking the different conformations by scoring function.

   The scoring function may be based on statistically preferred contacts, MM force fields or pre-existing protein-ligand binding affinities (Morris and Lim-Wilby, 2008).

Molecular docking comes with many inconsistencies (Chen, 2015). Docked compounds are often criticized due to incorrect binding sites or choice of docked complex (Ferreira *et al.*, 2015). Due to this inconsistencies issues, all docked complexes in this study were verified with MD simulations and the stability of the ligand at the active site was demonstrated.

## 3.8 References:


Adcock, S. A. and McCammon, J. A. (2006a) 'Molecular dynamics: survey of methods for simulating the activity of proteins.', *Chemical reviews*. Howard Hughes Medical Institute, 106(5), pp. 1589–615. doi: 10.1021/cr040426m.

Adcock, S. A. and McCammon, J. A. (2006b) 'Molecular dynamics: survey of methods for simulating the activity of proteins.', *Chemical reviews*, 106(5), pp. 1589–615. doi: 10.1021/cr040426m.

Atkins, P. and Paula, J. De (2009) *Atkins' physical chemistry*, *Chemistry*. doi: 10.1021/ed056pA260.1.

Atkins, P. W. and Friedman, R. (2011) *Molecular Quantum Mechanics*, *Oxford Universiy Press*.

Bahrami, M. *et al.* (2014) 'The Schrödinger–Newton equation and its foundations', *New Journal of Physics*. IOP Publishing, 16(11), p. 115007. doi: 10.1088/1367-2630/16/11/115007.

Bajorath, J. (2012) 'Progress in computational medicinal chemistry', *Journal of Medicinal Chemistry*, pp. 3593–3594. doi: 10.1021/jm300429z.

Beringer, J. and Others (2014) '2014 Review of Particle Physics', *Physical Review D*, 38#9(September 2014), pp. 1–1676. doi: 10.1088/1674-1137/38/9/090001.

Bludman, S. and Daitch, P. B. (1954) 'Validity of the Born-Oppenheimer approximation', *Physical Review*, 95(3), pp. 823–830. doi: 10.1103/PhysRev.95.823.

Born, M. and Oppenheimer, J. R. (1927) 'Born-Oppenheimer approximation', *Ann. Phys. (Leipzig)*, 84(may), p. 457. doi: 10.1007/978-3-662-44593-8.

Bornemann, F. A., Nettesheim, P. and Schütte, C. (1998) 'Quantum-classical molecular dynamics as an approximation to full quantum dynamics', *The Journal of Chemical Physics*. American Institute of Physics, 105(3), p. 1074. doi: 10.1063/1.471952.

Bose, S. N. (1924) 'Planck 's Law and Light Quantum Hypothesis .', *Zeitschrift für Physik*, 26(Received), pp. 1–4. doi: 10.1007/BF01327326.

Bowen, J. P. and Allinger, N. L. (2007) ‘Molecular Mechanics: The Art and Science of Parameterization’, *Reviews in Computational Chemistry*, 2, pp. 81–97. doi: 10.1002/9780470125793.ch3.

Brooks, B. R. *et al.* (2009) ‘CHARMM: The biomolecular simulation program’, *Journal of Computational Chemistry*. Wiley Subscription Services, Inc., A Wiley Company, 30(10), pp. 1545–1614. doi: 10.1002/jcc.21287.

Brüschweiler, R. (2003) ‘Efficient RMSD measures for the comparison of two molecular ensembles’, *Proteins: Structure, Function and Genetics*, 50(1), pp. 26–34. doi: 10.1002/prot.10250.

Case, D. A. *et al.* (2005) ‘The Amber biomolecular simulation programs’, *Journal of Computational Chemistry*, 26(16), pp. 1668–1688. doi: 10.1002/jcc.20290.

Chen, Y. C. (2015) ‘Beware of docking!’, *Trends in Pharmacological Sciences*. Elsevier Ltd, 36(2), pp. 78–95. doi: 10.1016/j.tips.2014.12.001.

Christen, M. *et al.* (2005) ‘The GROMOS software for biomolecular simulation: GROMOS05’, *Journal of Computational Chemistry*, pp. 1719–1751. doi: 10.1002/jcc.20303.

Cornell, W. D. *et al.* (1995) ‘A Second Generation Force Field for the Simulation of Proteins, Nucleic Acids, and Organic Molecules’, *Journal of the American Chemical Society*. American Chemical Society, 117(19), pp. 5179–5197. doi: 10.1021/ja00124a002.

Cournia, Z., Smith, J. C. and Ullmann, G. M. (2005) ‘A molecular mechanics force field for biologically important sterols’, *Journal of Computational Chemistry*, 26(13), pp. 1383–1399. doi: 10.1002/jcc.20277.

D’Espagnat, B. (2011) ‘Quantum Physics and Reality’, *Foundations of Physics*, 41(11), pp. 1703–1716. doi: 10.1007/s10701-011-9582-z.

Deslauriers, L. (2011) ‘Physics Class’, *Science*, 862(May), pp. 862–864. doi: 10.1126/science.1201783.

Dronamraju, K. R. (1999) ‘Erwin Schrödinger and the origins of molecular biology.’,

*Genetics*, 153(3), pp. 1071–6.

Earl, D. J. and Deem, M. W. (2008) 'Monte Carlo Simulations', in. Humana Press, pp. 25–36. doi: 10.1007/978-1-59745-177-2_2.

Elsawy, K. M., Hodgson, M. K. and Caves, L. S. D. (2005) 'The physical determinants of the DNA conformational landscape: An analysis of the potential energy surface of single-strand dinucleotides in the conformational space of duplex DNA', *Nucleic Acids Research*, 33(18), pp. 5749–5762. doi: 10.1093/nar/gki888.

Ferreira, L. G. *et al.* (2015) *Molecular docking and structure-based drug design strategies*, *Molecules*. doi: 10.3390/molecules200713384.

Galindo-Murillo, R., Roe, D. R. and Cheatham, T. E. (2015) 'Convergence and reproducibility in molecular dynamics simulations of the DNA duplex d(GCACGAACGAACGAACGC)', *Biochimica et Biophysica Acta - General Subjects*, 1850(5), pp. 1041–1058. doi: 10.1016/j.bbagen.2014.09.007.

Genheden, S. and Ryde, U. (2015) 'The MM/PBSA and MM/GBSA methods to estimate ligand-binding affinities.', *Expert opinion on drug discovery*, 10(5), pp. 449–61. doi: 10.1517/17460441.2015.1032936.

González, M. A. (2011) 'Force fields and molecular dynamics simulations', *Collection SFN*, 12, pp. 169–200. doi: 10.1051/sfn/201112009.

Griffiths, D. J. (2005) *Introduction to Quantum Mechanics*, *Quantum*.

Guest, M. F. and Sherwood, P. (2002) 'Computational chemistry applications: Performance on high-end and commodity-class computers', in *Proceedings - International Symposium on High Performance Computing Systems and Applications*, pp. 290–301. doi: 10.1109/HPCSA.2002.1019173.

Guvench, O. and MacKerell, A. D. (2008) *Comparison of protein force fields for molecular dynamics simulations., Methods in molecular biology (Clifton, N.J.)*. doi: 10.1007/978-1-59745-177-2_4.

Halgren, T. A. and Damm, W. (2001) 'Polarizable force fields', *Current opinion in*

*structural biology*, 11(2), pp. 236–42. doi: 10.1016/S0959-440X(00)00196-2.

Hanson, N. (1959) 'Copenhagen Interpretation of Quantum Theory', *American Journal of Physics*, 27(1), pp. 1–15. doi: doi: 10.1119/1.1934739.

Hollowood, T. J. (2013) 'The Copenhagen Interpretation as an Emergent Phenomenon', *Arxiv Preprints*, p. 33. doi: 10.1088/1751-8113/46/32/325302.

Homeyer, N. and Gohlke, H. (2012) 'Free energy calculations by the Molecular Mechanics Poisson-Boltzmann Surface Area method', *Molecular Informatics*, 31(2), pp. 114–122. doi: 10.1002/minf.201100135.

Honarparvar, B. *et al.* (2014) 'Integrated Approach to Structure-Based Enzymatic Drug Design: Molecular Modeling, Spectroscopy, and Experimental Bioactivity', *Chemical Reviews*. American Chemical Society, 114(1), pp. 493–537. doi: 10.1021/cr300314q.

Hospital, A. *et al.* (2015) 'Molecular dynamics simulations: advances and applications.', *Advances and applications in bioinformatics and chemistry : AABC*, 8, pp. 37–47. doi: 10.2147/AABC.S70333.

Hu, H., Elstner, M. and Hermans, J. (2003) 'Comparison of a QM/MM force field and molecular mechanics force fields in simulations of alanine and glycine "dipeptides" (Ace-Ala-Nme and Ace-Gly-Nme) in water in relation to the problem of modeling the unfolded peptide backbone in solution', *Proteins: Structure, Function and Genetics*, 50(3), pp. 451–463. doi: 10.1002/prot.10279.

Huang, H. J. *et al.* (2010) 'Current developments of computer-aided drug design', *Journal of the Taiwan Institute of Chemical Engineers*. Taiwan Institute of Chemical Engineers, 41(6), pp. 623–635. doi: 10.1016/j.jtice.2010.03.017.

Huang, Y. and Paul, D. R. (2007) 'Effect of molecular weight and temperature on physical aging of thin glassy poly(2,6-dimethyl-1,4-phenylene oxide) films', *Journal of Polymer Science Part B: Polymer Physics*. Wiley-Blackwell, 45(12), pp. 1390–1398. doi: 10.1002/polb.21173.

Hull, D. L., Tessner, P. D. and Diamond Jr., A. M. (1978) 'Planck's Principle', *Science*, 202(4369), pp. 717–723. doi: 10.1126/science.202.4369.71.

Jarosaw Meller (2001) ‘Molecular Dynamics’, *Encyclopedia of Life Sciences*, pp. 1–8. doi: 10.1021/jp909004y.

Jensen, F. (2002) ‘Introduction to Computational Chemistry’, *Design*, 2, p. 429.

Jensen, F. (2007) *Introduction to Computational Chemistry*, *Angewandte Chemie International Edition*. doi: 10.1007/s00214-013-1372-6.

Kang, L., Liu, Z. and Guo, Q. (2014) ‘A force fields-based multi-scale docking method in drug molecular design’, in *Proceedings 2014 IEEE International Conference on Security, Pattern Analysis, and Cybernetics, SPAC 2014*, pp. 139–142. doi: 10.1109/SPAC.2014.6982674.

Kober, M. (2009) ‘Copenhagen Interpretation of Quantum Theory and the Measurement Problem’, *arXiv*, p. 9.

Laskin, N. (2002) ‘Fractional Schrodinger equation’, *Physical Review E*, 66(5), p. 18. doi: 10.1103/PhysRevE.66.056108.

Leach, A. . (2001) *Molecular Modelling: Principles and Applications, 2nd Edition*.

Leszczynski, J. (2012) *Handbook of computational chemistry*, *Handbook of Computational Chemistry*. doi: 10.1007/978-94-007-0711-5.

Levitt, M. (1976) ‘A simplified representation of protein conformations for rapid simulation of protein folding.’, *Journal of molecular biology*, 104(1), pp. 59–107. Available at: http://www.ncbi.nlm.nih.gov/pubmed/957439 (Accessed: 14 January 2019).

Lewars, E. (2011) *Computational chemistry*, *Computational Chemistry*. doi: 10.1007/978-90-481-3862-3.

Lobanov, M. I., Bogatyreva, N. S. and Galzitskaia, O. V (no date) ‘[Radius of gyration is indicator of compactness of protein structure].’, *Molekuliarnaia biologiia*, 42(4), pp. 701–6. Available at: http://www.ncbi.nlm.nih.gov/pubmed/18856071 (Accessed: 12 July 2018).

Lobanov, M. Y., Bogatyreva, N. S. and Galzitskaya, O. V. (2008) ‘Radius of gyration as an indicator of protein structure compactness’, *Molecular Biology*, 42(4), pp. 623–628. doi: 10.1134/S0026893308040195.

Lu, X. *et al.* (2016) ‘QM/MM free energy simulations: recent progress and challenges’, *Molecular Simulation*. Taylor & Francis, 42(13), pp. 1056–1078. doi: 10.1080/08927022.2015.1132317.

Margreitter, C. and Oostenbrink, C. (2017) ‘MDplot : Visualise Molecular Dynamics’, *The R Journal*, 9(June), pp. 164–186.

Marques, H. M. and Brown, K. L. (2002) ‘Molecular mechanics and molecular dynamics simulations of porphyrins, metalloporphyrins, heme proteins and cobalt corrinoids’, *Coordination Chemistry Reviews*, 225(1–2), pp. 123–158. doi: 10.1016/S0010-8545(01)00411-8.

Martínez, L. (2015) ‘Automatic Identification of Mobile and Rigid Substructures in Molecular Dynamics Simulations and Fractional Structural Fluctuation Analysis’, *PLoS ONE*. Edited by J. Kleinjung. San Francisco, CA USA: Public Library of Science, 10(3), p. e0119264. doi: 10.1371/journal.pone.0119264.

Matsika, S. (2010) ‘The Born-Oppenheimer approximation’, *The Journal of chemical physics*, 133(22), p. 224103. doi: 10.1063/1.3511638.

Mittelstaedt, P. (2008) ‘Planck’s constant in the light of quantum logic’, in *International Journal of Theoretical Physics*, pp. 104–113. doi: 10.1007/s10773-007-9380-8.

Montoya, A., Mondragón, F. and Truong, T. N. (2002) ‘Adsorption on carbonaceous surfaces: Cost-effective computational strategies for quantum chemistry studies of aromatic systems’, *Carbon*, 40(11), pp. 1863–1872. doi: 10.1016/S0008-6223(02)00035-0.

Morris, G. M. and Lim-Wilby, M. (2008) ‘Molecular docking.’, *Methods in molecular biology (Clifton, N.J.)*, 443, pp. 365–382. doi: 10.1007/978-1-59745-177-2_19.

Müller, I. (2008) ‘Max Planck - A life for thermodynamics’, *Annalen der Physik (Leipzig)*, 17(2–3), pp. 73–87. doi: 10.1002/andp.200710274.

Nair, P. C. and Miners, J. O. (2014) ‘Molecular dynamics simulations: from structure function relationships to drug discovery.’, *In Silico pharmacology*, 2(4), pp. 1–4. doi: 10.1186/s40203-014-0004-8.

Pan, L. and Patterson, J. C. (2013) ‘Molecular Dynamics Study of Zn(Aβ) and Zn(Aβ)2’, *PLoS ONE*. Edited by J. Zheng. Public Library of Science, 8(9), p. e70681. doi: 10.1371/journal.pone.0070681.

Phillips, J. C. *et al.* (2005) ‘Scalable molecular dynamics with NAMD.’, *Journal of computational chemistry*, 26(16), pp. 1781–802. doi: 10.1002/jcc.20289.

Ponder, J. W. and Case, D. A. (2003) ‘Force fields for protein simulations’, *Advances in Protein Chemistry*, pp. 27–85. doi: 10.1016/S0065-3233(03)66002-X.

Quincey, P. (2013) ‘Planck’s constant as a natural unit of measurement’, *Physics Education*, 48(5), p. 597. doi: 10.1088/0031-9120/48/5/597.

Ramachandran, K. I., Deepa, G. and Namboori, K. (2008) *Computational Chemistry and Molecular Modeling*, *Computational Chemistry and Molecular Modeling: Principles and Applications*. doi: 10.1007/978-3-540-77304-7.

Ramírez, D. (2016) ‘Computational Methods Applied to Rational Drug Design’, *The Open Medicinal Chemistry Journal*, 10(1), pp. 7–20. doi: 10.2174/1874104501610010007.

Rastelli, G. *et al.* (2010) ‘Fast and accurate predictions of binding free energies using MM-PBSA and MM-GBSA’, *Journal of Computational Chemistry*, 31(4), pp. 797–810. doi: 10.1002/jcc.21372.

Richmond, T. J. (1984) ‘Solvent accessible surface area and excluded volume in proteins. Analytical equations for overlapping spheres and implications for the hydrophobic effect.’, *Journal of molecular biology*, 178(1), pp. 63–89. Available at: http://www.ncbi.nlm.nih.gov/pubmed/6548264 (Accessed: 2 April 2018).

Rohland, N. and Reich, D. (2012) ‘Cost-effective , high-throughput DNA sequencing’, *Genome research*, 22, pp. 939–946. doi: 10.1101/gr.128124.111.

Sauer, J. and Sierka, M. (2000) ‘Combining quantum mechanics and interatomic potential functions inab initio studies of extended systems’, *Journal of Computational Chemistry*. John Wiley & Sons, Ltd, 21(16), pp. 1470–1493. doi: 10.1002/1096-987X(200012)21:16<1470::AID-JCC5>3.0.CO;2-L.

Senn, H. M. and Thiel, W. (2009) ‘QM/MM methods for biomolecular systems.’, *Angewandte Chemie (International ed. in English)*, 48(7), pp. 1198–229. doi: 10.1002/anie.200802019.

Shao, J. *et al.* (2007) ‘Clustering molecular dynamics trajectories: 1. Characterizing the performance of different clustering algorithms’, *Journal of Chemical Theory and Computation*, 3(6), pp. 2312–2334. doi: 10.1021/ct700119m.

Shattuck, T. W. (2003) ‘Molecular Mechanics Tutorial’, *Structure*, (November).

Shurki, A. and Warshel, A. (2003) ‘Structure/function correlations of proteins using MM, QM/MM, and related approaches: methods, concepts, pitfalls, and current progress.’, *Advances in protein chemistry*, 66, pp. 249–313. Available at: http://www.ncbi.nlm.nih.gov/pubmed/14631821 (Accessed: 14 January 2019).

Stapp, H. P. (1972) ‘The Copenhagen Interpretation’, *American Journal of Physics*, 40(8), pp. 1098–1116. doi: 10.1119/1.1986768.

Tsai, C. S. (2002) ‘Molecular modeling: molecular mechanics’, *An introduction to computational biochemistry*, pp. 285–314.

Vakal, S. (2017) ‘Current approaches and tools for binding energy prediction in computer-aided drug design’, *Journal of Chemical and Pharmaceutical Science*, 10(1), pp. 685–694.

Vanommeslaeghe, K. *et al.* (2014) ‘Molecular mechanics.’, *Current pharmaceutical design*, 20(20), pp. 3281–92. doi: 10.1016/j.biotechadv.2011.08.021.Secreted.

Wallrapp, F. H. and Guallar, V. (2011) ‘Mixed quantum mechanics and molecular mechanics methods: Looking inside proteins’, *Wiley Interdisciplinary Reviews: Computational Molecular Science*, pp. 315–322. doi: 10.1002/wcms.27.

Wang, J. *et al.* (2004) ‘Development and testing of a general amber force field’, *Journal of Computational Chemistry*, 25(9), pp. 1157–1174. doi: 10.1002/jcc.20035.

Wang, J. *et al.* (2005) ‘Antechamber, An Accessory Software PackageFor Molecular Mechanical Calculation’, *J. Comput. Chem.*, 25(2), pp. 1157–1174. doi: 10.1234/2013/999990.

Woolley, R. G. (1991) ‘Quantum chemistry beyond the Born-Oppenheimer approximation’, *Journal of Molecular Structure: THEOCHEM*, 230, pp. 17–46. doi: 10.1016/0166-1280(91)85170-C.

Woolley, R. G. and Sutcliffe, B. T. (1977) ‘Molecular structure and the born—Oppenheimer approximation’, *Chemical Physics Letters*, 45(2), pp. 393–398. doi: 10.1016/0009-2614(77)80298-4.

Wudka, J. (1990) ‘Remarks on the Born-Oppenheimer approximation’, *Physical Review D*, 41(2), pp. 712–714. doi: 10.1103/PhysRevD.41.712.

Young, D. C. (2001) *Computational Chemistry: A Practical Guide for Applying Techniques to Real World Problems*. New York, USA: John Wiley & Sons, Inc. doi: 10.1002/0471220655.

Zettili, N. (2009) *Quantum Mechanics: Concepts and Applications, 2nd edn.*, *Contemporary Physics*. doi: 10.1080/00107514.2010.547600.

Zheng, M. *et al.* (2013) ‘Computational methods for drug design and discovery: Focus on China’, *Trends in Pharmacological Sciences*, pp. 549–559. doi: 10.1016/j.tips.2013.08.004.

Zinkernagel, H. (2011) ‘Some trends in the philosophy of physics’, *Theoria-Revista De Teoria Historia Y Fundamentos De La Ciencia*, pp. 215–241.

# CHAPTER 4

## The Perplexity of Synergistic Duality: Inter-Molecular Mechanisms of Communication in Bcr–Abl1

Ahmed A Elrashedy[1], Pritika Ramharack[1], Mahmoud E. S. Soliman[1*]

[1]Molecular Bio-computation and Drug Design Laboratory, School of Health Sciences, University of KwaZulu-Natal, Westville Campus, Durban 4001, South Africa

[*]Email: soliman@ukzn.ac.za

Telephone: +27 (0) 31 260 8048, Fax: +27 (0) 31 260 78

## Abstract

**Background:** Aberrant and proliferative expression of the oncogene Bcr-Abl in bone marrow cells is one of the prime causes of chronic myeloid leukemia (CML). It has been established that the tyrosine kinase domain of the Bcr-Abl protein is a potential therapeutic target for the treatment of CML. Although first and second line inhibitors against the enzyme are available, recent studies have indicated that monotherapeutic resistance has become an aggrieved challenge.

**Objective:** In recent studies, the dual inhibition of Bcr-Abl by Nilotinib and Asciminib was shown to overcome drug resistance. This prompted us to investigate the dynamic behind this novel drug combination.

**Methods:** By the utilization of a wide range of computational tools, we define and compare Bcr-Abl's structural and dynamic characteristics when bound as a dual inhibitor system.

**Results:** Conformational ensemble analysis presented a sustained inactive protein, as the activation loop, inclusive of the characteristic Tyr257, remained in an open position due to the unassailable binding of Asciminib at the allosteric site. Nilotinib also indicated more propitious binding at the catalytic site in the presence of Asciminib, thus exposing new avenues in treating Nilotinib-resistance. This was in countenance with intermolecular hydrogen bond interactions with key binding site residues GLU399, Asn259 and Thr252.

**Conclusion:** The investigations carried out in this study give rise to new possibilities in the treatment of resistance in CML, as well as assisting in the design of novel and selective inhibitors as dual anti-cancer drugs.

## 4.1 Introduction

Chronic myelogenous or myeloid leukemia (CML) is a cancer of white blood cells (WBCs), distinguished by an increase in leukemic blasts (white cells), also called granulocytes. As the CML matures, the granulocytes leak out of the bone marrow and circulate through the bloodstream, thus leading to a shortage of red blood cells and platelets, causing anemia, bruising and/or bleeding [1,2]. CML is present in about 15-25% of all adult leukemia [2], with an annual incidence rate of 1 to 2 cases per 100 000 [3]. Being Philadelphia chromosome positive, CML is characterized by a translocation between chromosome 9 and 22, thus leading to an alteration in the breakpoint cluster region (Bcr) and allowing for the formation of the Bcr-Abl gene [4]. A breakpoint in BCR leads to the formation of a fusion protein [5,6], which results in the phosphorylation of the Bcr-Abl protein [7,8]. This phosphorylated Bcr-Abl protein leads to deregulated tyrosine kinase activity, a characteristic feature of CML [9-10].

The Bcr-Abl protein is formed from two portions: first, the N-Terminal that comprises of the SH2 and SH3 domains and N-Terminal cap that plays a significant role in the regulation of kinase activity and secondly, the C-terminal which is composed of an array of signaling and recognition domains that are involved in many cellular functions, including a DNA-binding domain, and actin-binding domain [11] (Figure 4.1).

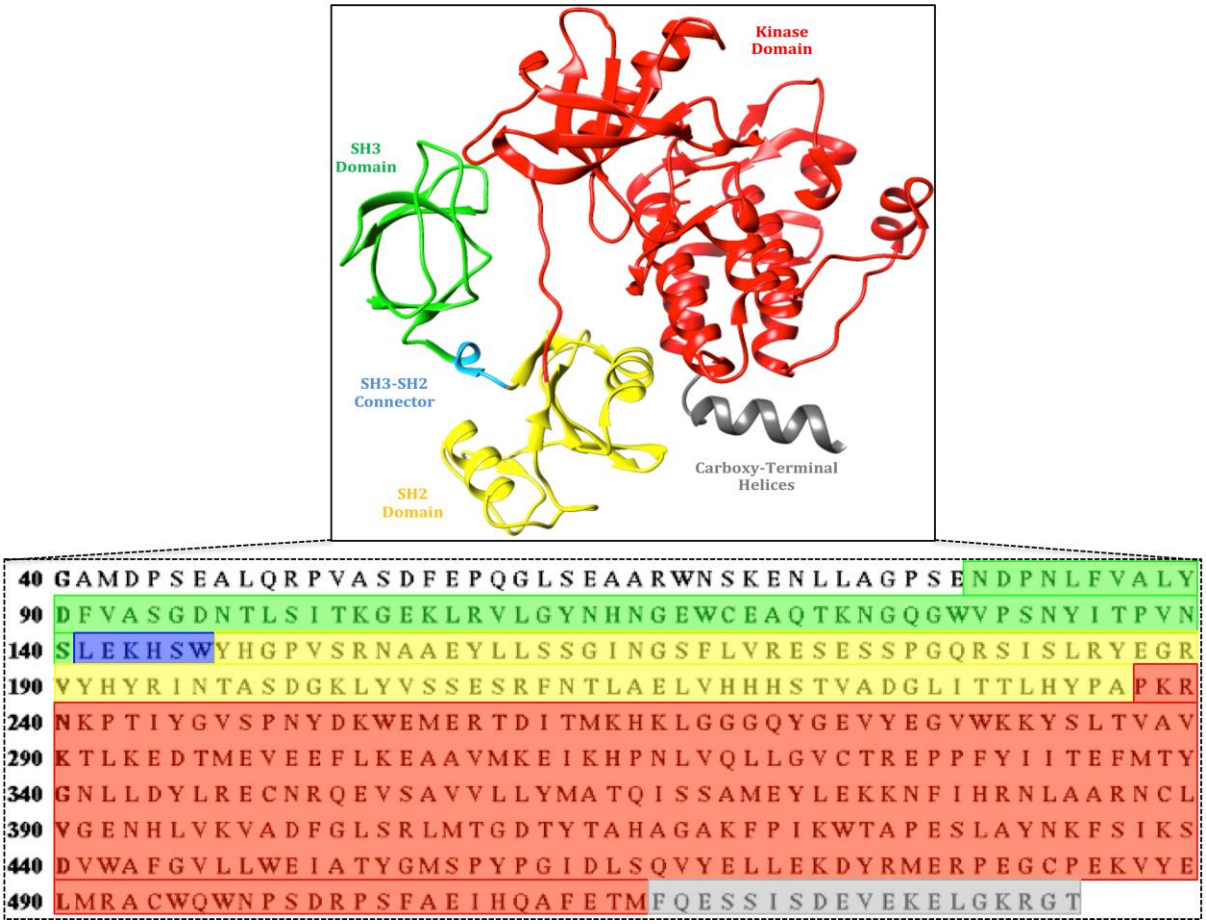


**Figure 4.1:** The 3-D crystal structure of the Bcr-Abl protein (PDB code: 1OPK). The SH3, SH2 and kinase domains are shown in green, yellow and red, respectively. The SH3-SH2 connector is depicted in blue and the carboxy-terminal helix in gray.

Under normal conditions, Abl is regulated with very low kinase activity, while in chronic myelogenous leukemia (CML), it is controlled by a series of intramolecular interactions from both SH3 and SH2 domains. Enzymatic studies of Bcr-Abl suggest the native enzyme may be distinguished into two principle components, being active and inactive/autoinhibited [12].

One of the most promising new drug therapies for CML is Asciminib. This drug binds allosterically to Bcr-Abl, targeting the myristoyl pocket (allosteric site to which natural

substrate, myristate binds) of the protein. In physiological conditions, the myristoylated N-terminus of ABL acts as a regulator of kinase activity, however, this is lost upon fusion with BCR in CML. The Asciminib drug was designed to restore the autoregulatory function of Bcr-Abl fusion protein, thus inhibiting oncogenic signaling. Recent studies have shown that monotherapy using Asciminib led to tumor regression in mice xenografted with KCL22 CML cell line. Despite this, however, all of the tumors eventually recurred [13–15]. Although this drug has been proven to inhibit the Bcr-Abl protein in multiple studies[16] , there are also numerous investigations on Asciminib-resistance susceptibility in multiple CML cell lines[13,17,18].

Imatinib has been previously reported to competitively bind to the ATP active site, thus leading to a loss in Bcr-Abl activity and an eventual suppression of CML [19]. Nilotinib, is structurally similar to the Imatinib, but with molecular alterations that provide higher affinity towards Bcr-Abl. Nilotinib is 10 to 50-fold more potent than Imatinib against ABL and shows higher efficacy against multiple CML mutants. The drug, together with Dastinib has been previously used against drug resistant CML, with Nilotinib being approved by the FDA as a drug of choice for the treatment of patients who become resistant to imatinib or in advanced stage of the disease [20–24]. Nilotinib has also been used as a multitherapy, treating various proteins including ABL, PDGFRA and KIT in gastrointestinal stromal tumors, as well as acute and chronic myeloid leukemia [25]. Figure 4.2 shows the structures of the currently available drugs against Bcr-Abl.

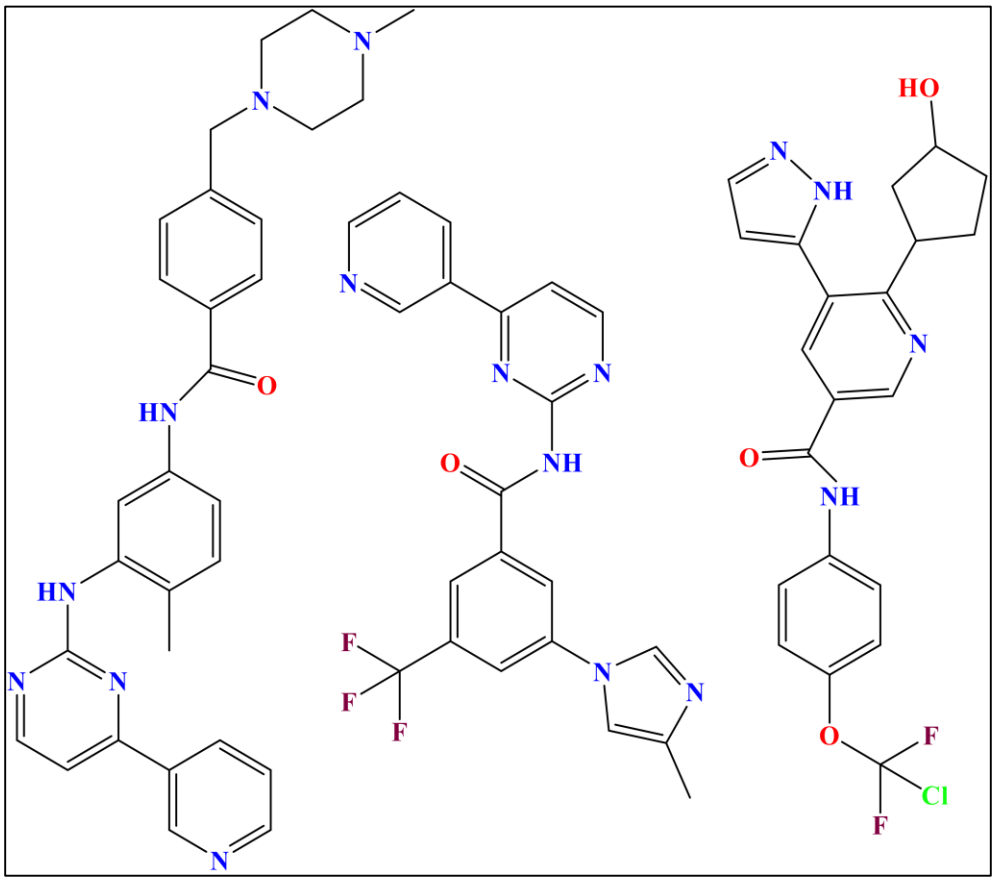


**Figure 4.2**: The 2-D structures of Bcr-Abl inhibitors: (**left**) Imatinib, (**centre**) Nilotinib, (right) Asciminib.

Combination therapy involving both catalytic and allosteric site inhibitors have shown abundant potential in improving the outcome of CML treatment and overcoming monotherapeutic resistance [13,15]. With the availability of drugs for both the allosteric and active site, there is an urgent need to get new insights into the structural basis of potential dual inhibition. This would allow for a greater understanding of effective co-administrative treatments against CML. A recent study by Wylie *et al* (2017) demonstrated, with the use of NMR and crystallography, the dual targeting of Bcr-Abl with potent inhibitor Asciminib at the allosteric, myristoyl pocket of the protein and Nilotinib at the catalytic pocket [17]. These results indicated Asciminib bound in a similar conformation to that of myristate and when bound in combination with Nilotinib, led to tumour regression in mice. It was interesting to note that even after the stopping the combination dosage, no evidence of

tumor re-growth was observed. To further assess the dosage of Asciminib in CML patients, a phase 1 clinical trial was initiated (ClinicalTrials.gov identifier: NCT02081378). To further validate the study, a crystal structure of the protein in complex with both Nilotinib and Asciminib was reported (PDB code: 5MO4) [17]. Preliminary results on patients receiving an escalated dose of the compound revealed well-tolerated dose-dependent pharmacokinetics. Other studies by Cowan-Jacob (2016) and Schoepfer *et al* (2018) further exemplified the potency of Asciminib as an allosteric inhibitor against the Bcr-Abl protein in CML [26,27]. Based on the above-mentioned experimental investigation, we present, in this study, the first account of the structural mechanism of inhibition induced by co-binding of allosteric (Asciminib) and catalytic (Nilotinib) inhibitors (Figure 4.3).

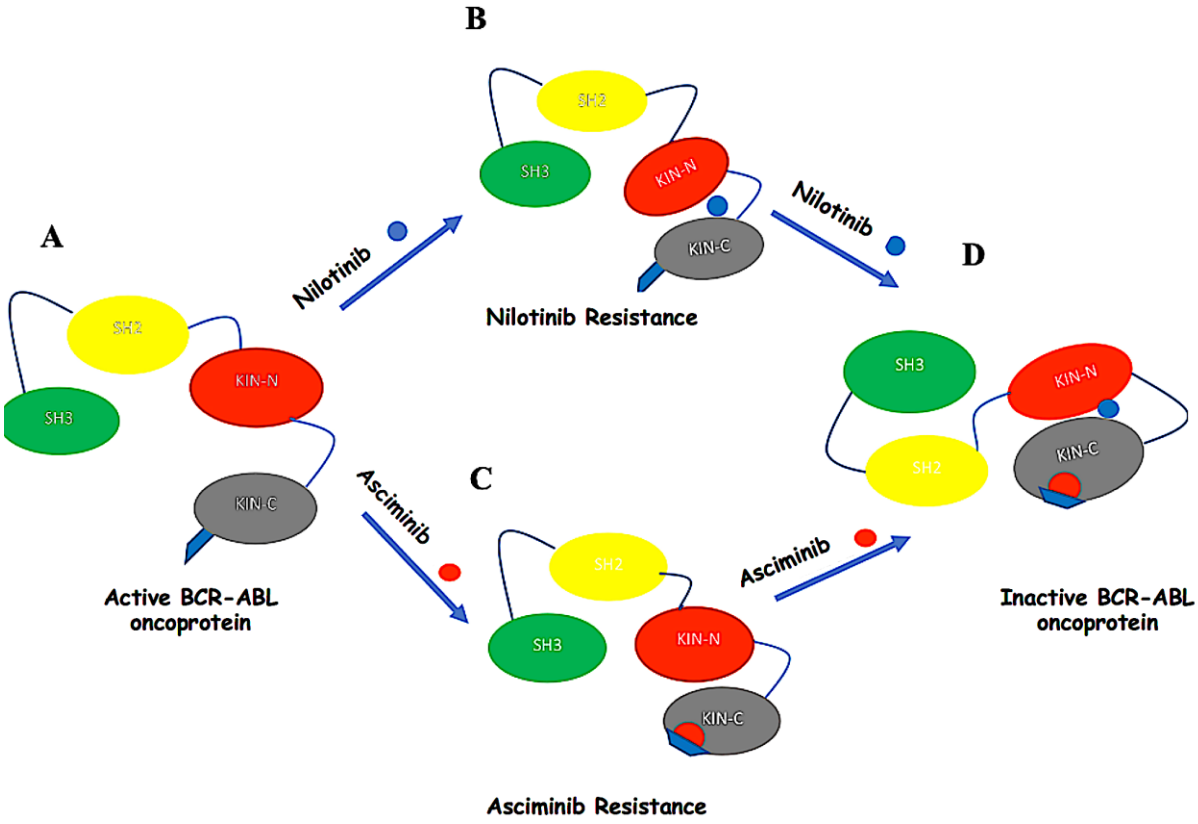


**Figure 4.3:** Schematic representation of the conformational equilibrium of Bcr-Abl in open and closed states in the presence and absence of inhibitors, **[A]** Apo Bcr-Abl active flexible, Without a ligand bound to the Allosteric site, the carboxy-terminal helix is flexible **[B]** Binding of nilotinib to the catalytic site shifts this equilibrium to the open state (active form) **[C]** Binding of Asciminib to the allosteric site fixes the carboxy-terminal helix (blue)

and stabilizes the closed state by reducing steric clashes. **[D]** Combined binding of Nilotinib and Asciminib shifts the equilibrium to the closed state (inactive rigid conformation).

Multi-targeted therapies have become extremely popular in cancer treatments over recent years. A study by Block *et al*., (2015) described the feasibility of therapeutics against a wide range of cancer targets, thus eliminating the potential of drug resistance as observed with monotherapies [28]. Molecules that control cell proliferation and death, including tyrosine kinase receptors can be targeted with two classes of compounds, being trastuzamab and imatinib. The main concern with these compounds is the problem of relapse and resistance [29]. Based on these results, there is now an agreement that molecules that target multiple agents may be more effective. Our study aims to add to the broad-spectrum approach elucidated on in the above-mentioned article, thus increasing the number of combinatorial low-toxicity agents that will simultaneously inhibit a network of targets in cancer metabolism.

By the utilization of a wide range of *in silico* tools, we define and compare Bcr-Abl's structural and dynamic characteristics when bound as a dual inhibitor system. Furthermore, we provide a binding landscape of this synergistic dual inhibition, thus providing an attenuation mechanism for Asciminib-resistance. Further studies beyond this investigation will be to test the dual inhibitory mechanism on other cancer targets, thus increasing the chance of a multitherapeutic combination.

## 4.2 Computational Methods

### *4.2.2 System Preparation*

The Bcr-Abl tyrosine kinase in complex with PD166326 and Myristic acid (PDB code: 1OPK)[12] was obtained from RSCB Protein Data Bank[30]. Although the crystal structure used in the study originates from the Mus musculus organism, superimposition of the crystal structure to mutated human Bcr-Abl (PDB code: 5MO4)[17] shows no significant structural or sequential differences between the organisms, thus permitting structural extrapolation to human CML (Figure S1). The 3-D structure of the inhibitors, Nilotinib and

Asciminib, were obtained from PubChem[31]. The Apo structure was prepared by manually deleting the solvent and any bound small molecules from the crystal structure. Docking was carried on both catalytic and allosteric active sites using Autodock Vina[32] to obtain the Nilotinib, Asciminib and Nilotinib-Asciminib complexes. In total, four systems were subjected to 190ns molecular dynamic simulations as described in "Molecular Dynamic Simulations" section. Protein and ligand alterations as well as visualizations were conducted in Chimera software [33].

### *4.2.2 Molecular Dynamic (MD) Simulations*

Molecular dynamic (MD) simulations are an important tool to determine the physical movements of atoms and molecules, thus providing insights on the dynamical evolution of biological systems[34]. The MD simulations were carried out on the systems using the GPU version of AMBER 14, with an integrated SANDER module and the FF14SB variant of the AMBER force field[35]. This was followed by a standard simulation protocol previously adopted in our preceding studies [36–38].

### *4.2.3Post-Dynamic Analysis*

The coordinates of the complexes were each saved every 1 ps, followed by analysis using the CPPTRAJ[39] module employed in AMBER 14 suit. All plots were completed using the Origin data analysis tool and Chimera[33].

### *4.2.4 Binding Free Energy Calculations*

Calculation of the binding fee energy of small ligand to protein is one of the most important end point methods currently used in computational biophysics [40]. To determine the free binding energy of each system, the Molecular Mechanics/GB Surface Area method (MM/GBSA) was employed[41]. The explicit solvent employed in the MD simulation was discarded and replaced with a dielectric continuum [42] . The changes (Δ) in each term between complex state and unbound state were calculated and contributed to the total relative binding free energy [42]. Molecular mechanics force fields were then employed to calculate energy contributions from the atomic coordinates of the enzyme, ligands and the complex in a gas phase [42].

Binding free energy was averaged over 19,000 snapshots extracted from the 190ns trajectory. The free binding energy (ΔG) calculated by this method for each molecular species employs typical molecular mechanic equations, which have been elaborated on in a number of our previous publications [38,43] and will not be reiterated herein.

### 4.3 Results and Discussion

#### 4.3.1 Synergistic Duality: Allosteric versus Catalytic Inhibition

The basic concept of catalytic inhibition can be explained as a competitive mechanism. In CML conditions, the natural substrate, in this instance, ATP, would bind to the active site of Bcr-Abl and allow for continued deregulated tyrosine kinase activity. When a competitive inhibitor, such as Nilotinib, is administered, it would compete with ATP to bind to the active site. In most cases, drugs are designed to bind more strongly than that of the natural substrate, this allows sustained inhibition of the protein. However, if it were that simple for a drug to inhibit a protein, there would be no need for the design of new, more effective treatments. Drug resistance and adverse molecular interactions mainly due to target mutations have opened the drug discovery domain to identifying alternative means of inhibiting a drug target. Allosteric inhibition entails the binding of a drug to a hydrophobic pocket, other than the active site, thus affecting the conformation of the catalytic region and inhibiting binding of the natural substrate. In the case of CML, however, the Bcr-Abl has shown resistance to allosteric binding of Asciminib alone [44], therefore requiring researchers to go back to the drawing board. To further explain the synergistic dual targeting that Wylie et al., (2017) proposed experimentally, Asciminib binds to the allosteric, myristoyl pocket with a higher affinity than that of myristoyl [17]. Intramolecular interactions than occur between the molecular groups of Asciminib and the allosteric site amino acids, which lead to structural modifications of the enzyme, eventually leading to modification of the catalytic site, allowing for increased interactions upon binding of Nilotinib. These structural dynamics that allow for this synergistic inhibition is elucidated on below. The binding free energy changes are also presented to corroborate the conformational analysis.

### 4.3.2 Drug duality leads to an unwavering structural ensemble

The Bcr-Abl protein contains a characteristic "activation loop" that remains in a closed position whilst inactivated and opens out when the protein is to be activated. Studies have shown that the site in which Nilotinib binds to allows for this activation loop to remain closed and thus inactive [45]. To assess this theory, snapshots were taken at 80ns, to identify whether each complex remained closed subsequent to the binding of Nilotinib. It was evident from these snapshots that the characteristic loop remained in a closed position among all three complexes.

The stability of the MD simulation was determined by measuring the variations in the root mean square deviation (RMSD) of the C-α atoms across the 190ns trajectory. The RMSD results for all the systems are illustrated in Figure 4**.** All systems reached convergence after approximately 125 ns (RMSD deviation < 2 °A). The Asciminib (2.89Å) and Nilotinib (2.93Å) systems showed much higher RMSD fluctuations throughout the simulation system compared to that of the Asciminib-Nilotinib system (2.145Å). Figure 4.4

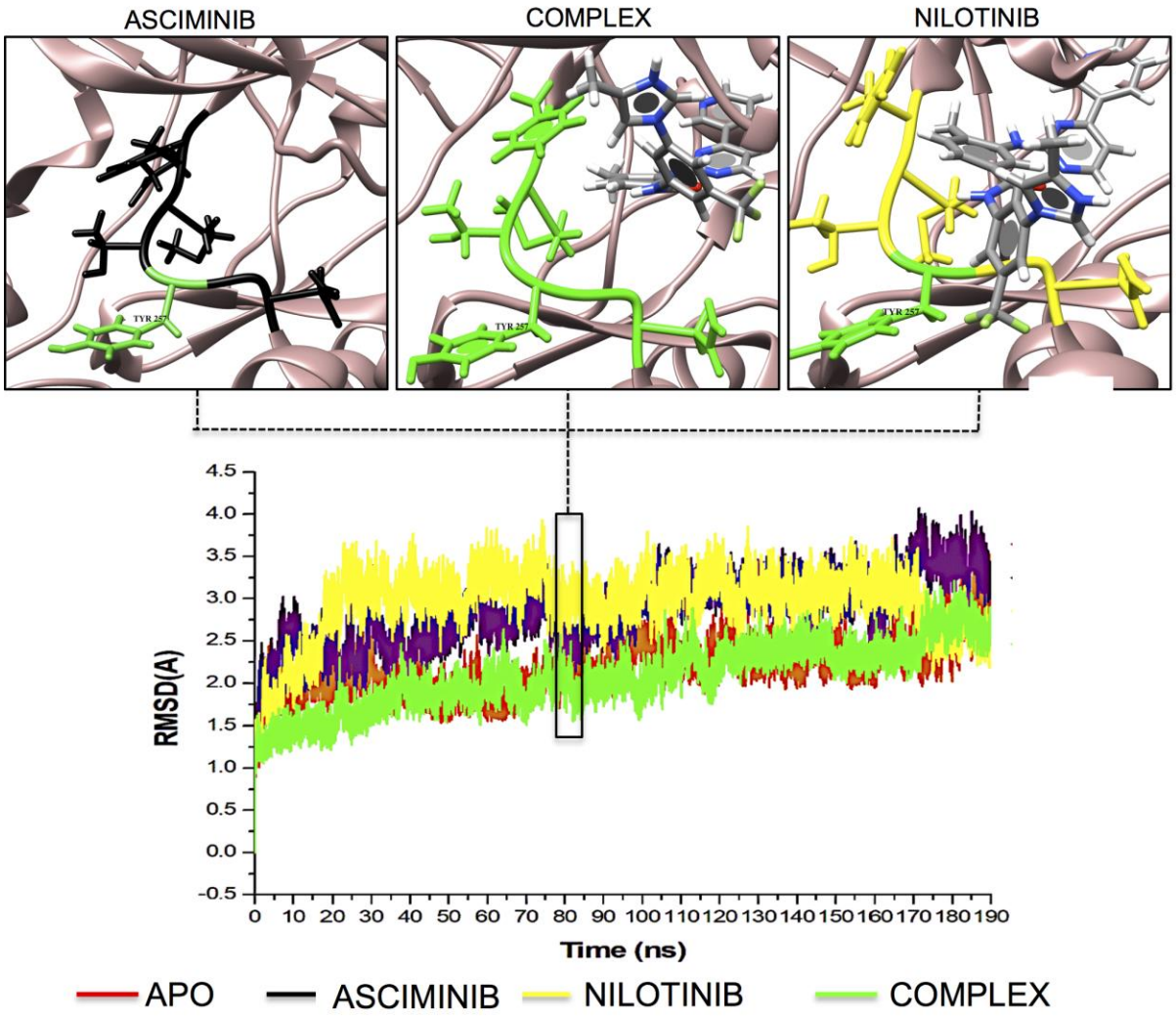


**Figure 4.4:** Root-mean-square deviation (RMSD) of the backbone atoms relative to the starting minimized structure over 190ns simulation for Apo, Asciminib, Nilotinib and Asciminib-Nilotinib systems. The "activation loop" of each system showed a closed structure, indicating a inactive protein.

The root mean square fluctuation (RMSF) of each residue in all four systems was analyzed to determine Bcr-Abl's structural changes upon ligand binding. Figure 4.5 clearly demonstrates greater residue fluctuations in the Asciminib system (14.54Å). This may be due to Bcr-Abl's flexibility to a closed state and previously illustratedL001 in figure 3. It is interesting to note that of the four systems, the Asciminib-Nilotinib system is the most

stable (9.98Å). This may be due to Nilotinib binding to the catalytic site of Bcr-Abl. These results could be potentially extrapolated to reveal that dual binding decreases the overall flexibility of Bcr-Abl (inactive form).

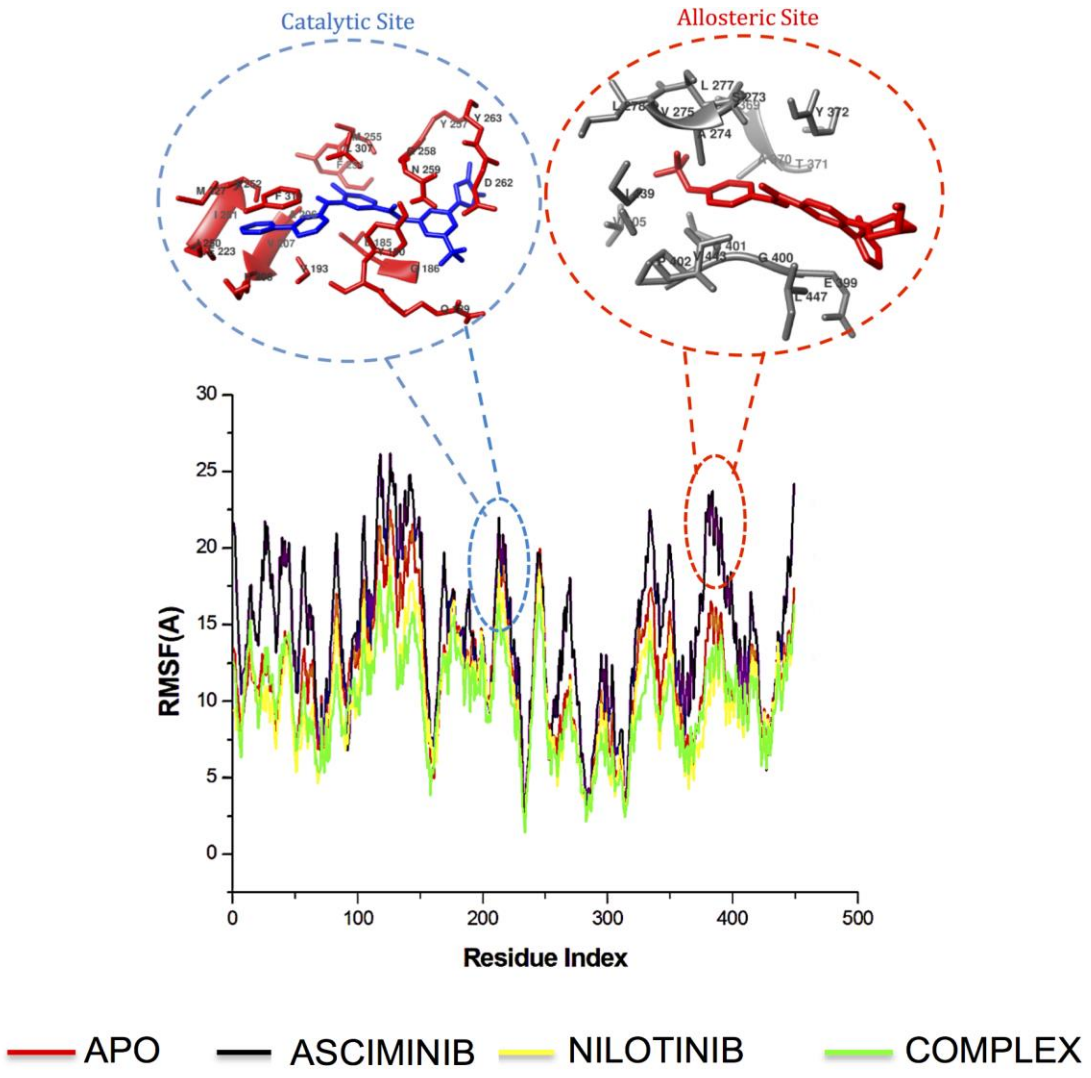


**Figure 4.5:** The RMSF of Bcr-Abl in each of the four systems relative to the starting minimized structure over 190 ns simulation.

The radius of gyration (Rg) was performed to give insights into the distribution of atoms from the center of mass of the complexes during MD simulations [46,47]. The Apo, Asciminib, Nilotinib and Asciminib-Nilotinib systems were measured, analyzed, and plotted as seen in figure S1. The Rg between the systems showed very similar structural

compactness, however, atomic distribution was seen in the Asciminib-Nilotinib system from 170-180ns.

Usually protein interactions are often accomplished by significant changes in the conformation, from folding to the unfolding of a protein. Bcr-Abl conformation studies had shown that the protein misfolding characterized its activity, indicating that the folded state characterized its activity [48,49]. To further support this statement, Solvent accessible surface area (SASA) was used to predict and determine the magnitude of compactness of each system's hydrophobic core (Figure S2). This was done by calculating the surface area of the protein visible to solvent across the duration of the molecular dynamics simulation which is essential in biomolecular stability [50].

Extrapolating from figure S1, the Asciminib-Nilotinib system showed an average surface area of 20578.21Å, indicating greater compactness compared to the rest of the systems. This, together with the results from RSMD, RMSF and radius of gyration prove that co-administration of Asciminib and Nilotinib results in a stable and more compact Bcr-Abl protein.

The results obtained from the above analysis prompted us to explore the thermodynamic binding landscape of Asciminib and Nilotinib to Bcr-Abl.

### 4.3.3 Co-binding of Asciminib and Nilotinib acts as a "thermodynamic safety-net"

To gain insight into the energetics of Bcr-Abl binding to Asciminib and Nilotinib, the total binding free energy of the three systems being, Asciminib and Nilotinib alone and then upon co-binding of the two drugs. The MM/GBSA approach was utilized to better understand the various energy contributions within the binding pocket.

As seen in Table 4.1, the difference in binding energy of Nilotinib when bound alone (-31.68 kcal/mol) to when co-bound (-38.19 kcal/mol) was 6.51 kcal/mol. This indicates more favorable binding when bound together with Asciminib. Although showing a smaller difference, the Asciminib also showed greater intramolecular energy when co-bound. The computed binding energies correlate well with the experimental $IC_{50}$ reported values [13,15]. The thermodynamic energy contribution of Nilotinib to the total binding free energy of the complex surmounts to the stability of Asciminib in the allosteric binding pocket and thus the stability of the complex during the simulation.

**Table 4.1**: Summary of free binding Energy contributions of Asciminib, Nilotinib and Asciminib-Nilotinib systems.

| **Energy Components (kcal/mol)** | | | | | |
|---|---|---|---|---|---|
| **Individual Binding of Ligands** | | | | | |
| | **$\Delta E_{vdW}$** | **$\Delta E_{elec}$** | **$\Delta G_{gas}$** | **$\Delta G_{solv}$** | **$\Delta G_{bind}$** |
| **Asciminib** | -47.74±0.06 | -20.29±0.14 | -68.04±0.17 | 28.99±0.12 | -39.04±0.08 |
| **Nilotinib** | -45.19 ± 0.06 | -142.23 ± 0.58 | -187.43 ± 0.57 | -159.75 ± 0.55 | -31.68 ± 0.062 |
| **Co-binding of Ligands** | | | | | |
| | **$\Delta E_{vdW}$** | **$\Delta E_{elec}$** | **$\Delta G_{gas}$** | **$\Delta G_{solv}$** | **$\Delta G_{bind}$** |
| **Asciminib** | -48.33±0.38 | -165.10±1.13 | -213.44±1.00 | -173.60±0.96 | -39.83±0.23 |
| **Nilotinib** | -45.12± 0.09 | -150.54 ±0.60 | -195.66 ±0.63 | -159.46 ± 0.58 | -38.19 ± 0.087 |

As evident from Table 1, that the electrostatic, Gibbs free energy, and solvation interactions were found to be the most favorable energy contributors to both Asciminib, Nilotinib binding to the protein.

Figure 4.6 illustrates the collective drug-binding landscape at an atomistic level. Catalytic site residues Asn259 and Thr252 formed stable hydrogen bonds with the hydroxyl and amino group of Nilotinib, while the amino group of Asciminib donated a hydrogen bond to residue Glu399. It is also interesting to note that highly electrostatic fluorine molecules were found at the based of the hydrophobic pocket in both the catalytic and active sites.

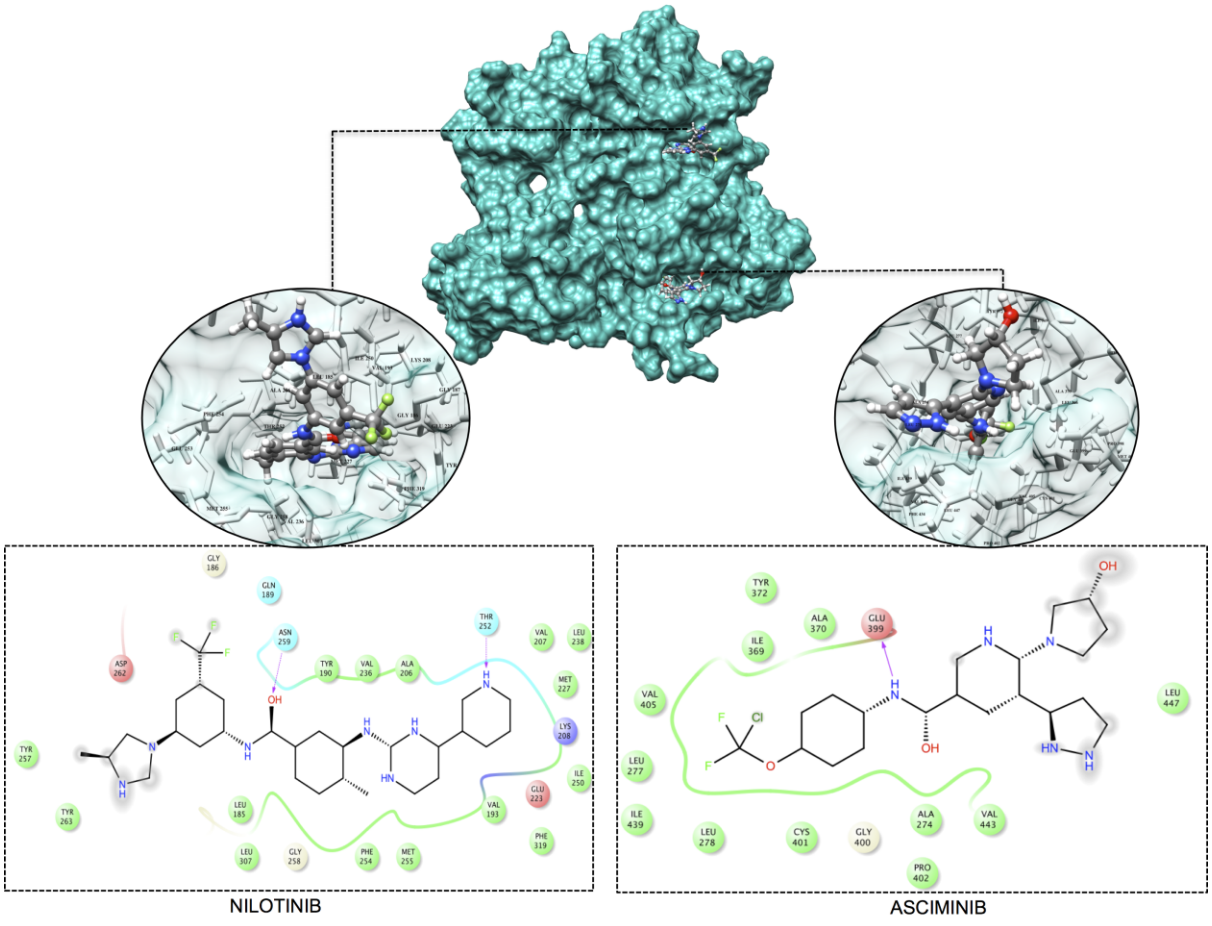


Figure 4.6: Surface representation of dual catalytic and allosteric inhibition of Bcr-Abl by Nilotinib and Asciminib. Nilotinib binds at the catalytic site while Asciminib binds at the allosteric pocket. Ligand interaction plot illustrates interactions between binding site

residues and the above drugs (grey haze demonstrates ionic interactions, pink arrows show hydrogen bonds and coloured lines indicate hydrophobic energy).

Based on the evidence from the above analysis, it may be deduced that the co-bound system demonstrated a more stable and compact system compared to the Apo and monotherapeutic systems. This corresponds to the thermodynamic energy calculations that displayed that the co-bound system had greater binding energies. Correlation of these results confers with the experimentally demonstrated synergistic effects generated upon co-binding of Asciminib and Nilotinib [15].

### 4.4 Conclusion

Computational analytical approaches were used to understand the dual inhibitory mechanism of Nilotinib and Asciminib against Bcr-Abl. To this end, comparative MD simulations and analyses were performed toward determining the binding landscape and structural features that are characteristic of this synergistic dual inhibition. Our findings correlated with earlier experimental studies reporting co-administration of these two drugs. Results demonstrated that the co-bound Bcr-Abl system induced a more stable, compact protein structure, when compared to systems in which Asciminib and Nilotinib were individually bound. Thermodynamic calculations indicated that Nilotinib exerts some level of stability and stronger Asciminib-Bcr-Abl interactions. As a result, the calculated binding free energy of Asciminib in the presence of Nilotinib was higher compared to when bound alone as elucidated in the thermodynamics. These revelations give insights into the possible structural dynamics at play, thus contributing to the experimental co-administration studies. We believe that this study will aid in the understanding synergistic dual inhibition for not only CML, but other cancer therapeutics as well.

**Acknowledgements**

The authors acknowledge the Center for High Performance Computing (http://www.chpc.ac.za) for their computational resources.

**Funding**

None

## *4.5 References:*


(1) Deininger, M. W. Diagnosing and Managing Advanced Chronic Myeloid Leukemia. *Am. Soc. Clin. Oncol. Educ. B.* **2015**, *35*, e381–e388.

(2) Granatowicz, A.; Piatek, C. I.; Moschiano, E.; El-Hemaidi, I.; Armitage, J. D.; Akhtari, M. An Overview and Update of Chronic Myeloid Leukemia for Primary Care Physicians. *Korean J. Fam. Med.* **2015**, *36* (5), 197–202.

(3) Baccarani, M.; Pileri, S.; Steegmann, J.-L.; Muller, M.; Soverini, S.; Dreyling, M. Chronic Myeloid Leukemia: ESMO Clinical Practice Guidelines for Diagnosis, Treatment and Follow-Up. *Ann. Oncol.* **2012**, *23*, vii72-vii77.

(4) Matutes, E.; Pickl, W. F.; van't Veer, M.; Morilla, R.; Swansbury, J.; Strobl, H.; Attarbaschi, A.; Hopfinger, G.; Ashley, S.; Bene, M. C.; et al. Mixed-Phenotype Acute Leukemia: Clinical and Laboratory Features and Outcome in 100 Patients Defined According to the WHO 2008 Classification. *Blood* **2011**, *117* (11), 3163–3171.

(5) Clark, S. S.; McLaughlin, J.; Timmons, M.; Pendergast, A. M.; Ben-Neriah, Y.; Dow, L. W.; Crist, W.; Rovera, G.; Smith, S. D.; Witte, O. N. Expression of a Distinctive BCR-ABL Oncogene in Ph1-Positive Acute Lymphocytic Leukemia (ALL). *Science* **1988**, *239* (484), 775–777.

(6) Konopka, J. B.; Watanabe, S. M.; Witte, O. N. An Alteration of the Human C-Abl Protein in K562 Leukemia Cells Unmasks Associated Tyrosine Kinase Activity. *Cell* **1984**, *37* (3), 1035–1042.

(7) Laneuville, P. Abl Tyrosine Protein Kinase. *Semin. Immunol.* **1995**, *7* (4), 255–266.

(8) Liu, J.; Campbell, M.; Guo, J. Q.; Lu, D.; Xian, Y. M.; Andersson, B. S.; Arlinghaus, R. B. BCR-ABL Tyrosine Kinase Is Autophosphorylated or Transphosphorylates P160 BCR on Tyrosine Predominantly within the First BCR Exon. *Oncogene* **1993**, *8* (1), 101–109.

(9) Pendergast, A. M.; Quilliam, L. A.; Cripe, L. D.; Bassing, C. H.; Dai, Z.; Li, N.; Batzer, A.; Rabun, K. M.; Der, C. J.; Schlessinger, J. BCR-ABL-Induced

Oncogenesis Is Mediated by Direct Interaction with the SH2 Domain of the GRB-2 Adaptor Protein. *Cell* **1993**, *75* (1), 175–185.

(10) Ben-Neriah, Y.; Daley, G. Q.; Mes-Masson, A. M.; Witte, O. N.; Baltimore, D. The Chronic Myelogenous Leukemia-Specific P210 Protein Is the Product of the Bcr/Abl Hybrid Gene. *Science* **1986**, *233* (4760), 212–214.

(11) Yang, J.; Campobasso, N.; Biju, M. P.; Fisher, K.; Pan, X.-Q.; Cottom, J.; Galbraith, S.; Ho, T.; Zhang, H.; Hong, X.; et al. Discovery and Characterization of a Cell-Permeable, Small-Molecule c-Abl Kinase Activator That Binds to the Myristoyl Binding Site. *Chem. Biol.* **2011**, *18* (2), 177–186.

(12) Nagar, B.; Hantschel, O.; Young, M. A.; Scheffzek, K.; Veach, D.; Bornmann, W.; Clarkson, B.; Superti-Furga, G.; Kuriyan, J. Structural Basis for the Autoinhibition of C-Abl Tyrosine Kinase. *Cell* **2003**, *112* (6), 859–871.

(13) Wylie, A.; Schoepfer, J.; Berellini, G.; Cai, H.; Caravatti, G.; Cotesta, S.; Dodd, S.; Donovan, D.; Erb, B.; Furet, P.; Gangal, G.; Grotzfeld, R.; Hassan, Q.; Hood, T.; Iyer, I.; Jacob, S.; Ja, W. ABL001, a Potent Allosteric Inhibitor of BCR-ABL, Prevents Emergence of Resistant Disease When Administered in Combination with Nilotinib in an in Vivo Murine Model of Chronic Myeloid Leukemia. *Blood* **2014**, *124*, 398–398.

(14) Eadie, L. N.; Saunders, V. A.; Leclercq, T. M.; Branford, S.; White, D. L.; Hughes, T. P. The Allosteric Inhibitor ABL001 Is Susceptible to Resistance in Vitro Mediated By Overexpression of the Drug Efflux Transporters ABCB1 and ABCG2. *Blood* **2015**, *126* (23), 4841–4841.

(15) Wylie, A. A.; Schoepfer, J.; Jahnke, W.; Cowan-Jacob, S. W.; Loo, A.; Furet, P.; Marzinzik, A. L.; Pelle, X.; Donovan, J.; Zhu, W.; et al. The Allosteric Inhibitor ABL001 Enables Dual Targeting of BCR? ABL1. *Nature* **2017**, *543* (7647), 733–737.

(16) Ottmann, O. G.; Alimena, G.; DeAngelo, D. J.; Goh, Y.-T.; Heinrich, M. C.; Hochhaus, A.; Hughes, T. P.; Mahon, F.-X.; Mauro, M. J.; Minami, H.; et al.

ABL001, a Potent, Allosteric Inhibitor of BCR-ABL, Exhibits Safety and Promising Single- Agent Activity in a Phase I Study of Patients with CML with Failure of Prior TKI Therapy. *Blood* **2015**, *126* (23), 138–138.

(17) Wylie, A. A.; Schoepfer, J.; Jahnke, W.; Cowan-Jacob, S. W.; Loo, A.; Furet, P.; Marzinzik, A. L.; Pelle, X.; Donovan, J.; Zhu, W.; et al. The Allosteric Inhibitor ABL001 Enables Dual Targeting of BCR–ABL1. *Nature* **2017**, *543* (7647), 733–737.

(18) Hughes, T. P.; Goh, Y.-T.; Ottmann, O. G.; Minami, H.; Rea, D.; Lang, F.; Mauro, M. J.; DeAngelo, D. J.; Talpaz, M.; Hochhaus, A.; et al. Expanded Phase 1 Study of ABL001, a Potent, Allosteric Inhibitor of BCR-ABL, Reveals Significant and Durable Responses in Patients with CML-Chronic Phase with Failure of Prior TKI Therapy. *Blood* **2016**, *128* (22), 625–625.

(19) Druker, B. J.; Sawyers, C. L.; Kantarjian, H.; Resta, D. J.; Reese, S. F.; Ford, J. M.; Capdeville, R.; Talpaz, M. Activity of a Specific Inhibitor of the BCR-ABL Tyrosine Kinase in the Blast Crisis of Chronic Myeloid Leukemia and Acute Lymphoblastic Leukemia with the Philadelphia Chromosome. *N. Engl. J. Med.* **2001**, *344* (14), 1038–1042.

(20) Hassan, A. Q.; Sharma, S. V.; Warmuth, M. Allosteric Inhibition of BCR-ABL. *Cell Cycle* **2010**, *9* (18), 3734–3738.

(21) Giles, F. J.; Le Coutre, P. D.; Pinilla-Ibarz, J.; Larson, R. A.; Gattermann, N.; Ottmann, O. G.; Hochhaus, A.; Radich, J. P.; Saglio, G.; Hughes, T. P.; et al. Nilotinib in Imatinib-Resistant or Imatinib-Intolerant Patients with Chronic Myeloid Leukemia in Chronic Phase: 48-Month Follow-up Results of a Phase II Study. *Leukemia* **2013**, *27* (1), 107–112.

(22) Rogers, G.; Hoyle, M.; Thompson Coon, J.; Moxham, T.; Liu, Z.; Pitt, M.; Stein, K. Dasatinib and Nilotinib for Imatinib-Resistant or -Intolerant Chronic Myeloid Leukaemia: A Systematic Review and Economic Evaluation. *Health Technol. Assess.* **2012**, *16* (22), 1–265.

(23) Jarwoski, A.; Sweeney, R. P. Nilotinib : A New Tyrosine Kinase Inhibitor for the Treatment of Chronic Myelogeneous Leukemia. *Pharmacotherapy* **2008**, *28* (11), 1374–1382.

(24) Blay, J. Y.; Von Mehren, M. Nilotinib: A Novel, Selective Tyrosine Kinase Inhibitor. *Semin. Oncol.* **2011**, *38* (1), 1–13.

(25) Bleeker, F. E.; Bardelli, A. Genomic Landscapes of Cancers: Prospects for Targeted Therapies. *Pharmacogenomics* **2007**, *8* (12), 1629–1633.

(26) Cowan-Jacob, S. W. The Role of Structure and Biophysics in the Discovery of Allosteric Kinase Inhibitors: ABL001, a Potent and Specific Inhibitor of BCR-ABL. *Acta. Crystallogr.* **2016**, *72* (a1), s4–s5.

(27) Schoepfer, J.; Jahnke, W.; Berellini, G.; Buonamici, S.; Cotesta, S.; Cowan-Jacob, S. W.; Dodd, S.; Drueckes, P.; Fabbro, D.; Gabriel, T.; et al. Discovery of Asciminib (ABL001), an Allosteric Inhibitor of the Tyrosine Kinase Activity of Bcr-Abl1. *J. Med. Chem.* **2018**, *61* (18), 8120–8135.

(28) Block, K. I.; Gyllenhaal, C.; Lowe, L.; Amedei, A.; Ruhul Amin, A. R. M.; Amin, A.; Aquilano, K.; Arbiser, J.; Arreola, A.; Arzumanyan, A.; et al. Designing a Broad-Spectrum Integrative Approach for Cancer Prevention and Treatment. *Semin. Cancer Biol.* **2015**, *35* (3), S276–S304.

(29) Giordano, S.; Petrelli, A. From Single- to Multi-Target Drugs in Cancer Therapy: When Aspecificity Becomes an Advantage. *Curr. Med. Chem.* **2008**, *15* (5), 422–432.

(30) Berman, H. M.; Battistuz, T.; Bhat, T. N.; Bluhm, W. F.; Philip, E.; Burkhardt, K.; Feng, Z.; Gilliland, G. L.; Iype, L.; Jain, S.; et al. The Protein Data Bank. *Biol. Crystallogr.* **2002**, *58*, 899–907.

(31) Kim, S.; Thiessen, P. A.; Bolton, E. E.; Chen, J.; Fu, G.; Gindulyte, A.; Han, L.; He, J.; He, S.; Shoemaker, B. A.; et al. PubChem Substance and Compound Databases. *Nucl. A. Res.* **2016**, *44* (1), 1202–1213.

(32) Trott, O.; Olson, A. J. AutoDock Vina: Improving the Speed and Accuracy of

Docking with a New Scoring Function, Efficient Optimization, and Multithreading. *J. Comput. Chem.* **2010**, *31* (2), 455–461.

(33) Pettersen, E. F.; Goddard, T. D.; Huang, C. C.; Couch, G. S.; Greenblatt, D. M.; Meng, E. C.; Ferrin, T. E. UCSF Chimera--a Visualization System for Exploratory Research and Analysis. *J. Comput. Chem.* **2004**, *25* (13), 1605–1612.

(34) Adcock, S. A.; McCammon, J. A. Molecular Dynamics: Survey of Methods for Simulating the Activity of Proteins. *Chem. Rev.* **2006**, *106* (5), 1589–1615.

(35) Case, D. A.; Cheatham, T. E.; Darden, T.; Gohlke, H.; Luo, R.; Merz, K. M.; Onufriev, A.; Simmerling, C.; Wang, B.; Woods, R. J. The Amber Biomolecular Simulation Programs. *J. Comput. Chem*. 2005, 1668–1688.

(36) Ramharack, P.; Soliman, M. E. S. Zika Virus NS5 Protein Potential Inhibitors: An Enhanced in Silico Approach in Drug Discovery. *J. Biomol. Struct. Dyn.* **2018**, *36* (5), 1118–1133.

(37) El Rashedy, A. A.; Olotu, F. A.; Soliman, M. E. S. Dual Drug Targeting of Mutant Bcr-Abl Induces Inactive Conformation: New Strategy for the Treatment of Chronic Myeloid Leukemia and Overcoming Monotherapy Resistance. *Chem. Biodivers.* **2018**.

(38) Ramharack, P.; Oguntade, S.; Soliman, M. E. S. Delving into Zika Virus Structural Dynamics – a Closer Look at NS3 Helicase Loop Flexibility and Its Role in Drug Discovery. *RSC Adv.* **2017**, *7* (36), 22133–22144.

(39) Roe, D. R.; Cheatham, T. E. PTRAJ and CPPTRAJ: Software for Processing and Analysis of Molecular Dynamics Trajectory Data. *J. Chem. Theory Comput.* **2013**, *9*, 3084–3095.

(40) Ylilauri, M.; Pentikäinen, O. T. MMGBSA as a Tool to Understand the Binding Affinities of Filamin-Peptide Interactions. *J. Chem. Inf. Model.* **2013**, *53* (10), 2626–

(41) Hou, T.; Wang, J.; Li, Y.; Wang, W. Assessing the Performance of the MM/PBSA and MM/GBSA Methods. 1. The Accuracy of Binding Free Energy Calculations Based on Molecular Dynamics Simulations. *J. Chem. Inf. Model.* **2011**, *51* (1), 69–

82.

(42) Hayes, J. M.; Archontis, G. MM-GB (PB) SA Calculations of Protein-Ligand Binding Free Energies. *InTech* **2011**, 171–190.

(43) Agoni, C.; Ramharack, P.; Soliman, M. E. S. Co-Inhibition as a Strategic Therapeutic Approach to Overcome Rifampin Resistance in Tuberculosis Therapy: Atomistic Insights. *Future Med. Chem.* **2018**, *10* (14), 1665–1675.

(44) Eadie, L. N.; Saunders, V. A.; Branford, S.; White, D. L.; Hughes, T. P. The New Allosteric Inhibitor Asciminib Is Susceptible to Resistance Mediated by ABCB1 and ABCG2 Overexpression. *Oncotarget* **2018**, *9* (17), 13423–13437.

(45) Reddy, E. P.; Aggarwal, A. K. The Ins and Outs of Bcr-Abl Inhibition. *Genes and Cancer* **2012**, *3* (5–6), 447–454.

(46) Pan, L.; Patterson, J. C.; Deshpande, A.; Cole, G.; Frautschy, S. Molecular Dynamics Study of Zn(Aβ) and Zn(Aβ)2. *PLOS ONE* **2013**, *8* (9), e70681.

(47) Wijffels, G.; Dalrymple, B.; Kongsuwan, K.; Dixon, N. Conservation of Eubacterial Replicases. *IUBMB. Life* **2005**, *57* (6), 413–419.

(48) Panjarian, S.; Iacob, R. E.; Chen, S.; Engen, J. R.; Smithgall, T. E. Structure and Dynamic Regulation of Abl Kinases. *J. Biol. Chem.* **2013**, *288* (8), 5443–5450.

(49) Maru, Y. Molecular Biology of Chronic Myeloid Leukemia. *Cancer Sci.* **2012**, *103* (9), 1601–1610.

(50) Marsh, J. A.; Teichmann, S. A. Relative Solvent Accessible Surface Area Predicts Protein Conformational Changes upon Binding. *Struct. Eng.* **2011**, *19* (6), 859–867.

# CHAPTER 5

## Dual drug targeting of mutant Bcr-Abl induces inactive conformation: New strategy for the treatment of chronic myeloid leukemia and overcoming monotherapy resistance

Ahmed A El Rashedy[a], Fisayo A. Olotu[a], Mahmoud E. S. Soliman[a,b*]

[a]Molecular Modeling and Drug Design Research Group, School of Health Sciences, University of KwaZulu-Natal, Westville Campus, Durban 4001, South Africa

[b]College of Pharmacy and Pharmaceutical Sciences, Florida Agricultural and Mechanical University, FAMU, Tallahassee, Florida 32307, USA.

*Corresponding Author: Mahmoud E.S. Soliman

Email: soliman@ukzn.ac.za

Telephone: +27 (0) 31 260 8048, Fax: +27 (0) 31 260 7872

**Abstract**

Bcr-Abl is an oncogenic fusion protein which expression enhances tumorigenesis, and has been highly associated with chronic myeloid leukemia (CML). Acquired drug resistance in mutant Bcr-Abl has enhanced pathogenesis with the use of single therapy agents such as Nilotinib. Moreover, allosteric targeting has been identified to consequentially inhibit Bcr-Abl activity, which led to the recent development of ABL-001 (asciminib) that selectively binds the myristoyl pocket. Experimental studies have revealed that the combination of Nilotinib and ABL-001 induced a "bent" conformation in the C-terminal helix of Bcr-Abl; a benchmark of inhibition, thereby exhibiting a greater potency in the treatment of CML, surmounting the setbacks of drug resistance, disease regression and relapse. Therefore, we report the first account of the dynamics and conformational analysis of oncogenic T334I Bcr-Abl by dual targeting. Our findings revealed that unlike in the Bcr-Abl-Nilotinib complex, dual targeting by both inhibitors induced the bent conformation in the C-terminal helix that varied with time. This was coupled with significant alteration in Bcr-Abl stability, flexibility and compactness and an overall structural re-orientation inwards towards the hydrophobic core, which reduced the solvent-exposed residues indicative of protein folding. This study = will facilitate allosteric targeting and the design of more potent allosteric inhibitors for resistive target proteins in cancer.

**Keywords:** Bcr-Abl; oncogenic; catalytic; allosteric; myristoyl; C-terminal helix

## 5.1. Introduction

The success of targeted therapy with kinase inhibitors has been best shown in Bcr-Abl, wherein a drug such as imatinib selectively diminishes kinase activity with significant pharmacological effect in the treatment of chronic myelogenous leukemia (CML) [1]. However, the potency of kinase inhibitors in cancer therapeutics has been invariably impeded by the emergence of acquired resistance, thereby presenting one of the major challenges to the effective deployment of these agents in the clinic [1]. Prior to oncogenesis, activation of Abelson tyrosine kinase (ABL) occurs by the combination of the *BCR* (breakpoint cluster region) gene with the gene that codes for the intracellular non-receptor tyrosine kinase, which translates into the formation of an enormous protein of approximately 1150 residues. This possesses two distinct halves; the N-terminal half constitutes an N-terminal cap, SH3 and an SH2 domain sequentially while the C-terminal half is made up response elements for varying functionality, which includes domain for DNA and actin binding [2]. This is in close proximity to the phosphorylation site in the C-terminal half, and also includes proline-rich segments for nuclear localization and export signaling [3]. The N-terminal cap contains an approximate of 80 residues that play critical role in autoinhibition. This domain is followed by the SH3 domain, SH2 and ultimately a tyrosine kinase domain (Nagar et al. 2003). The interaction between the SH3 and the SH2 domains facilitates autoinhibition, which involves the binding of the SH3 domain to the linker sequence (polyproline) between the SH2 and kinase domains. This is followed by the interaction between the SH2 domain and the kinase domain's C-terminal lobe to form a clamp structure (Hantschel et al. 2003; Nagar et al. 2006). The binding of the SH3 domains to peptides to form polyproline type II helices while on the other hand, SH2 domains interact with and bind to peptides that contain phosphotyrosine. In its normal state, the c-Abl is regulated with very low kinase activity, while in diseased states such as in chronic myeloid leukemia (CML), it is upregulated by a complex intramolecular interplay between the SH2, SH3, and the kinase domain [4, 5]. In this case, oncogenic activation is driven by the fusion of Bcr to c-Abl at its $NH_2$ terminus (Hantschel et al. 2003; Panjarian et al. 2013). The linker region between SH2 and catalytic domains form a polyproline type

II helix, which binds the SH3 domain, bringing it into close proximity with the catalytic domain [4] (Figure 5.1).

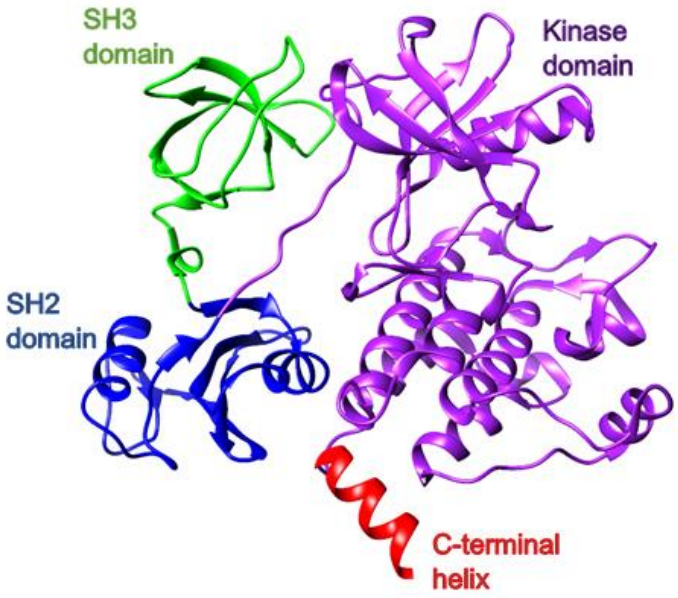


**Figure 5.1:** Structural highlight of Bcr-Abl domains showing the SH2, SH3, kinase domains and the C-terminal helix.

Regulation of c-Abl occurs via an autoinhibitory mechanism, which has been elucidated to occur through the binding of myristoyl to the myristoyl pocket, an allosteric site situated on c-Abl. This results in its conformational reorientation to an inactive auto-inhibited kinase state evidenced by the bending of the C-terminal helix [6]. However, Bcr-Abl is not myristoylated due to the absence of the first Abl exon and the disruption of its regulatory mechanism by pertinent auto-phosphorylation results into uncontrolled oncogenic activity as seen in chronic myeloid leukemia [6]. Inactivation of c-Abl has been the basis of CML therapy and this has resulted into the design and use of imatinib, a target specific ATP-competitive inhibitor which functions by blocking the binding of ATP to the catalytic site, leading to the inactivity of Bcr-Abl and eventual amelioration of CML and improves overall survival of patients [7]. However, point mutations, which occur at this domain, has accounted for acquired resistance and reduced sensitivity to imatinib therapy. Advancement in therapeutic intervention led to the development of more potent kinase inhibitors such as nilotinib and dasatinib to treat CML associated with Imatinib resistance

[8, 9]. Nilotinib (Figure 5.2A) shares more similarity with imatinib in its mode of binding and target specificity coupled with its physicochemical properties [10, 11]. Although not modified by myristoylation, the presence of the pocket for myristate binding on Bcr-Abl presented additional target site for therapy, which led to the design of site-specific molecules to mimic the binding of myristate and facilitate auto-inhibitory regulation [12]. These classes of inhibitors are ATP non-competitive but rather bind to the myristoyl pocket of the ABL kinase domain [13], thereby decreasing Bcr-Abl aberrant kinase activity. Such inhibitors include GNF-2, GNF-5 and most recently, ABL-001 (asciminib), which possesses more potency and selectivity among this class of allosteric inhibitors. ABL-001 (Figure 5.2B), among others was able to bind specifically at the myristoyl pocket thereby inducing a 'bend' in the C-terminal helix, which structurally characterizes auto-inhibitory modulation [2, 14].

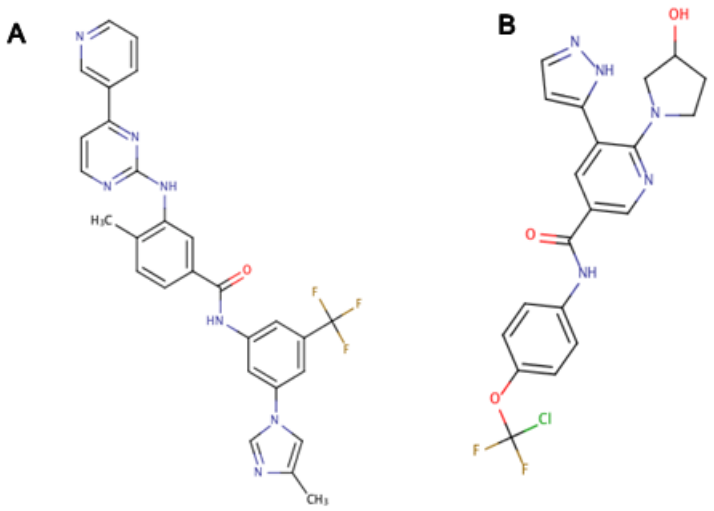


**Figure 5.2:** 2D structure of c-Abl inhibitors: **[A]** Nilotinib **[B]** ABL-001

Combination therapy involving both the catalytic and allosteric (myristoyl pocket) inhibitors have been identified has a rationale for improving outcomes of CML treatment and surmounts setbacks associated with lone administration of either inhibitors such as resistance and intolerance [6, 14]. In other words, allosteric inhibition complements the therapeutic activity of a kinase inhibitor to effect the inactivation of Bcr-Abl oncogenic fusion protein as structurally evidenced by the bending of its C-terminal helix. Activated Bcr-Abl fusion oncoprotein has been described to exhibit flexibility in the linker chains

characteristic of an increased kinase activity while binding of inhibitors to its active and allosteric induces rigidity, which is characteristic of inhibited Bcr-Abl (Gray and Fabbro, 2014; Hantschel, 2012) similar to a c-ABL autoinhibited state for reduced kinase activity (Nagar et al. 2006; Panjarian et al. 2013). This is schematically represented below (Figure 5.3).

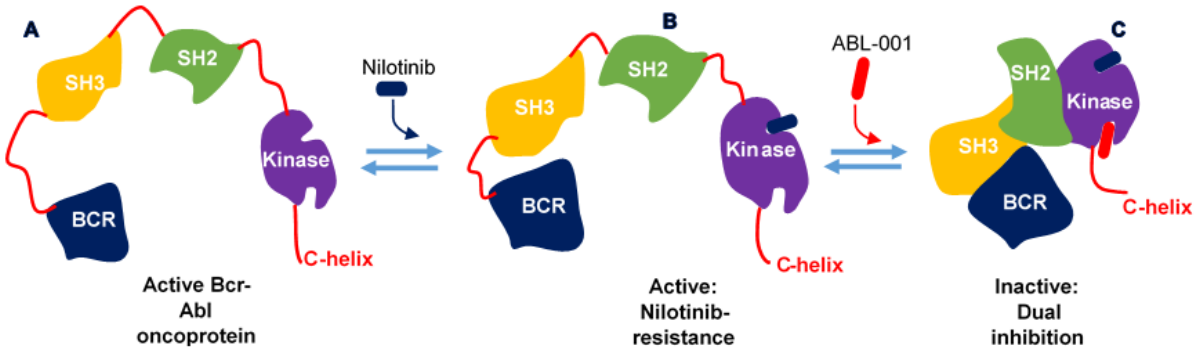


**Figure 5.3:** Schematic representation of the structural effect of single-agent and dual inhibition on Bcr-Abl protein complex relative to its activation and inactivation conformation. **[A]** Active flexible and straight C-terminal helix **[B]** Active flexible and straight C-terminal helix **[C]** Inactive Rigid and bent C-terminal helix conformation.

There is therefore need to have an insight into the structural basis of dual inhibition in abrogating oncogenic Bcr-Abl kinase activity relative to induction of inactive C-terminal conformation. Therefore, in this study we present the first account of the dynamics and conformational basis of kinase inactivity effected by dual inhibitory mechanisms of ABL001 (allosteric) and Nilotinib (catalytic) (Figure 5.4).

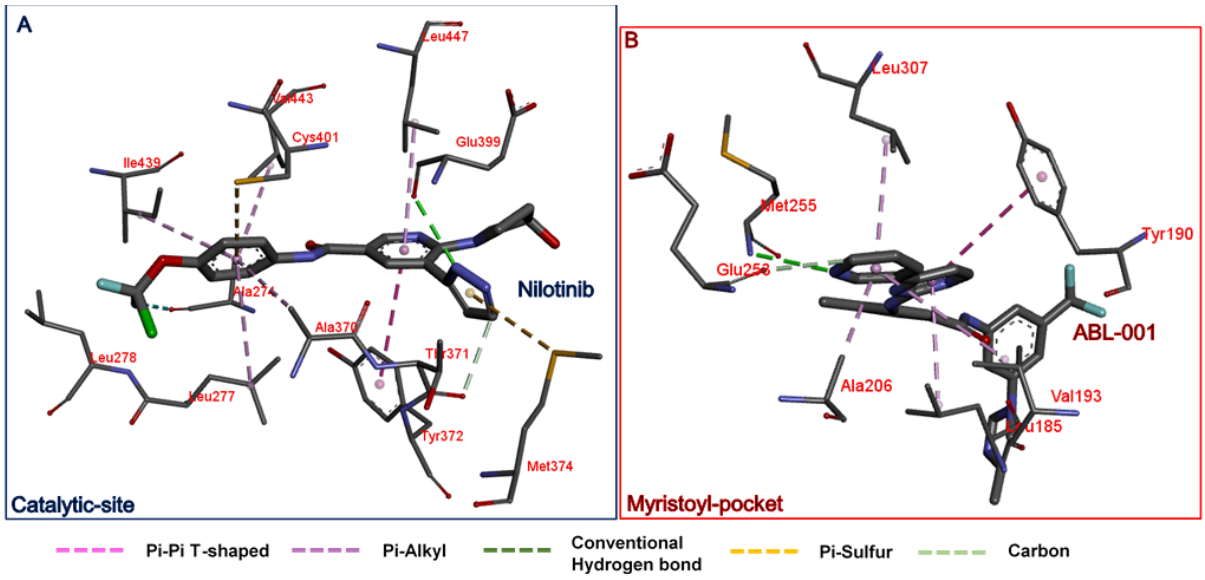


**Figure 5.4:** Target site interactions between inhibitors and site residues showing bond types involved in stabilization at the respective sites. **[A]** Nilotinib and catalytic site residues **[B]** ABL-001 and myristoyl-pocket residues

This is to provide further insight into structural basis of inactivation induced by co-administration of allosteric and catalytic inhibitors. These findings would further validate the rationale of combination therapy in the treatment of CML and also aids the structure-based design of other potent allosteric inhibitors to enhance the efficacy of kinase inhibitors.

## 5.2 Result and Discussion

### 5.2.1 Protein stability

Stability of the protein systems was comparatively determined by measuring the root mean square deviation (RMSD) of the C-α atoms across the 200ns of the MD simulations. Moreover, deviation in protein structure as calculated by the RMSD could correspond to the stability of the protein wherein a high value implies a low stability and a low value could indicate an increase in protein stability. As seen in Figure 5.5, deviations in both systems varied with time wherein a highly unstable structure characterized mutant Bcr-Abl inhibited by Nilotinib alone.

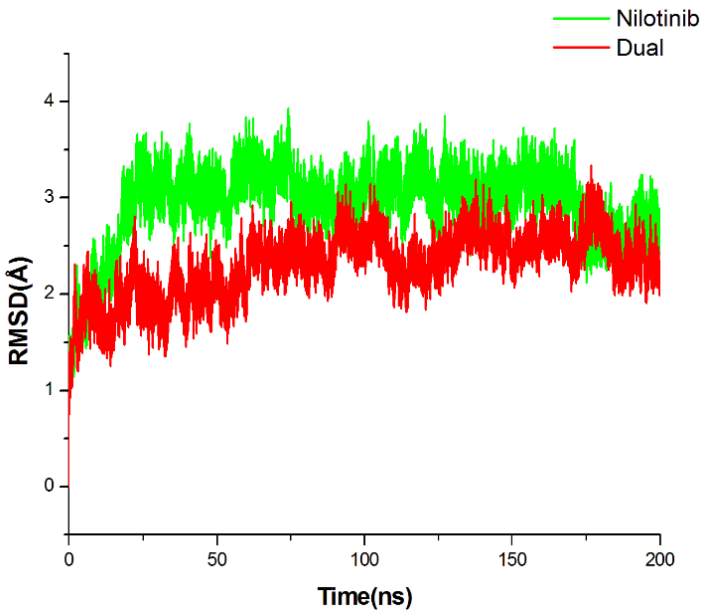


**Figure 5.5:** Comparative C-α RMSD plot of single-agent (Nilotinib) and dual (Nilotinib+ABL-001) targeted Bcr-Abl complex

This could suggest one of the basis of mutation-induced acquired resistance to monotherapy with the kinase inhibitor; Nilotinib. However, dual targeting by Nilotinib and ABL-001 induced a reduction in C-α atoms deviation which could correlate with increase in stability. This could provide insight into the structural attributes of mutant Bcr-Abl targeted with ABL-001 and Nilotinib in the treatment of CML as revealed experimentally [14]. Average RMSD values include 3.03Å for BN while the allosteric inhibitor lowered the deviation to 2.33Å in the BAN complex.

### 5.2.2 Flexibility and activity interplay

Conformational studies have associated a compact and rigid structure with an inactive oncogenic Bcr-Abl fusion protein while flexibility characterizes its activity and resistance [2, 15]. Therefore, in order to structurally determine the effect of dual inhibition on the flexibility protein system, we measured the C-α root mean square fluctuation (RMSF), which is a metrics for estimating flexibility. The result revealed that both inhibitors

significantly lowered the overall residual fluctuation indicative of rigidity, which characterizes the inactive form of the protein (Figure 5.6).

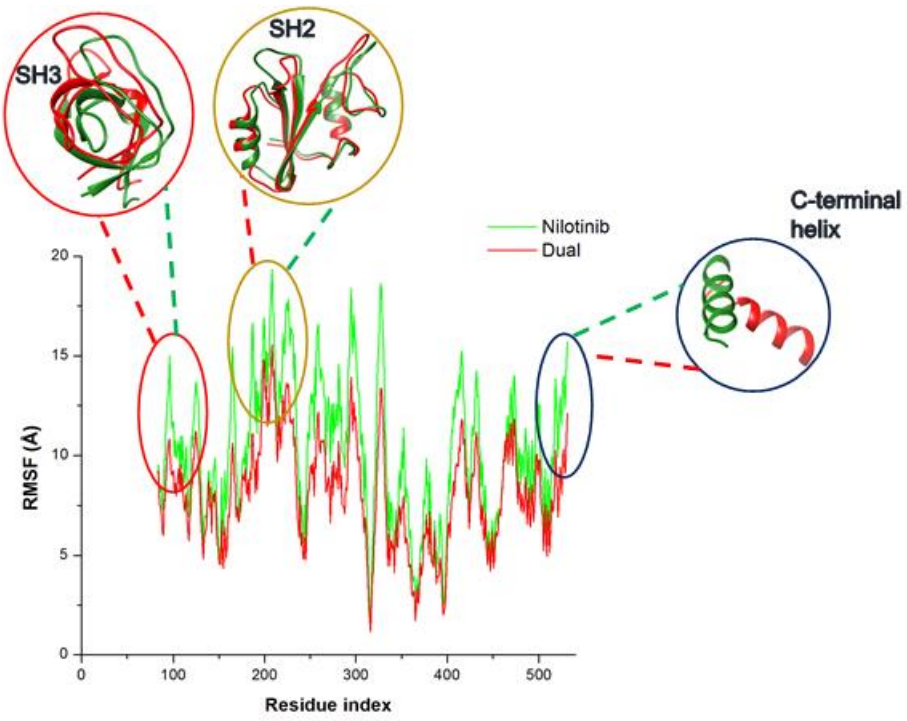


**Figure 5.6:** C- α RMSF plot showing the effect of single-agent and dual targeting on residual fluctuation and overall flexibility relative to inactivation. Inset are the SH3 (red), SH2 (gold) and the C-terminal helix (blue).

In other words, combination of Nilotinib and the allosteric inhibitor; ABL-001 reduces flexibility. However, with the catalytic inhibitor, Nilotinib alone, mutant Bcr-Abl maintained high flexibility, which characterizes the active form. This could indicate mutant Bcr-Abl Nilotinib-resistivity and serve as a basis for structural characterization. Reduction in flexibility was revealed as shown in the figure above across the respective domains that constitute Bcr-Abl fusion proteins. The complex with both inhibitors (BAN) has an average RMSF value of 7.68Å that was significantly lower than in BN: 12.08Å.

### 5.2.3 Exposed surface area and protein folding

The solvent accessible surface area (SASA) analysis is useful in understanding the folding-unfolding process of a protein in conformational studies as it measures the surface area of the protein exposed to solvent across the duration of the molecular dynamics simulation.

Moreover, the process of folding decreases the protein surface exposed to the solvent while an increase in the exposed surface depicts an unfolding process [16]. Conformational Bcr-Abl studies had also revealed that protein misfolding characterizes its activity while inactive in its folded state [17, 18]. Our result agrees accordingly as shown in the SASA plot, which reveals that allosteric combined with catalytic targeting reduces the number of solvent exposed surfaces (Figure 5.7).

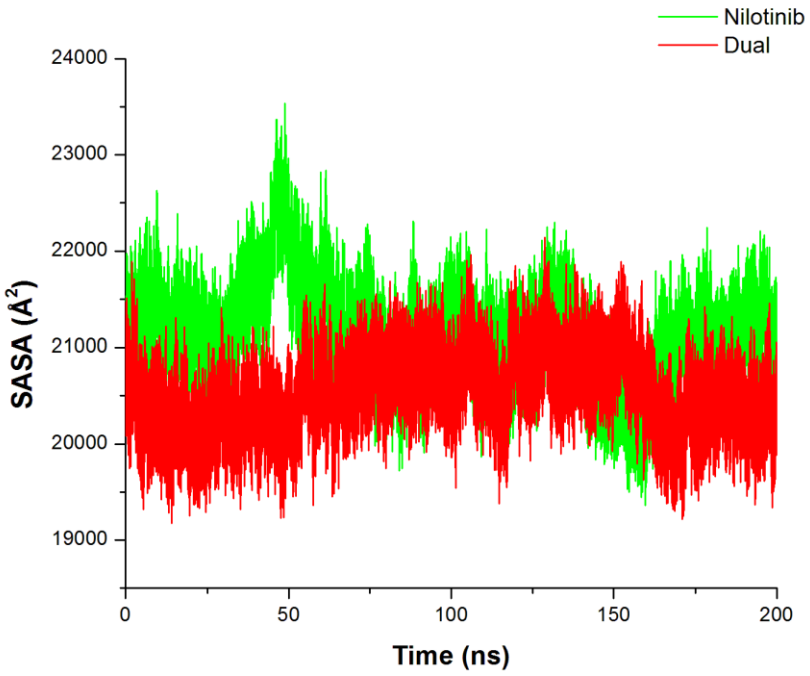


**Figure 5.7:** Comparative SASA plot showing single and dual inhibition-induced exposure of surfaces

This is indicative of protein unfolding which characterizes inactive Bcr-Abl state. However, there was an increase in the surfaces exposed to solvent in BN. In other words, dual targeting caused an inward re-orientation of residual side chains that were exposed to solvent towards the hydrophobic core of the protein. This could further suggest the potency of dual targeting in the treatment of Nilotinib resistant CML as compared to regimen with Nilotinib alone. Compactness of both systems (singly and dually inhibited) was measured by estimating the radius of gyration (RoG) where a high RoG value depicts a reduction or loss of structural compactness and vice versa (Lobanov, Bogatyreva, and Galzitskaya, 2008). The result is shown in Figure 5.8 and reveals that there was a loss of compactness

in the structure of Bcr-Abl that was dually inhibited with Nilotinib and ABL001 as compared with that which was inhibited with Nilotinib alone. Moreover, the variations in structural compactness among the two systems could be relative to inhibition using single and dual inhibitors respectively as shown in other results.

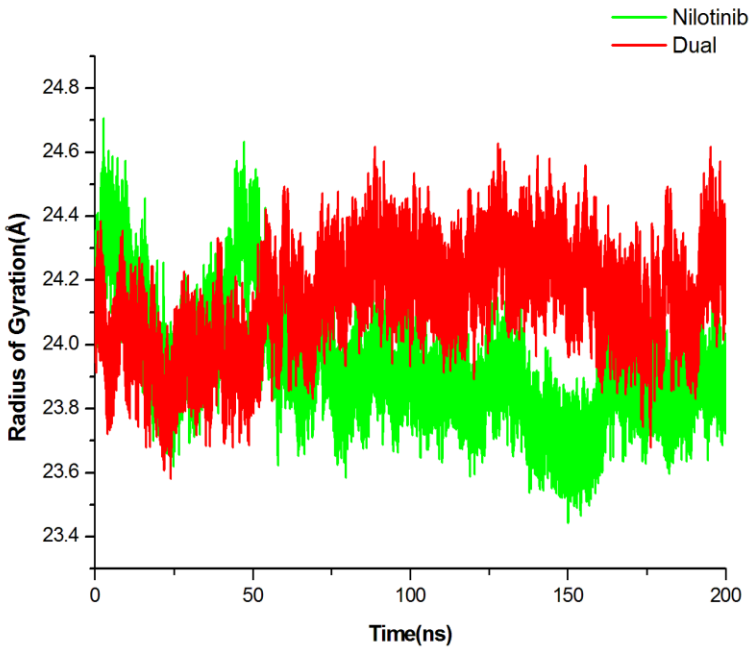


**Figure 5.8:** RoG plot showing the effect of single (Nilotinib) and dual (Nilotinib and ABL001) inhibition on the compactness of Bcr-Abl structure.

### 5.2.4 Systemic induction of inactive C-terminal helix conformation

Conformational re-orientation of the C-terminal helix is crucial to the regulation of c-Abl activity and inactivity during its auto-inhibition, a regulatory mechanism in normal conditions. This occurs upon its myristoylation as a result of the binding of myristate to its binding pocket, resulting into a 'bent' C-terminal helix conformation, a highlight of an inactive or auto-inhibited c-Abl kinase [2, 14]. Although Bcr-Abl oncogenic fusion protein is not myristoylated due to the lack of the first Abl exon [19], it still possess the myristate-binding pocket. This has been the subject of allosteric targeting in order to mimic auto-inhibitory type of regulation as it occurs in non-diseased conditions. Trajectory visualization revealed inhibition by nilotinib alone gradually assumed a straight C-terminal helix conformation (slightly bent at some trajectories as shown in Figure 9) at around 50ns

and was steady until the end of the MD simulation. The distinct fluctuations in structure was seen in the RMSF plot. However, the bent C-terminal conformation was induced by dual inhibition with both Nilotinib and ABL-001. Other than inducing a 'bend' in the C-terminal helix, it appears that allosteric targeting by ABL-001 locked this conformation across the 200ns of MD simulation. This reveals the mechanistic effect of allosteric targeting in the potency of dual inhibition relative to Bcr-Abl inactivation and ultimately, CML treatment.

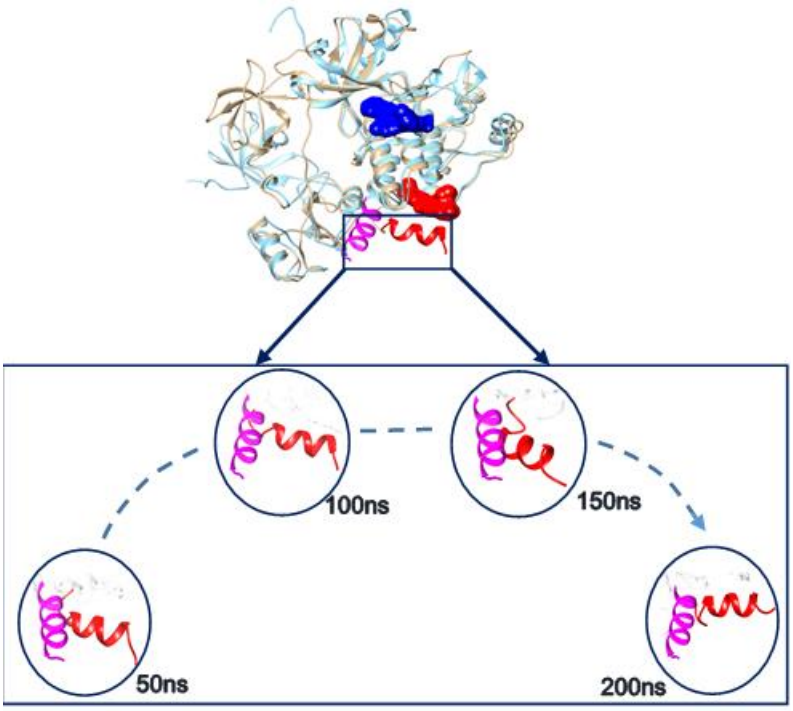


**Figure 5.9:** Superimposed single (gold) and dual (blue) targeted Bcr-Abl complex. Inset shows the trajectory visualization of the C-terminal helix conformations of the singly inhibited Bcr-Abl (Nilotinib alone - Magenta) and the dually inhibited Bcr-Abl (Nilotinib and ABL001 - Red) across the MD simulation time.

## 5.3. Conclusion

Advancement in the treatment of CML has been a subject of research due to the emergence of acquired resistance to kinase inhibitors due to mutations in the kinase domain of the target Bcr-Abl fusion oncoprotein. These inhibitors were designed as competitive inhibitors to prevent the binding of ATP to its kinase domain thereby preventing auto-

phosphorylation, which accounts for its dysregulation in diseased conditions. Examples include Imatinib and Nilotinib. Setbacks in CML therapy with kinase inhibitors due to resistance and reduction in drug sensitivity led to allosteric targeting with second site inhibitors at the myristate-binding pocket in order to mimic the normal auto-inhibitory regulatory mechanism. An example of such allosteric inhibitor is ABL001 (Asciminib). Moreover, treatment of CML with the combination of both inhibitors has been shown to improve outcomes with no recurrence after treatment cessation compared to single agent treatment with kinase inhibitors. Since structural re-orientation characterize activation and inactivation of Bcr-Abl most importantly the straight and bent C-terminal helix conformation. In this study, we provided the structural basis of dual inhibitory mechanisms of Nilotinib (kinase inhibitor) and ABL001 (allosteric inhibitor) compared to single agent by Nilotinib alone, to support studies wherein combination therapies where used for improved treatment outcomes in CML. Our findings agreed with earlier experimental studies and revealed that single-agent inhibition with Nilotinib was unable to induce a 'bend' in the C-terminal helix but maintained its characteristic active straight conformation. Also, the protein was shown to exhibit high residual fluctuation, flexibility and a low stability that characterizes Bcr-Abl active conformation. However, both inhibitors induced an overall structural re-orientation in active Bcr-Abl, which increased its stability and conferred rigidity; structural attributes of inactive fusion Bcr-Abl oncoproteins. Also, dual inhibition reduced the residual side chains exposed to solvent as revealed by surface analysis indicative of protein folding, while single agent inhibition by Nilotinib had a higher exposed surface indicative of an unfolded or misfolded protein which has been experimentally shown to characterize its activity. Taken together, in agreement with previous experimental studies, therapies with allosteric combined with catalytic inhibitors possess a great propensity for inactivating Bcr-Abl and ultimately improved outcomes in the treatment of CML with acquired resistance to single-agent kinase inhibitors. This study will provide structural insight into the basis of dual inhibitory mechanisms and aid the design and development of more potent allosteric inhibitors to enhance inhibitory activities with kinase inhibitors.

## 5.4. Experimental section - Computational Methodology

### 5.4.1 System Preparation

Crystal structure of c-Abl tyrosine kinase was retrieved from RSCB Protein Data Bank (PDBID: 1OPK) [2] and was used to obtain the inactive C-terminal helix protein conformation while missing residues were added using Modeller [20].

Further preparation of the retrieved structure involved the removal of co-crystallized substrates that are irrelevant to study. Such include myristoyl acid present in the myristoyl binding pocket (allosteric site). This model was used because it constitute the kinase, SH2 and SH3 domains that characterizes Bcr-Abl oncogenic fusion protein unlike in other structures which were distinctively crystallized. T334I point mutation was carried out at the catalytic site (kinase domain) of the protein complex using UCSF chimera [18] to obtain the Nilotinib-resistant mutant. Both inhibitors; Nilotinib (ID: 644214) and ABL001 (ID: 72165228) were obtained from Pubchem [21]. Protein-inhibitor docking was carried sequentially at the catalytic and myristic-binding pocket using Autodock Vina [22] to obtain the Bcr-Abl-Nilotinib (BN) and ABL-001-Bcr-Abl-Nilotinib (BAN) complexes; both set up for molecular dynamics simulations. Molecular docking preceded the definition of grid boxes around the target sites (active and allosteric) of Bcr-Abl to which the inhibitors were docked respectively. System visualization and preparation was carried out using UCSF chimera [23].

### 5.4.2 Molecular dynamics (MD) simulations

This was carried out on the systems with the GPU version of AMBER 14 with an integrated SANDER module [24]. This followed a standard simulation protocol, which has been previously adopted in our previous studies [25, 26] and enumerated as follows. Parameterization of the inhibitors was carried out using the ANTECHAMBER module wherein atomic partial charges (Gasteiger – gaff, using the bcc charge scheme) were generated [27] while the ff99SB AMBER force field was used to parameterize the proteins. Using the LEAP module, hydrogen atoms were added and system neutralized by the addition of counter ions, thereby generating ligand, protein and complex topologies and parameter files. The systems were explicitly solvated with water using the TIP3P

orthorhombic box size of 10Å, which enclosed all atoms of the protein [24]. Prior to running the LEAP module, the *pdb4amber* script was executed to protonate the histidine residues at a constant pH (cpH). This was employed to automatically modify the protein system for use with tleap (Case et al. 2005). Both complexes were minimized initially for 2000 minimization steps applying a restraint potential of 500kcal/mol and then fully minimized for another 1000 steps of steepest descent without restrain. This was followed by gradual heating the system with a temperature range of 0-300k for 50ps after which the system was equilibrated for 500ps and the temperature and pressure kept constant at 300k and 1bar respectively using the Berendsen barostat [28]. Without restraints, 200ns MD simulation was initiated using a time step of 1fs and coordinates saved at 1ps interval followed by subsequent analysis of trajectories using the integrated PTRJ and CPPTRAJ module [29]. Visualization of the complexes and data plots were carried out using the graphical user interface of UCSF chimera [23] and Microcal Origin analytical software [30].

**Acknowledgements**

The authors acknowledge the School of Health Sciences, University of KwaZulu-Natal for their support financially and infrastructurally. Furthermore, we would also thank the Center for High Performance Computing; (http://www.chpc.ac.za), for their computational resources.

**Conflict of interest**

The authors declare no conflict of interest.

## *5.5 References:*


[1] Hassan, A. Q., Sharma, S. V., and Warmuth, M. (2010) Allosteric inhibition of BCR-ABL, *Cell Cycle 9*, 3710-3714.

[2] Nagar, B., Hantschel, O., Young, M. A., Scheffzek, K., Veach, D., Bornmann, W., Clarkson, B., Superti-Furga, G., and Kuriyan, J. (2003) Structural basis for the autoinhibition of c-Abl tyrosine kinase, *Cell 112*, 859-871.

[3] Van Etten, R. A. (1999) Cycling, stressed-out and nervous: cellular functions of c-Abl, *Trends in cell biology 9*, 179-186.

[4] Hantschel, O., and Superti-Furga, G. (2004) Regulation of the c-Abl and Bcr-Abl tyrosine kinases, *Nature reviews. Molecular cell biology 5*, 33-44.

[5] Colicelli, J. (2010) ABL tyrosine kinases: evolution of function, regulation, and specificity, *Science signaling 3*, re6.

[6] Greuber, E. K., Smith-Pearson, P., Wang, J., and Pendergast, A. M. (2013) Role of ABL family kinases in cancer: from leukaemia to solid tumours, *Nature reviews. Cancer 13*, 559-571.

[7] Hochhaus, A., O'Brien, S. G., Guilhot, F., Druker, B. J., Branford, S., Foroni, L., Goldman, J. M., Muller, M. C., Radich, J. P., Rudoltz, M., Mone, M., Gathmann, I., Hughes, T. P., and Larson, R. A. (2009) Six-year follow-up of patients receiving imatinib for the first-line treatment of chronic myeloid leukemia, *Leukemia 23*, 1054-1061.

[8] Weisberg, E., Manley, P. W., Breitenstein, W., Bruggen, J., Cowan-Jacob, S. W., Ray, A., Huntly, B., Fabbro, D., Fendrich, G., Hall-Meyers, E., Kung, A. L., Mestan, J., Daley, G. Q., Callahan, L., Catley, L., Cavazza, C., Azam, M., Neuberg, D., Wright, R. D., Gilliland, D. G., and Griffin, J. D. (2005) Characterization of AMN107, a selective inhibitor of native and mutant Bcr-Abl, *Cancer cell 7*, 129-141.

[9] Shah, N. P., Tran, C., Lee, F. Y., Chen, P., Norris, D., and Sawyers, C. L. (2004) Overriding imatinib resistance with a novel ABL kinase inhibitor, *Science 305*, 399-401.

[10] Kantarjian, H., Jabbour, E., Grimley, J., and Kirkpatrick, P. (2006) Dasatinib, *Nature reviews. Drug discovery 5*, 717-718.

[11] Vajpai, N., Strauss, A., Fendrich, G., Cowan-Jacob, S. W., Manley, P. W., Grzesiek, S., and Jahnke, W. (2008) Solution conformations and dynamics of ABL kinase-inhibitor complexes determined by NMR substantiate the different binding modes of imatinib/nilotinib and dasatinib, *The Journal of biological chemistry 283*, 18292-18302.

[12] Hantschel, O., Nagar, B., Guettler, S., Kretzschmar, J., Dorey, K., Kuriyan, J., and Superti-Furga, G. (2003) A myristoyl/phosphotyrosine switch regulates c-Abl, *Cell 112*, 845-857.

[13] Zhang, J., Adrian, F. J., Jahnke, W., Cowan-Jacob, S. W., Li, A. G., Iacob, R. E., Sim, T., Powers, J., Dierks, C., Sun, F., Guo, G. R., Ding, Q., Okram, B., Choi, Y., Wojciechowski, A., Deng, X., Liu, G., Fendrich, G., Strauss, A., Vajpai, N., Grzesiek, S., Tuntland, T., Liu, Y., Bursulaya, B., Azam, M., Manley, P. W., Engen, J. R., Daley, G. Q., Warmuth, M., and Gray, N. S. (2010) Targeting Bcr-Abl by combining allosteric with ATP-binding-site inhibitors, *Nature 463*, 501-506.

[14] Wylie, A. A., Schoepfer, J., Jahnke, W., Cowan-Jacob, S. W., Loo, A., Furet, P., Marzinzik, A. L., Pelle, X., Donovan, J., Zhu, W., Buonamici, S., Hassan, A. Q., Lombardo, F., Iyer, V., Palmer, M., Berellini, G., Dodd, S., Thohan, S., Bitter, H., Branford, S., Ross, D. M., Hughes, T. P., Petruzzelli, L., Vanasse, K. G., Warmuth, M., Hofmann, F., Keen, N. J., and Sellers, W. R. (2017) The allosteric inhibitor ABL001 enables dual targeting of Bcr-Abl1, *Nature 543*, 733-737.

[15] Reddy, E. P., and Aggarwal, A. K. (2012) The ins and outs of bcr-abl inhibition, *Genes & cancer 3*, 447-454.

[16] Lins, L., Thomas, A., and Brasseur, R. (2003) Analysis of accessible surface of residues in proteins, *Protein science : a publication of the Protein Society 12*, 1406-1417.

[17] Panjarian, S., Iacob, R. E., Chen, S., Engen, J. R., and Smithgall, T. E. (2013) Structure and dynamic regulation of Abl kinases, *The Journal of biological chemistry 288*, 5443-5450.

[18] Maru, Y. (2012) Molecular biology of chronic myeloid leukemia, *Cancer science 103*, 1601-1610.

[19] Hantschel, O. (2012) Structure, regulation, signaling, and targeting of abl kinases in cancer, *Genes & cancer 3*, 436-446.

[20] Eswar, N., Webb, B., Marti-Renom, M. A., Madhusudhan, M. S., Eramian, D., Shen, M. Y., Pieper, U., and Sali, A. (2007) Comparative protein structure modeling using MODELLER, *Current protocols in protein science Chapter 2*, Unit 2 9.

[21] Kim, S., Thiessen, P. A., Bolton, E. E., Chen, J., Fu, G., Gindulyte, A., Han, L., He, J., He, S., Shoemaker, B. A., Wang, J., Yu, B., Zhang, J., and Bryant, S. H. (2016) PubChem Substance and Compound databases, *Nucleic acids research 44*, D1202-1213.

[22] Trott, O., and Olson, A. J. (2010) AutoDock Vina: improving the speed and accuracy of docking with a new scoring function, efficient optimization, and multithreading, *Journal of computational chemistry 31*, 455-461.

[23] Pettersen, E. F., Goddard, T. D., Huang, C. C., Couch, G. S., Greenblatt, D. M., Meng, E. C., and Ferrin, T. E. (2004) UCSF Chimera--a visualization system for exploratory research and analysis, *Journal of computational chemistry 25*, 1605-1612.

[24] Case, D. A., Cheatham, T. E., 3rd, Darden, T., Gohlke, H., Luo, R., Merz, K. M., Jr., Onufriev, A., Simmerling, C., Wang, B., and Woods, R. J. (2005) The Amber biomolecular simulation programs, *Journal of computational chemistry 26*, 1668-1688.

[25] Machaba, K. E., Cele, F. N., Mhlongo, N. N., and Soliman, M. E. (2016) Sliding Clamp of DNA Polymerase III as a Drug Target for TB Therapy: Comprehensive Conformational and Binding Analysis from Molecular Dynamic Simulations, *Cell biochemistry and biophysics 74*, 473-481.

[26] Ramharack, P., and Soliman, M. E. S. (2017) Zika virus NS5 protein potential inhibitors: an enhanced in silico approach in drug discovery, *Journal of biomolecular structure & dynamics*, 1-16.

[27] Salomon-Ferrer, R., Gotz, A. W., Poole, D., Le Grand, S., and Walker, R. C. (2013) Routine Microsecond Molecular Dynamics Simulations with AMBER on GPUs. 2.

Explicit Solvent Particle Mesh Ewald, *Journal of chemical theory and computation 9*, 3878-3888.

[28] Berendsen, H. J., Postma, J. v., van Gunsteren, W. F., DiNola, A., and Haak, J. (1984) Molecular dynamics with coupling to an external bath, *The Journal of chemical physics 81*, 3684-3690.

[29] Roe, D. R., and Cheatham, T. E., 3rd. (2013) PTRAJ and CPPTRAJ: Software for Processing and Analysis of Molecular Dynamics Trajectory Data, *Journal of chemical theory and computation 9*, 3084-3095.

[30] Seifert, E. (2014) OriginPro 9.1: scientific data analysis and graphing software-software review, *Journal of chemical information and modeling 54*, 1552.

# CHAPTER 6

## A Synergistic Combination against Chronic Myeloid Leukemia: An Intra-Molecular Mechanism of Communication in Bcr–Abl Resistance

Ahmed A Elrashedy[1], Patrick Appiah-Kubi[1], Mahmoud E. S. Soliman[1,2]

[1]Molecular Bio-computation and Drug Design Lab, School of Health Sciences, University of KwaZulu-Natal, Westville Campus, Durban 4001, South Africa

*Corresponding Author: Mahmoud E.S. Soliman

[2]College of Pharmacy and Pharmaceutical Sciences, Florida Agricultural and Mechanical University, FAMU, Tallahassee, Florida 32307, USA.

Email: soliman@ukzn.ac.za

Telephone: +27 (0) 31 260 8048, Fax: +27 (0) 31 260 78

**Abstract**

The constitutive Bcr-Abl active protein fusion has been identified as the main cause of chronic myeloid leukemia (CML). The emergence of T334I, and D381N point mutations in Bcr-Abl confer drug resistance. A recent experimental study shows a synergistic effect in supressing this resistance when Nilotinib and ABL001 are co-administered to target both the catalytic and allosteric binding site of Bcr-Abl protein, respectively. However, the structural mechanism by which this synergistic effect occurs have not been clearly elucidated. To obtain insight into the observed synergistic effect, molecular dynamics simulations have been employed to investigate the inhibitory mechanism as well as the structural dynamics that characterize this effect. Structural dynamic analyses indicate that the synergistic binding effect results in a more compact and stable protein conformation. In addition, binding free energy calculation suggests a dominant energy effect of nilotinib during co-administration. van der Waals energy interactions was observed to be the main energy component driving this synergistic effect. Furthermore, per-residue energy decomposition analyses identified Glu481, Ser453, Ala452, Tyr454, Phe401, Asp400, Met337, Phe336, Ile334, And Val275 as key residues that contribute largely to the synergistic effect. The findings highlighted in this study provide molecular understanding of the dynamics and mechanisms that mediate the synergistic inhibition in Bcr-Abl protein in chronic myeloid leukemia treatment.

**Keyword:** Bcr-Abl, Mutation, CML, ABL001, Nilotinib.

## 6.1 Introduction

Chronic myeloid leukemia (CML) is a rare hematopoietic stem cell disorder categorized by an acquired balanced chromosomal translocation, which gives rise to a constitutively active tyrosine kinase (Bcr-Abl) [1, 2]. Chronic myeloid leukemia pathogenesis involves the fusion of the breakpoint cluster region (Bcr) gene on chromosome 22 with the Abelson murine leukemia (Abl1) gene on chromosome 9 resulting in the expression of Bcr-Abl oncoprotein [3]. This fusion is defined as the Philadelphia chromosome positive ($Ph^+$) , and is characterized by a reciprocal translocation between chromosomes 9 and 22, t(9;22)(q34;q11) [4]. Bcr-Abl oncoprotein is found exclusively in the cytoplasm of the cell and when contrasted with typical ABL, shows deregulated tyrosine kinase action [5, 6] thereby clarifying Bcr-Abl role in leukemia. Chronic myeloid leukemia (CML) accounts for about 15% of newly diagnosed leukemia cases in adults [7] In CML, immature white blood cells are gradually produced crowding in the bone marrow thereby interfering with normal blood cell production. Further progression of the disease leads to the shortage of red blood cells and platelets, causing anemia, bruising and/or bleeding [8].

The Bcr-Abl protein comprises of some domains from both BCR and ABL1 [9]. The BCR domains mainly include an N-terminal coiled-coil domain and a Serine/Threonine Kinase domain. The ABL1 domains consist of an N-Terminal cap that plays a significant role in the regulation of kinase activity, the three Src homology domains (SH3, SH2 and SH1/tyrosine kinase domain), and the C-terminal actin-binding domain (**Figure 6.1**). The structural fold of ABL1 kinase forms the catalytic domain containing both N and C-terminal lobes linked by a short flexible chain referred to as the hinge regions. The cleft formed between the two lobes forms the adenosine triphosphate (ATP)-binding site, which includes the phosphate binding loop or P-loop [10]. The N- and C- lobes contribute conserved residues essential for the catalytic transfer of γ-phosphate from ATP onto the tyrosine residue in the substrate protein. The relative positions of the two lobes and the active site conserved residues coordinate catalytic reactions and dynamic interchanges between active and inactive conformation of the kinase domain. Since most kinases adopt similar active conformations, the inactive conformations of the kinase domains are remarkably diverse, thus providing opportunities for selective inhibitor discovery [11–14].

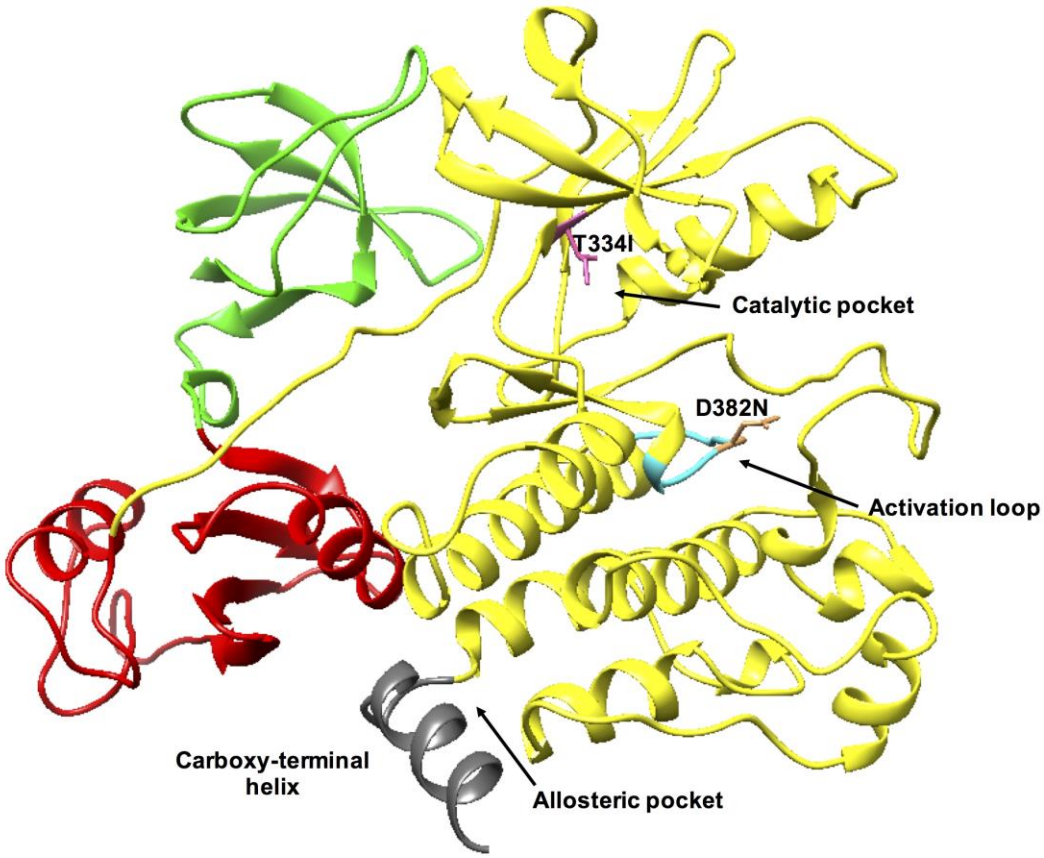


**Figure 6.1.** The 3-D crystal structure of the Abl kinase protein (PDB code: 5MO4). The SH3, SH2 and SH1/kinase domains are shown in green, red and yellow, respectively.

The discovery of Bcr–Abl as a requirement in CML pathogenesis, and the imperative role of ABL tyrosine-kinase activity for Bcr–Abl mediated transformation, made ABL kinase an attractive therapeutic target in CML interventions [4]. This has resulted in a substantial transformation in the therapeutic landscape of CML with the development of tyrosine kinase inhibitors (TKIs) that potently inhibit the interaction of Bcr-Abl and ATP. This approach has resulted in a 10-year survival rate improvement from about 20% to 80%-90% [7, 15].

Most of the developed Bcr-Abl small-molecule inhibitors are ATP competitive inhibitors which occupy the ATP-binding site [16]. However, the ATP-binding site is highly prone to mutations. Interestingly, more than 50 different point mutations have been recognized in imatinib–resistant patients [17]. Mutations at the gatekeeper are considered the most recalcitrant mutations. Asciminib (ABL001) (**Figure 6.2**) is a highly allosteric selective non-ATP competitive inhibitor of oncogenic Bcr-Abl activity [dissociation constant ($K_d$) = 0.5–0.8 nM] recently discovered [18]. ABL001 binds to the myristoyl binding pocket at the N-terminus of ABL1 inducing a conformational change that disables the protein's active site, thus, inducing an inactive C-terminal helix conformation [18, 19]. Recently, mono therapeutic treatment using ABL001 had led to tumor regression in mice xenografted with KCL22 CML cell line. Despite the regression, all of the tumors eventually recurred [20–22]. Although this drug has been established to inhibit the Bcr-Abl protein in multiple studies [23], there are also numerous investigations on ABL001-resistance susceptibility in multiple CML cell lines [19, 21, 24].

Imatinib mesylate (IM, STI-571 or Gleevec) has been previously reported to competitively bind to the ATP active site, thus leading to a loss in Bcr-Abl activity and eventual suppression of CML [25]. Nilotinib (AMN-107, Tasigna) is structurally like imatinib but with molecular alterations that provide higher affinity towards Bcr-Abl (**Figure 6.2**). Nilotinib is 10-50-fold more potent than imatinib against ABL and shows higher efficacy against imatinib-resistant chronic myelogenous leukemia. Nilotinib was approved by FDA as a drug of choice for the treatment of patients resistant to imatinib or in an advanced stage of the disease [26].

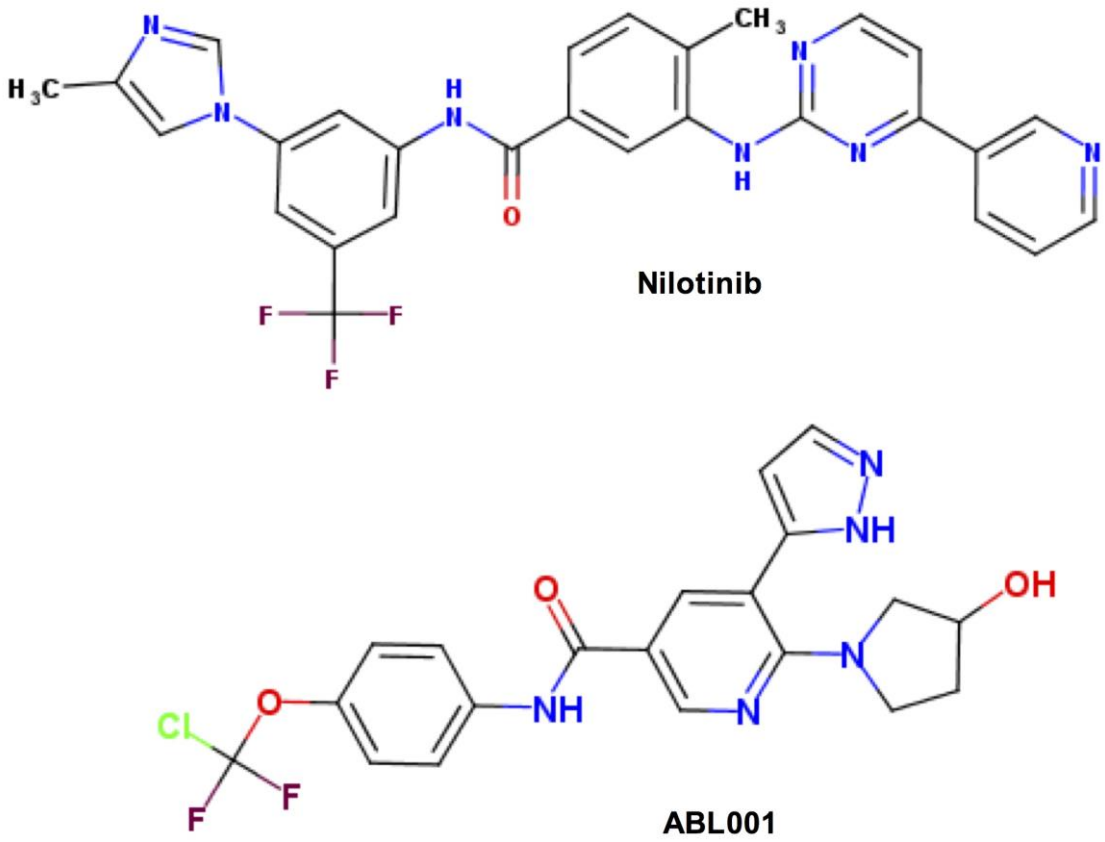


**Figure 6.2.** 2D structure of Nilotinib and ABL001

Combination therapy involving both catalytic and allosteric site inhibitors have been shown to improve the outcome of CML treatment and overcoming resistance [20, 21] (**Figure 6.3**). Wylie *et al* (2017) reported conclusive experimental evidence that co-administration of Nilotinib and ABL001 bound at both catalytic, and allosteric site respectively suppresses the emergency of T334I and D381N resistance [19]. With the availability of drugs for both allosteric and active site, obtaining insights into the structural basis of potential dual inhibition is therefore imperative. This will enhance our understanding of the effectiveness of co-administrative treatments against CML.

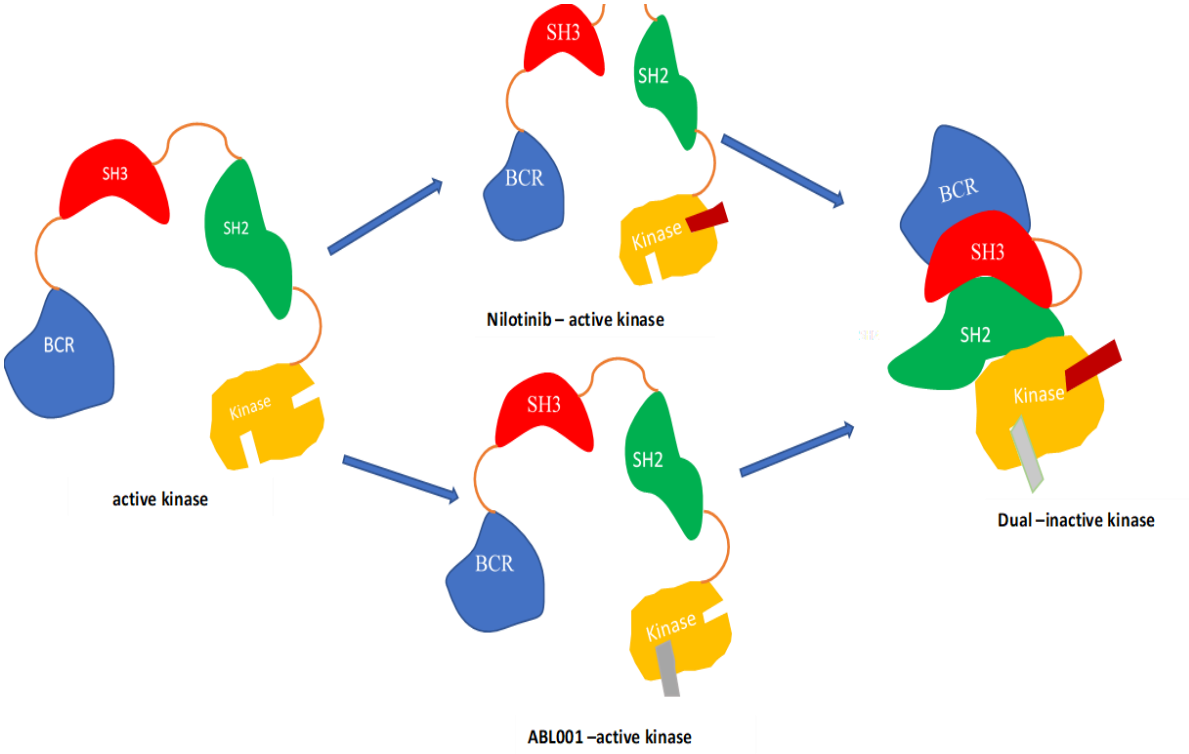


**Figure 6.3**. Schematic diagram showing the structural effects of single-agents and dual inhibition on Bcr-Abl protein complex relative to its activation and inactivation conformation.

In this study, we explored the synergistic therapeutic effect of Bcr-Abl co-inhibition, investigated the underlying structural dynamics and inhibitory mechanisms of Nilotinib and ABL001 combination therapy to overcome T334I, and D382N resistance. We utilized a wide range of *in silico* approaches to define and compare Bcr-Abl's structural dynamics and binding energy characteristics when jointly inhibited by Nilotinib and ABL001 compared with the effect of each drug alone. The joint blockade of Bcr-Abl by Nilotinib and ABL-001 renders a synergistic effect on Bcr-Abl by inducing a more stable and compact protein conformation. The binding energy analysis showed that the joint effect of the two drugs was much better when combined compared with the binding effects of each drug alone. Our results provide a rational basis for the combination therapy using both inhibitors for Bcr-Abl pathway in CML treatment.

## 6.2 Computational Methods

### 6.2.1 System Preparation

Prior to Molecular dynamic (MD) simulations, Bcr-Abl tyrosine kinase in complex with ABL001 (**asciminib**) and Nilotinib was obtained from RSCB Protein Data Bank (PDB code: 5MO4) [19]. The Apo structure was manually prepared by deleting the solvent and any bound small molecules from the crystal structure. The T334I, and D381Npoint mutations were manually introduced with Chimera software. Missing residues were modelled using MODELER 9.19 [27] integrated with chimera software [28]. A 200ns MD simulations were performed on the four prepared systems (**Table 6.1**). Protein and ligand alterations , as well as visualizations, were conducted in Chimera software [28].

**Table 1**. The four studied systems and their abbreviations used in the entire paper.

| Studied Systems | Abbreviations | Time Step (ns) |
|---|---|---|
| Bcr-Abl Apo | BA-Apo | 200 |
| Bcr-Abl in complex with ABL001 alone | BA-ABL001 | 200 |
| Bcr-Abl in complex with Nilotinib alone | BA-Nilotinib | 200 |
| Bcr-Abl in complex with both ABL001 and Nilotinib | BA-Co-inhibition | 200 |

### 6.2.2 Molecular Dynamic (MD) Simulation

Molecular dynamic (MD) simulation is an important tool to determine the physical movements of atoms and molecules, thus, providing insights on the dynamical evolution of biological systems [29]. The MD simulations were carried out on the systems using the GPU version of AMBER14 with SANDER module and the FF14SB variant of the AMBER force field [30]. Restrained Electrostatic Potential (RESP) [31] and General Amber Force Field (GAFF) [32] procedures were used during Antechamber run to complete atomic partial charges for the ligands. The receptor and ligands were optimized, and counterions added for neutralization using the LEAP module for all studied systems [33]. The systems

were completely suspended in an orthorhombic box of TIP3P water molecules, such that all atoms were within 10Å of any box edge [34].

All systems were minimized into two separate minimization stages. An initial partial minimization of 2000 steps were achieved with an applied restraint potential of 100 kcal/mol Å, followed by 1000 steps of full minimization by conjugate gradient algorithm without restrain. The system was heated from 0K to 300K for 50ps, such that the system maintained a fixed number of atoms and a fixed volume (NVT) with a potential harmonic restraint of 10 kcal/mol Å and a collision frequency of $1.0ps^{-1}$. The systems were further equilibrated at 300k for 500ps in the isothermal-isobaric ensemble (NPT) at a constant pressure of 1bar without constrains using the Berendsen barostat.

A total of 200ns NTP ensemble MD production was performed for each system. In each simulation, SHAKE algorithm was employed to constrict the bonds of hydrogen atoms. The time step of each simulation was set to 2fs with a constant pressure of 1 bar maintained by the Berendsen barostat, a pressure-coupling constant of 2ps, a temperature of 300K and Langevin thermostat with collision frequency of $1.0ps^{-2}$. Trajectory files were generated and subjected to post-dynamic analysis.

### 6.2.3 Post-Dynamic Analysis

The trajectories generated after MD simulations were each saved every 1ps, followed by analysis using the CPPTRAJ [35] module employed in AMBER 14 suit. All plots and visualizations were completed using the Origin data analysis tool [36] and Chimera [28] respectively.

### 6.2.4 Binding Free Energy Calculations

Computing of the binding free energy of small ligand to protein is an important endpoint method currently used in computational biophysics [37]. To determine the free binding energy of each system, the Molecular Mechanics-Generalized-Born Surface Area method (MM-GBSA) procedure in AMBER14 was employed [38]. The explicit solvent employed in the MD simulation was discarded and replaced with a dielectric continuum [39]. The

changes (Δ) in each term between complex state and unbound state were calculated for the total relative binding free energy [39]. Molecular mechanics force fields were then employed to calculate energy contributions from the atomic coordinates of the enzyme, ligands and the complex in a gas phase [39]. This technique was used to calculate the binding free energy of ABL001, Nilotinib in all systems.

Binding free energy was averaged over 2000 snapshots extracted from the entire 200ns trajectory at an interval of 100. The computing of the binding free energy (ΔG) for each molecular species (complex, ligand,and receptor) can be represented as:

$$\Delta G_{bind} = G_{complex} - G_{receptor} - G_{ligand} \quad (1)$$

$$\Delta G_{bind} = E_{gas} + G_{sol} - TS \quad (2)$$

$$E_{gas} = E_{int} + E_{vdw} + E_{ele} \quad (3)$$

$$G_{sol} = G_{GB} + G_{SA} \quad (4)$$

$$G_{SA} = \gamma SASA \quad (5)$$

The term $E_{gas}$, $E_{int}$, $E_{ele}$, and $E_{vdw}$ symbolize the gas-phase energy, internal energy, Coulomb energy, and van der Waals energy respectively. The $E_{gas}$ was directly assessed from the FF14SB force field terms. Solvation free energy ($G_{sol}$), was assessed from the energy involvement from the polar states ($G_{GB}$), and non-polar states (G). The non-polar solvation energy ($G_{SA}$), was determined from the solvent accessible surface area (SASA), using a radius of 1.4 Å, whereas the polar solvation ($G_{GB}$) contribution assessed by solving the GB equation. S and T symbolize the total entropy of the solute and temperature respectively.

### 6.2.5 Per-Residue Free Energy Decomposition Analysis

To further identify key active site residues responsible for inhibitor recognition, the computed total binding free energy was decomposed to each residue. The binding interactions between each residue and the inhibitor were calculated using the MM-GBSA per-residue decomposition process in AMBER14.

## 6.3 Results and Discussion

### 6.3.1 Overall Structural Stability and Dynamics of the simulated systems

The stability of the simulated systems was observed by measuring the root mean square deviation (RMSD) from the crystallographic structure. The average RMSD C-α atoms of the trajectories for all the systems demonstrate that equilibration was achieved after 20ns (**Figure 6.4a**). The recorded average RMSD values for the entire frames of the systems were 2.95Å, 2.50Å, 2.28Å, 1.96Å for BA-Apo, BA-Nilotinib, BA-ABL001, and BA-Co-inhibition respectively. These results show that the co-inhibition of Bcr-Abl by ABL001 and Nilotinib induces a more stable protein conformation than when ABL001 or Nilotinib binds alone.

Furthermore, to compare the amino acid residue flexibility upon ligand binding, the root mean square fluctuation (RMSF) of the protein backbone was measured over 200ns to observe inhibitor binding effects towards Bcr-Abl protein structural dynamics. The computed average atomic fluctuations for BA-Apo, BA-Nilotinib, BA-ABL001, and BA-Co-inhibition were 1.22Å, 1.14Å, 1.38Å, and 1.00Å, respectively (**Figure 6.4b**). These results indicate a lower residue fluctuation during BCL-ABL co-inhibition, suggesting that the co-binding of ABL001and Nilotinib decreases the overall protein flexibility compared to when ABL001 or Nilotinib binds alone to Bcr-Abl.

To observe the overall Bcr-Abl protein compactness upon ligand binding, the radius of gyration (ROG) was computed by measuring the mass-weighted root mean square distance of a collection of atoms from the center of mass of complex during the MD simulations [40, 41]. The average ROG values are 23.78Å, 23.71Å, 24.03Å and 23.54Å for BA-Apo, BA-Nilotinib, BA-ABL001, and BA-Co-inhibition respectively (**Figure 6.4c**). The observed lower ROG value for co-inhibition of Bcr-Abl by ABL001 and Nilotinib compared with Bcr-Abl single drug inhibition by ABL001 or Nilotinib only, reflects a similar pattern as seen in the RMSF and RMSD values. The observed pattern suggests that the co-inhibition of Bcr-Abl by ABL001 and Nilotinib results in a more rigid stable protein structure than when ABL001 or Nilotinib binds alone, which results in improved binding energy as evidenced by the binding energy results (**Table 6.2**).

To further gain insight on how the protein surface interacts with solvent molecules and to obtain insight into the relation of the compactness of the protein hydrophobic core, the solvent accessible surface area (SASA) of the protein upon ligand binding was computed (**Figure 6.4d**).

This was accomplished by measuring the surface area of the protein visible to solvent across the 200ns MD simulation, which is essential for biomolecular stability [42]. The overall SASA indicates that co-inhibition of Bcr-Abl by ABL001 and Nilotinib less expose the protein surface to solvent molecules compared to mono-therapeutic inhibition. The computed average SASA values for BA-Apo, BA-Nilotinib, BA-ABL001, and BA-Co-inhibition systems were 20420.93A$^2$, 19912.11A$^2$, 20053.69A$^2$, and 19526.81A$^2$ respectively. The SASA results together with the observations from RSMD, RMSF and ROG calculations further confirms that the co-administration of ABL001 and Nilotinib results in a more stable compact protein conformation than when each of the drugs binds alone.

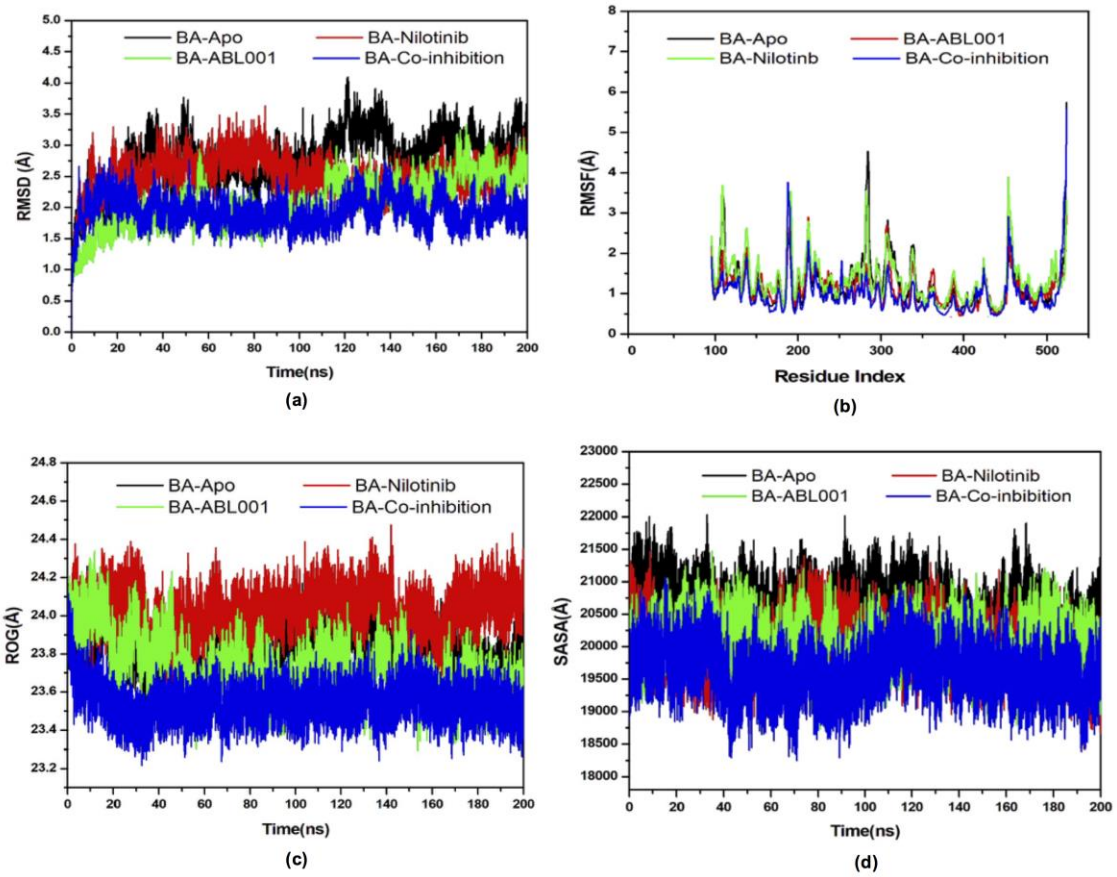

**Figure 6.4**. (a) RMSD of Cα atoms of the protein backbone atoms (b) RMSF of each residue of the protein backbone Cα atoms (c) Radius of Gyration (ROG) of Cα atoms of protein residues, and (d) Solvent accessible surface area (SASA) of the backbone atoms relative to the starting minimized over 200ns for BA-Apo, BA-Nilotinib, BA-ABL001, and BA-Co-inhibition systems.

### 6.3.2 Mechanism of binding interactions based on Binding Free Energy Calculation

The total binding free energy was calculated to gain insight into the binding energetics of ABL001 and Nilotinib when each bind alone and when in co-inhibition to Bcr-Abl. The MM-GBSA program in AMBER14 was used in calculating the binding free energies by extracting snapshots from the trajectories of the compounds.

As can be seen in **Table 6.2**, the difference in binding energy of Nilotinib when bound alone (-62.77 kcal/mol) and when bound in a complex with ABL001 (-67.51 kcal/mol) was -4.74 kcal/mol. The same is true for ABL001 with a binding free energy difference of -1.85 kcal/mol when bound alone (-40.97 kcal/mol) and when bound in a complex with Nilotinib (-42.82 kcal/mol). This indicates a more favorable binding of Nilotinib and ABL001when bound in a complex with each other than when each bound alone. The computed binding energies correlate well with the experimental $IC_{50}$ reported values [20, 21].

**Table 2**. Summary of binding free energy components calculated for ABL001 and Nilotinib when each bound alone and when in co-inhibition with each other to Bcr-Abl systems. All values are given in kcal/mol. Standard deviation given by σ.

| Compounds | Individual binding | | | | Co-inhibition of inhibitors | | | |
|---|---|---|---|---|---|---|---|---|
| | ABL001 | | Nilotinib | | ABL001 | | Nilotinib | |
| | Mean | σ | Mean | σ | Mean | σ | Mean | σ |
| $\Delta E_{vdW}$ | -49.30 | 0.05 | -70.87 | 0.04 | -48.80 | 0.18 | -74.94 | 0.20 |

| | | | | | | | | |
|---|---|---|---|---|---|---|---|---|
| $\Delta E_{elec}$ | -20.44 | 0.12 | -28.72 | 0.06 | -30.96 | 0.49 | -29.85 | 0.38 |
| $\Delta G_{gas}$ | -69.74 | 0.14 | -99.59 | 0.07 | -79.77 | 0.50 | -104.79 | 0.41 |
| $\Delta G_{solv}$ | 28.77 | 0.10 | 36.82 | 0.05 | 36.94 | 0.38 | 37.28 | 0.30 |
| $\Delta G_{bind}$ | -40.97 | 0.07 | -62.77 | 0.05 | -42.82 | 0.21 | -67.51 | 0.25 |

The MM-GBSA method further allows the decomposition of the total binding free energy into the individual contributing energy components, thus providing a detailed understanding of the complex binding process. The nonpolar solvation and van der Waals interaction energies are observed in all the systems to be responsible for favorable binding free energies whereas polar solvation energy terms contribute unfavorably to the binding of the inhibitors. The thermodynamic energy contribution of Nilotinib to the total binding free energy of the complex surmounts to the stability of ABL001 in the allosteric binding pocket and thus the stability of the complex during the simulation.

### 6.3.3 Identification of the key residues responsible for inhibitor binding

To identify the key active site residues involved in the co-inhibition process, the total binding free energy of ABL001 and Nilotinib toward Bcr-Abl protein was further decomposed into the contribution of each active site residue. The residue interaction energy information is shown in **Figure 6.5**. As can be observed from **Figure 6.5a**, the major favourable energy contributions to ABL001 binding predominately originate from residues GLU481 (-2.20 kcal/mol), SER453 (-2.11 kcal/mol), ALA452 (-2.23 kcal/mol), and TYR454 (-1.54 kcal/mol) whereas in **Figure 6.5b** residues PHE401 (-3.13 kcal/mol), ASP400 (-1.79 kcal/mol), MET377 (-1.66 kcal/mol), PHE336 (-2.20kcal/mol), ILE334 (-2.5kcal/mol), and VAL275 (-1.77kcal/mol) largely contribute to Nilotinib binding with binding energy contributions $\Delta G_{bind}$ > -1.5 kcal/mol.

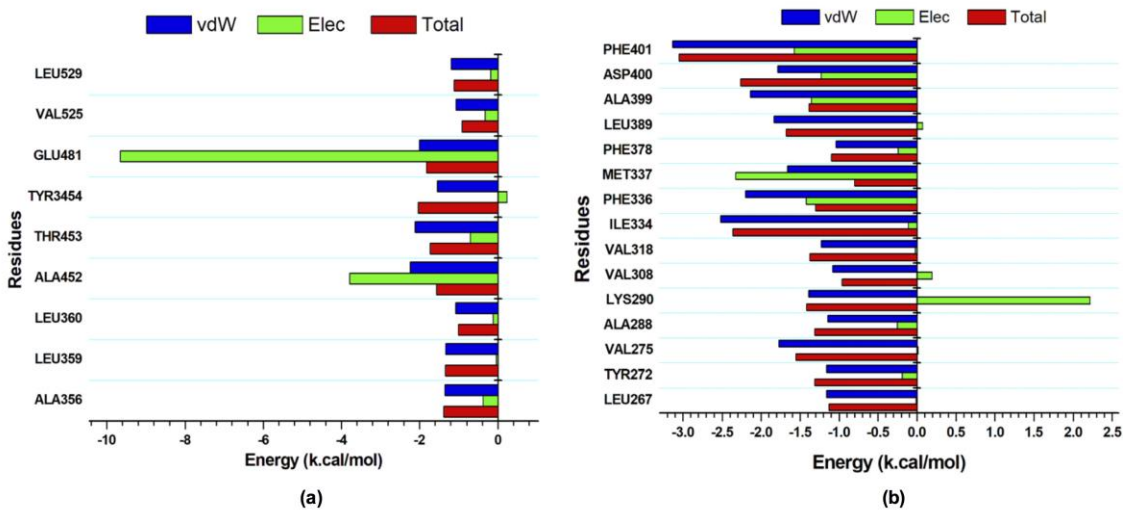


**Figure 6.5.** Per-residue decomposition plot showing the energy contributions of the most interacting residues at (a) the allosteric binding site with ABL001 and (b) the catalytic active site with Nilotinib.

### 6.3.4 Bcr-Abl Co-Inhibition Interactions and Ligand Binding Mode Analysis

Figure 6.6 illustrates that the catalytic site residues Asp400, and Phe401 form a stable hydrogen bond with the hydroxyl group of Nilotinib whereas Met377 forms a hydrogen bond with the amino group of pyrimidine ring of Nilotinib. The amino group of ABL001 donates a hydrogen bond to residue Glu399 at the allosteric site via its terminal oxygen atom with a negatively binding of -2.003 kcal/mol, indicating its importance for binding. It is worth to note that highly electrostatic fluorine molecules were found at the base of the hydrophobic pocket in both the catalytic and allosteric sites.

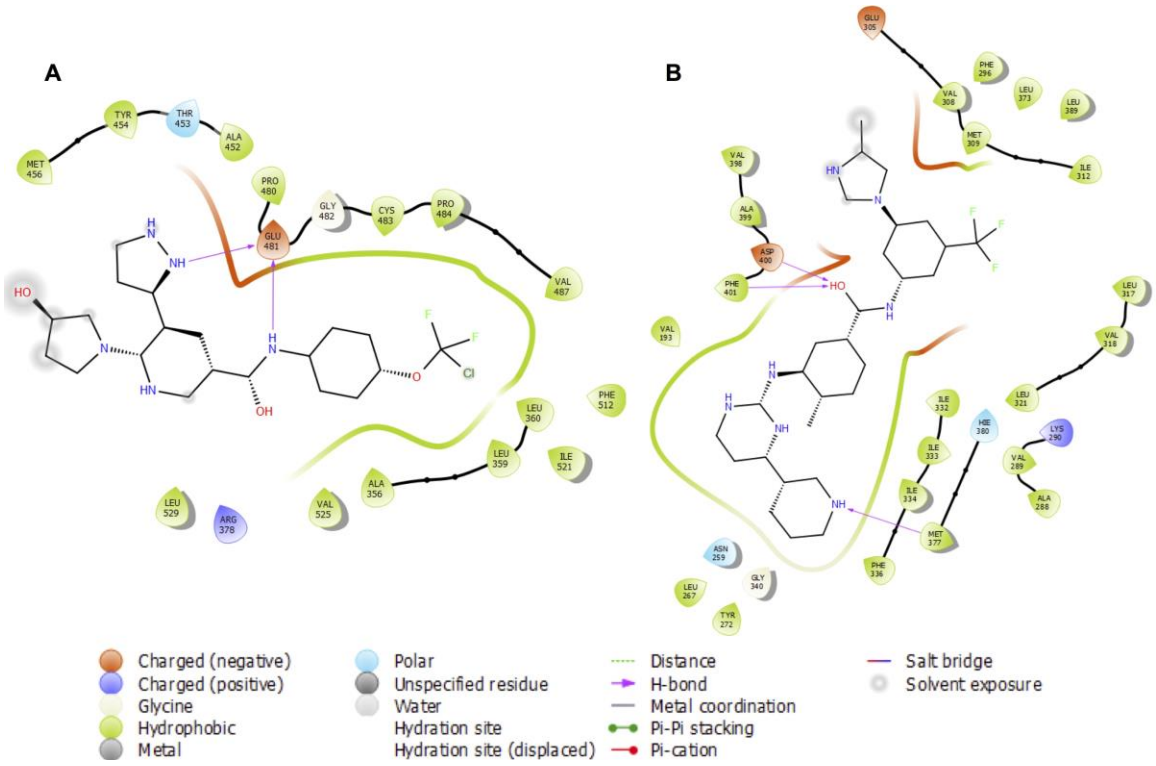


**Figure 6.6**: The key interactions between the catalytic active site and allosteric active site residues of Bcr-Abl with ABL001 (A) and Nilotinib (B).

### 6.4 Conclusion

In this study, comparative MD simulation and binding free energy analysis were employed to investigate the co-inhibitory mechanism of Nilotinib and ABL001 in the presence and absence of each other against Bcr-Abl. Recent experimental evidence shows that co-administration of Nilotinib and ABL001 bound at both catalytic, and allosteric site respectively suppresses the emergency of T334I, and D381N resistance. To this end, we investigated the inhibitory mechanism and structural dynamic features that characterize this synergistic co-inhibition. Results from this study demonstrated that the co-inhibition of Bcr-Abl system induced a more stable, compact protein structure when compared to systems in which ABL001 or Nilotinib binds alone. The calculated binding free energy of ABL001 or Nilotinib during co-inhibition was higher compared to when each bound alone. The binding free energy component analysis suggests that the major energy component driving this synergistic effect is van der Waals energy component. The decomposition of the total energies into individual active site residue contributions revealed that amino acid

residues Glu481, Ser453, Ala452, and Tyr454 are important residues that contribute largely to the binding of ABL001, whereas Phe401, Asp400, Met377, Phe336, Ile334, and Val275 are key to the binding of Nilotinib.

The findings highlighted in this study provide a molecular understanding of the dynamics and mechanisms that mediate the synergistic inhibition in Bcr-Abl protein. Our findings will further assist in the optimization of the inhibitory activity of these compounds in chronic myeloid leukemia treatment.

**Acknowledgment**

The authors acknowledge the College of Health Science, University of KwaZulu-Natal for financial support and Centre of High Performance Computing (CHPC) Cape Town, RSA, for computational resources (www.chpc.ac.za).

**Conflict of interest**

The authors declare no conflict of interest.

## *6.5 Reference:*


1. Apperley JF (2015) Chronic myeloid leukaemia. Lancet (London, England) 385:1447–1459. https://doi.org/10.1016/S0140-6736(13)62120-0

2. Druker BJ (2001) Current treatment approaches for chronic myelogenous leukemia. Cancer J 7 Suppl 1:S14-8

3. Rowley JD (1973) A new consistent chromosomal abnormality in chronic myelogenous leukaemia identified by quinacrine fluorescence and Giemsa staining. Nature 243:290

4. Ren R (2005) Mechanisms of BCR–ABL in the pathogenesis of chronic myelogenous leukaemia. Nat Rev Cancer 5:172

5. Pendergast AM, Quilliam LA, Cripe LD, et al (1993) BCR-ABL-induced oncogenesis is mediated by direct interaction with the SH2 domain of the GRB-2 adaptor protein. Cell 75:175–185

6. Ben-Neriah Y, Daley GQ, Mes-Masson AM, et al (1986) The chronic myelogenous leukemia-specific P210 protein is the product of the bcr/abl hybrid gene. Science (80- ) 233:212–214

7. Jabbour E, Kantarjian H (2018) Chronic myeloid leukemia: 2018 update on diagnosis, therapy and monitoring. Am J Hematol 93:442–459

8. Granatowicz A, Piatek CI, Moschiano E, et al (2015) An overview and update of chronic myeloid leukemia for primary care physicians. Korean J Fam Med 36:197–202

9. Panjarian S, Iacob RE, Chen S, et al (2013) Structure and dynamic regulation of Abl kinases. J Biol Chem 288:5443–50. https://doi.org/10.1074/jbc.R112.438382

10. Huse M, Kuriyan J (2002) The Conformational Plasticity of Protein Kinases. Cell 109:275–282. https://doi.org/10.1016/S0092-8674(02)00741-9

11. Nagar B, Bornmann WG, Pellicena P, et al (2002) Crystal structures of the kinase domain of c-Abl in complex with the small molecule inhibitors PD173955 and

imatinib (STI-571). Cancer Res 62:4236–43

12. Schindler T, Bornmann W, Pellicena P, et al (2000) Structural mechanism for STI-571 inhibition of abelson tyrosine kinase. Science 289:1938–42

13. Zhang J, Yang PL, Gray NS (2009) Targeting cancer with small molecule kinase inhibitors. Nat Rev Cancer 9:28–39. https://doi.org/10.1038/nrc2559

14. Nagar B (2007) c-Abl tyrosine kinase and inhibition by the cancer drug imatinib (Gleevec/STI-571). J Nutr 137:1518S–1523S; discussion 1548S

15. Huang X, Cortes J, Kantarjian H (2012) Estimations of the increasing prevalence and plateau prevalence of chronic myeloid leukemia in the era of tyrosine kinase inhibitor therapy. Cancer 118:3123–3127. https://doi.org/10.1002/cncr.26679

16. Battistutta R, De Moliner E, Sarno S, et al (2001) Structural features underlying selective inhibition of protein kinase CK2 by ATP site-directed tetrabromo-2-benzotriazole. Protein Sci 10:2200–6. https://doi.org/10.1110/ps.19601

17. Shah NP, Nicoll JM, Nagar B, et al (2002) Multiple BCR-ABL kinase domain mutations confer polyclonal resistance to the tyrosine kinase inhibitor imatinib (STI571) in chronic phase and blast crisis chronic myeloid leukemia. Cancer Cell 2:117–25

18. Schoepfer J, Jahnke W, Berellini G, et al (2018) Discovery of asciminib (ABL001), an allosteric inhibitor of the tyrosine kinase activity of Bcr-Abl1

19. Wylie AA, Schoepfer J, Jahnke W, et al (2017) The allosteric inhibitor ABL001 enables dual targeting of BCR–ABL1. Nature 543:733–737. https://doi.org/10.1038/nature21702

20. Wylie AA, Schoepfer J, Jahnke W, et al (2017) The allosteric inhibitor ABL001 enables dual targeting of BCR?ABL1. Nature 543:733–737. https://doi.org/10.1038/nature21702

21. Wylie A, Schoepfer J, Berellini G, et al (2014) ABL001, a Potent Allosteric Inhibitor of BCR-ABL, Prevents Emergence of Resistant Disease When Administered in

Combination with Nilotinib in an in Vivo Murine Model of Chronic Myeloid Leukemia. Blood 124:398–398

22. Eadie LN, Saunders VA, Leclercq TM, et al (2015) The Allosteric Inhibitor ABL001 Is Susceptible to Resistance in Vitro Mediated By Overexpression of the Drug Efflux Transporters ABCB1 and ABCG2. Blood 126:4841–4841

23. Ottmann OG, Alimena G, DeAngelo DJ, et al (2015) ABL001, a Potent, Allosteric Inhibitor of BCR-ABL, Exhibits Safety and Promising Single- Agent Activity in a Phase I Study of Patients with CML with Failure of Prior TKI Therapy. Blood 126:138–138

24. Hughes TP, Goh Y-T, Ottmann OG, et al (2016) Expanded Phase 1 Study of ABL001, a Potent, Allosteric Inhibitor of BCR-ABL, Reveals Significant and Durable Responses in Patients with CML-Chronic Phase with Failure of Prior TKI Therapy. Blood 128:625–625

25. Druker BJ, Sawyers CL, Kantarjian H, et al (2001) Activity of a Specific Inhibitor of the BCR-ABL Tyrosine Kinase in the Blast Crisis of Chronic Myeloid Leukemia and Acute Lymphoblastic Leukemia with the Philadelphia Chromosome. N Engl J Med 344:1038–1042. https://doi.org/10.1056/NEJM200104053441402

26. Hassan AQ, Sharma S V., Warmuth M (2010) Allosteric inhibition of BCR-ABL. Cell Cycle 9:3734–3738. https://doi.org/10.4161/cc.9.18.13232

27. Webb B, Sali A (2014) Protein structure modeling with MODELLER. Protein Struct Predict 1–15

28. Pettersen EF, Goddard TD, Huang CC, et al (2004) UCSF Chimera—a visualization system for exploratory research and analysis. J Comput Chem 25:1605–1612

29. Adcock SA, McCammon JA (2006) Molecular dynamics: survey of methods for simulating the activity of proteins. Chem Rev 106:1589–615. https://doi.org/10.1021/cr040426m

30. Case DA, Cheatham TE, Darden T, et al (2005) The Amber biomolecular simulation programs. J Comput Chem 26:1668–1688. https://doi.org/10.1002/jcc.20290

31. Burger SK, Schofield J, Ayers PW (2013) Quantum Mechanics/Molecular Mechanics Restrained Electrostatic Potential Fitting. J Phys Chem B 117:14960–14966

32. Sprenger KG, Jaeger VW, Pfaendtner J (2015) The General AMBER Force Field (GAFF) Can Accurately Predict Thermodynamic and Transport Properties of Many Ionic Liquids. J Phys Chem B 119:5882–5895

33. Shao Y, Molnar LF, Jung Y, et al (2006) Advances in methods and algorithms in a modern quantum chemistry program package. Phys Chem Chem Phys 8:3172–3191

34. Jorgensen WL, Chandrasekhar J, Madura JD, et al (1983) Comparison of simple potential functions for simulating liquid water. J Chem Phys 79:926–935. https://doi.org/10.1063/1.445869

35. Roe DR, Cheatham TE (2013) PTRAJ and CPPTRAJ: Software for Processing and Analysis of Molecular Dynamics Trajectory Data. J Chem Theory Comput 9:3084–3095

36. Seifert E (2014) OriginPro 9.1: Scientific data analysis and graphing software - Software review. J Chem Inf Model 54:1552–1552. https://doi.org/10.1021/ci500161d

37. Ylilauri M, Pentikäinen OT (2013) MMGBSA as a tool to understand the binding affinities of filamin-peptide interactions. J Chem Inf Model 53:2626–2633. https://doi.org/10.1021/ci4002475

38. Hou T, Wang J, Li Y, Wang W (2011) Assessing the performance of the MM/PBSA and MM/GBSA methods. 1. The accuracy of binding free energy calculations based on molecular dynamics simulations. J Chem Inf Model 51:69–82. https://doi.org/10.1021/ci100275a

39. Hayes JM, Archontis G (2011) MM-GB (PB) SA Calculations of Protein-Ligand Binding Free Energies. InTech 171–190. https://doi.org/10.5772/37107

40. Pan L, Patterson JC, Deshpande A, et al (2013) Molecular Dynamics Study of Zn(Aβ) and Zn(Aβ)2. PLoS One 8:70681–70688.

https://doi.org/10.1371/journal.pone.0070681

41. Wijffels G, Dalrymple B, Kongsuwan K, Dixon N (2005) Conservation of Eubacterial Replicases. IUBMB Life 57:413–419. https://doi.org/10.1080/15216540500138246

42. Richmond TJ (1984) Solvent accessible surface area and excluded volume in proteins. Analytical equations for overlapping spheres and implications for the hydrophobic effect. J Mol Biol 178:63–89

# CHAPTER 7

## 7.1 Conclusion

Despite the notable achievement of kinase inhibitors in the treatment of CML patients, recent reports suggest a 5–10% clinical relapse due to drug resistance following long-term Imatinib therapy. As a result, finding viable therapeutic approaches to fight against Imatinib resistance has become extremely important. Over the last few years, significant resistance to kinase inhibitors has been revealed in many approaches, however researchers continue to work diligently in the design of therapeutically efficient techniques and potential drug molecules that can be co-administered with kinase inhibitors to curb the threat of kinase inhibitor resistance.

The main objectives of this thesis were to reveal molecular insight that may potentially eliminate the emergence of resistance to Nilotinib ( kinase inhibitor) by the novel ABL001 (Allosteric inhibitor) co-bound to Bcr-Abl. The study also sought to provide molecular understanding between the interplay of a single active site mutation as well as mutations in both the catalytic active site and activation loop which are responsible for the emerging resistance in Nilotinib amongst single binding of Nilotinib or upon co-binding with ABL001 at the allosteric site.

The results of this work have confirmed the following conclusions:

1. Dual inhibition with both Nilotinib and ABL001 induced a more stable and compact Bcr-Abl than when Bcr-Abl bound to either Nilotinib or ABL0001 alone.
2. Thermodynamic calculations have shown that ABL001 has greater stability and stronger Nilotinib –Bcr-Abl interactions, which was complemented by remarkable compactness of binding site residues of Nilotinib and enhanced interactions of van der Waals with dual binding.
3. The calculated binding free energy of Nilotinib in the presence of ABL001 was higher as compared to each drug bound individually to Bcr-Abl, possibly

explaining the reasons for suppressing the resistance of Nilotinib as previously experimentally predicted.

4. Per-residue energy decomposition analyses identified Glu481, Ser453, Ala452, Tyr454, Phe401, Asp400, Met337, Phe336, Ile334, And Val275 as key residues that contribute largely to the synergistic effect.
5. The study also investigated the impact of a mutation at the catalytic site in addition to mutations of both catalytic and activation loop of Bcr-Abl revealing that Nilotinib binding affinity and H-bond interactions were decreased with a resultant induced structural rearrangement around the mutant sites in Bcr-Abl when either Nilotinib or ABL001 is bound.
6. Dual binding has shown stronger bound to Bcr-Abl compared to monotherapy by either Nilotinib or ABL001 amidst the mutations. Results are compatible with the previous report of the dramatic impact of the mutation on the attachment of Nilotinib to Bcr-Abl, while also conferring with the experimental prediction of the suppression of Nilotinib resistance upon dual binding.

Overall, this study has provided essential conformational and structural molecular insights into the design and development of new Bcr-Abl inhibitors through molecular modeling and CADD.

### 7.2 Future Perspectives

Using computational tools, the studies reported in this thesis complemented and justified previously reported experimental findings, providing consistent molecular insights which can be utilized in future studies. Computational perspective presented in these studies opened up the scope for future studies, which can serve as the basis for future research.

1. Findings from this thesis support that dual binding with Nilotinib and ABL001 on Bcr-Abl suppresses the emergence of either Nilotinib or ABL001 resistance as previously predicted experimentally. Further research could still, however, be carried out to provide potential pharmacophoric features in the design and development of new small molecules inhibitors that can singly target Bcr-Abl to suppress ATP kinase inhibitor resistance. Single

acting drugs will reduce the risk of toxicity and will be relatively less expensive than the co-administration of two separate drugs.

2- To additionally examine the validity of the simulation and parameters proposed for the expressive the system studied, the simulation could be performed in longer periods of molecular dynamic simulations for each system. A longer system run can be used to evaluate parameters proposed and to further understand the impact of co-binding Nilotinib and ABL001 on the emergence of either Nilotinib or ABL001 resistance as well the revealing the impact of single active site mutation.

# APPENDIX

## Appendix A:

Ahmed A Elrashedy, Pritika Ramharack, Mahmoud E. S. Soliman (2019 The Perplexity of Synergistic Duality: Inter-Molecular Mechanisms of Communication in Bcr–Abl , Anticancer Agents Med Chem. 2019 Jun 20. doi: 10.2174/1871520619666190620120144.

## Appendix B:

Ahmed A El Rashedy , Fisayo A. Olotua, Mahmoud E. S. Solimana (2018) Dual Drug Targeting of Mutant Bcr-Abl Induces Inactive Conformation: New Strategy for the Treatment of Chronic Myeloid Leukemia and Overcoming Monotherapy Resistance , *Chem Biodivers. 2018 Mar;15(3):e1700533. doi: 10.1002/cbdv.201700533.*

## Appendix C:

Ahmed A Elrashedy, Patrick Appiah-Kubi, Mahmoud E. S. Soliman (2019) A Synergistic Combination Against Chronic Myeloid Leukemia: An Intra-molecular Mechanism of Communication in Bcr-Abl Resistance, Protein J. Apr;38(2):142-150. doi: 10.1007/s10930-019-09820-z.